Underlying Mechanisms of Prolyl Oligopeptidase Inhibition, Deletion, and Restoration on the α-Synuclein Aggregation Process

Reinis Svarcbahs

Division of Pharmacology and Pharmacotherapy
Faculty of Pharmacy
University of Helsinki

Doctoral School in Health Sciences
Doctoral Programme in Drug Research

ACADEMIC DISSERTATION

To be presented, with the permission of the Faculty of Pharmacy of the University of Helsinki, for public examination in lecture room 2041, Viikki Biocenter 2, on 25 January 2019, at 12 noon.

Helsinki 2019

Supervisors

Docent Timo T. Myöhänen, PhD
Division of Pharmacology and Pharmacotherapy
Faculty of Pharmacy
University of Helsinki
Finland

Professor Raimo K. Tuominen, MD, PhD
Division of Pharmacology and Pharmacotherapy
Faculty of Pharmacy
University of Helsinki
Finland

Reviewers

Associate professor Anna Erlandsson, PhD
Department of Public Health and Caring Sciences
Uppsala University
Sweden

Docent Jouni Sirviö
University of Eastern Finland
&
Sauloner Ltd
Finland

Opponent

Professor Deniz Kirik, MD, PhD
Brain Repair and Imaging in Neural Systems
Lund University
Sweden

ISBN 978-951-51-4817-9 (paperback)
ISBN 978-951-51-4818-6 (PDF)
ISSN 2342-3161 (paperback)
ISSN 2342-317X (online)

Unigrafia
Helsinki 2019

ABSTRACT

Neurodegenerative disorders are characterized by accumulation of toxic protein species that are followed by a gradual loss of neurons in certain brain regions and person's loss of movement and dementia. The cause of the protein accumulation is not fully understood but is partially influenced by the disturbances in the protein degradation pathways, post-translational protein modifications that facilitate either gain-of-toxicity or loss-of-function of these proteins. In Parkinson's disease, the best-known aggregation prone protein is alpha-synuclein (aSyn) that is the main component of Lewy bodies, the histopathological hallmarks of Parkinson's disease and other synucleinopathies. Several studies suggest that aSyn aggregates can damage neurons by various mechanisms, and propagate toxicity by cell-to-cell transfer thus making it a tempting target for drug therapy. Current drug therapies can only relieve symptoms of neurodegenerative diseases but do not address, for example, protein aggregate clearance or pharmacological deceleration of the inclusion formation.

In previous studies, prolyl oligopeptidase (PREP) has been shown to enhance the aggregation of aSyn. PREP inhibitors have been shown to reduce the aggregation and increase the clearance of aggregates via enhanced autophagy. However, the mechanisms of how PREP affects aSyn aggregation and regulates autophagy, and if this has a long-term impact on aSyn toxicity, have not been studied. The aim of this study was to investigate the role of PREP deletion, restoration, overexpression, and catalytical inhibition on the cellular signaling pathways and aSyn aggregation. The first part of the work was done in PREP knockout cells and knockout mice where the aSyn protein was overexpressed alone or together with PREP. We showed that absence of PREP decreases aSyn-overexpression mediated behavioral and cellular toxicity in mouse brain. Additionally, we found that PREP knockout cells exhibit reduced stress response and toxicity in the presence of protein overload, have increased autophagic activity, and remove excess aSyn into the cell media.

The second part studied effects of chronic PREP inhibition by KYP-2047 on aSyn aggregation and on motor disturbances in the aSyn viral vector overexpression Parkinson's disease mouse model. The main finding showed that after chronic PREP inhibition, animals lost pathological unilateral motor behavior due to reduction in aSyn oligomer species in the nigrostriatal pathway.

The third part concentrated on mapping the role of PREP in the pathways responsible for the autophagy initiation. The main finding was discovery of PREP's role in negatively regulating one of the most important protein phosphatase complexes, protein phosphatase 2A (PP2A), via direct protein-protein interaction. Besides, this interaction could be altered with PREP

inhibitor treatment that resulted in upregulation of PP2A activity and explained the functional results of autophagy induction after PREP inhibition.

In summary, the findings of this study underline mechanisms through which PREP might be mediating aSyn related pathology and underlines the potential of PREP inhibition as an attractive drug target in reducing aSyn aggregate formation and boosting clearance from the affected brains. PREP involvement in the PP2A network regulation and additional functional data warrants further PREP investigation in the context of other neurodegenerative disorders and PP2A-related ailments.

ACKNOWLEDGEMENTS

I first came to the Division of Pharmacology and Pharmacotherapy in fall 2013. Now, almost 6 years later, but still under 30 years of age, it is time to reminisce and thank people who were involved in this work. During these years I have worked in an encouraging and friendly environment.

I wish to express my deepest gratitude to the following persons:

My supervisor Dr. Timo T. Myöhänen for his supervision during all these years. Timo is warmly thanked for giving me the opportunity to work in his group, for guidance and both emotional and financial support on my way to becoming a scientist. I appreciate the fact that he could always find time for me, whether in person, via messenger late at night or by hands-on guidance. I feel privileged to have worked in Timo's group and during my study years, it has become as a second family to me.

Professor Raimo Tuominen for welcoming me at the division when I came to Finland as a Master's student for my ERASMUS exchange and for creating an inspiring and creative atmosphere. Additionally, Professor Raimo Tuominen is thanked for agreeing to act as a custos in the public defence of this thesis and for giving advice during the years.

Reviewers of this thesis, Associate Professor Anna Erlandsson and Dr. Jouni Sirviö, are thanked for the constructive comments and suggestions, which substantially improved the thesis manuscript.

I would like to thank Professor Deniz Kirik for agreeing to act as my opponent in the public defence of this thesis.

I wish to express my gratitude to all my co-authors for their contribution, which has made this work possible. Especially I would like to thank Ulrika Julku, Susanna Norrbacka, Dr. Mari Savolainen, and Dr. Maria Jäntti for sharing their knowledge during my PhD project and for becoming cherished friends (it would not have been possible without sharing a dark sense of humour).

I also thank Dr. Brandon Harvey for the memorable visit in his laboratory, in NIDA, and for the opportunity to learn from some of the best scientists I know. Including Dr. Christopher Richie who shared his expertise and gave me the great opportunity to learn molecular biology methods.

The current and former colleagues of the Division of Pharmacology and Pharmacotherapy are warmly thanked for their help during all these years. Particularly, Juho-Matti, Johanna, and Sakari, I appreciate our scientific and not so scientific discussions over the years. I would like to express my gratitude to laboratory technicians Susanna Norrbacka and Kati Rautio. I would especially like to thank Kati Rautio, without her, I would still most likely be doing sectioning.

It goes without saying that my warmest appreciation belongs to all past and present members of Myöhänen research group and the Department of

Pharmacology for making this such a great place to work. Moreover, to Katrina, Jenni, Emmi, FNC, and Anna-Maija for our 'Wine Tuesdays'. I greatly appreciate your friendship and the positive environment that you have created.

I would also like to thank all my friends from other science departments and outside the world of science for continuous encouragement and most importantly all the free time activities from dinners and late-nights, to travels and networking activities. Klaus, Dr. Rodrigo, Katia, and Dr. Miguel, Janis, Elina, and Dace, I am lucky to have so many great friends around me. Especially, I want to thank my best friend Dr. Yajie Zhao for shared passions, company, and for being like a family member.

I am grateful to my parents Inguna and Arijs, my sister Made and her family for their unconditional support in all phases of my life. Finally, I am deeply grateful to my beloved partner Dr. Li Liao, whose support and encouragement has been irreplaceable during this process. You mean the world to me.

Helsinki, December 2018

Reinis Svarcbahs

CONTENTS

LIST OF ORIGINAL PUBLICATIONS

This thesis is based on the following publications:

I Svarcbahs R, Julku UH, Norrbacka S, Myöhänen TT (2018) Removal of prolyl oligopeptidase reduces alpha-synuclein toxicity in cells and *in vivo*. Scientific Reports 8:1552.

II Svarcbahs R*, Julku UH*, Myöhänen TT (2016) Inhibition of Prolyl Oligopeptidase Restores Spontaneous Motor Behavior in the α-Synuclein Virus Vector–Based Parkinson's Disease Mouse Model by Decreasing α-Synuclein Oligomeric Species in Mouse Brain. The Journal of Neuroscience 36:12485-12497. *equal contribution

III Svarcbahs R, Jäntti M, Julku UH, Chavero M, Urvas L, Norrbacka S, and Myöhänen TT. Prolyl oligopeptidase is a novel regulator for protein phosphatase 2A (submitted).

The publications are referred to in the text by their roman numerals. Supplementary results are also presented for the III study. Reprints were made with the permissions of copyright holders.

ABBREVIATIONS

AAV	adeno-associated virus
AD	Alzheimer's disease
ALP	autophagy-lysosome pathway
aSyn	α-Synuclein
Atg	autophagy related
B55α	PP2A 55 kDa regulatory subunit B alpha
bcl2	B-cell lymphoma 2
bcl-xL	B-cell lymphoma-extra large
BL	baseline
cas9	CRISPR associated protein 9
CMA	chaperone-mediated autophagy
coIP	co-immunoprecipitation
CRISPR	clustered Regularly Interspaced Short Palindromic Repeats
DAPK	death-associated protein kinase
DCFDA	2',7'-dichlorofluorescin diacetate
DMSO	dimethyl sulfoxide
GAP-43	growth associated protein 43
GAPDH	glyceraldehyde 3-phosphate dehydrogenase
GFP	green fluorescent protein
GLuc	Gaussian princeps luciferase
HEK-293	human embryonic kidney cells
Hsc70	heat shock cognate 71 kDa protein
ICC	immunocytochemistry
IHC	immunohistochemistry
JNK1	c-Jun N-terminal kinase 1
Lamp2a	lysosome membrane protein type 2A
LB	Lewy body
LBD	Lewy body disease
LC3II	microtubule-associated protein 1 light chain 3
LPS	lipopolysaccharides
mTOR	the Mammalian target of rapamycin
MTT	3-(4,5-dimethylthiazol-2-yl)-2,5-diphenyl-tetrazolium bromide
NBR1	next to BRCA1 gene 1 protein
OD	optical density
p62	sequestosome 1/ubiquitin-binding protein p62
PBS	phosphate-buffered saline
PFA	paraformaldehyde
PCA	protein-fragment complementation assay
PD	Parkinson's disease
PME1	protein phosphatase methylesterase 1
PP2A	protein phosphatase 2A

PP2Ac	PP2A catalytical subunit
PREP	prolyl oligopeptidase
PREPko	prolyl oligopeptidase knockout
PK	proteinase K
p-S129	phosphorylated Serine-129
PTPA	protein phosphatase 2 phosphatase activator
ROS	reactive oxygen species
SDS	sodium dodecyl sulfate
SIAH	seven in absentia homolog
SN	substantia nigra
SNARE	soluble N-ethylmaleimide-sensitive factor activating receptor
SNpc	substantia nigra pars compacta
TBS-T	tris-buffered saline with 0.05% Tween-20
TH	tyrosine hydroxylase
TH+	tyrosine hydroxylase positive
ULK1	unc-51-like kinase 1
UPS	ubiquitin proteasomal system
VPS34	vacuolar protein sorting 34
WB	western blot
wt	wild-type

1 INTRODUCTION

Synucleinopathies are a subset of neurodegenerative disorders that are characterized by the accumulation of α-synuclein (aSyn) inclusion bodies in neurons, neuronal projections, and glial cells. Parkinson's disease (PD), Lewy body disease (LBD), and multiple system atrophy cause multisystem failure due to aSyn accumulation that is followed by a progressive loss in neuronal functions and death of the affected cellular subpopulations. Additionally, aSyn accumulation has been described in Alzheimer's disease (AD) cases. Progression of the aforementioned conditions are slow, while in most cases the cause of disease is idiopathic as the disease origin cannot be traced to a known cause or a certain mechanism (Crews et al., 2009; Beitz, 2014; McCann et al., 2014; Barker and Williams-Gray, 2016). Neurodegenerative disorder prevalence increases with the passage of an individual's years. With an increasingly ageing population the need for curative treatments will only become more acute as currently available therapies are aimed at palliative treatments and fail to address the need for reduction of pathological aSyn burden on the affected cellular processes.

The accepted PD pathophysiological mechanism is that the loss of or aberrations in the dopaminergic neurons leads to depletion of dopamine in the striatal dopaminergic projections. Consequently, synaptic failure due to insufficient dopamine signaling is the major cause of the motor symptoms bradykinesia, postural instability, rigidity, and tremor (George et al., 2013). While pathological identification of PD is based on the presence of Lewy bodies (LB) in the affected brain regions the consensus of whether LBs influence neuronal cell death or is a protective mechanism that sequesters harmful aSyn intermediary species has not been reached (Schulz-Schaeffer, 2010). However, recent reports are contesting the widely held notion of direct causality between LBs and neuronal loss (Milber et al., 2012; Iacono et al., 2015).

Presently, dysfunction in the protein degradation machinery, ubiquitin-proteasomal system (UPS), or autophagy-lysosomal pathway (ALP) has been implicated as one of the causes in most of the proteinopathies and has a distinctive role in the processing and aggregation of aSyn. Activation of these systems has been studied as a potential drug target that would potentially alleviate aSyn aggregate accumulation (Ebrahimi-Fakhari et al., 2012). One of the potential drug targets capable of reducing autophagy is prolyl oligopeptidase (PREP), a serine protease (Savolainen et al., 2014) that has been shown to directly interact with aSyn and increase aSyn aggregation rate (Brandt et al., 2008; Savolainen et al., 2015).

This literature review focuses on the aSyn pathophysiology, namely aSyn aggregate clearance and processing by the two major protein degradation systems and discusses the effects of aSyn post-translational modification on

these pathways. The experimental part of the thesis will describe the role of PREP or lack thereof on the aSyn aggregation process both in cellular and in *in vivo* models. PREP inhibition will be discussed as a potential treatment for synucleinopathies. Lastly, a new physiological role of PREP and its implication on the protein phosphatase 2A (PP2A) cellular network will be described.

2 REVIEW OF THE LITERATURE

2.1 Brief overview on alpha-synuclein

aSyn is a 14 kDa large protein with a lysine-rich N-terminus, which is important for the interactions with lipid membranes, while the C-terminus is intrinsically disordered and has been suggested to modulate aSyn's nuclear localization and interaction with proteins and small molecules (Ulmer et al., 2005; Uversky and Eliezer, 2009). Under native conditions aSyn predominantly exists in a monomeric state (Eliezer et al., 2001) but, in recent years, researchers have demonstrated possible existence of a tetrameric aSyn that under physiological conditions resists aggregation (Eliezer et al., 2001; Dettmer et al., 2016).

aSyn was initially identified from the electric ray neuronal tissue and immunostaining was predominantly observed in the synaptic and nuclear regions, hence the name of the protein (Maroteaux et al., 1988). aSyn was later linked to the β-amyloid inclusions and initially called non-β-amyloid-component of AD (Ueda et al., 1993). Shortly afterwards, the distinction between the alpha and beta isoforms of synuclein was identified (Jakes et al., 1994) and ten years later it was demonstrated that aSyn is not an essential protein as double knock-out of both aSyn isoforms does not result in animal lethality (Chandra et al., 2004). Currently, the physiological functions of aSyn are not fully understood (Lashuel et al., 2012). However, its predominant localization in synapses (Iwai et al., 1995), presence in the distal pool of synaptic vesicles (Kahle et al., 2000b; Lee et al., 2008b), and role in the SNARE (soluble N-ethylmaleimide-sensitive factor activating receptor) complex assembly points to a role for aSyn in neurotransmitter release, synaptic plasticity, and synaptic exocytosis (Burre et al., 2010). This is supported by studies in aSyn knockout animals and after aSyn overexpression where changes in activity-dependent dopamine release are seen (Abeliovich et al., 2000; Yavich et al., 2004; Scott et al., 2010).

2.1.1 aSyn aggregation overview

The identification of aSyn as a major component of LB and Lewy neurites that are the main hallmarks of PD and other synucleinopathies prompted large interest in aSyn research (Spillantini et al., 1997; Spillantini et al., 1998). Especially, when familial cases of duplications (Chartier-Harlin et al., 2004), triplications (Singleton et al., 2003), and point mutations (Polymeropoulos et al., 1997; Kruger et al., 1998; Zarranz et al., 2004) of the *SNCA* gene were linked to early onset PD and the onset of the disease was inversely correlated to the number of *SNCA* repeats (Fuchs et al., 2007). Even though there is support for the idea that accumulation of aSyn propagates pathology, a

viewpoint has also emerged that aSyn aggregation can sequester physiologically active aSyn that in turn leads to the loss-of function toxicity (Perez and Hastings, 2004; Cookson, 2006; Kanaan and Manfredsson, 2012).

Pathologically, LBD is characterized by the accumulation of aSyn that results in the degeneration of the nigrostriatal tract, neocortical and limbic brain areas (Braak and Braak, 2000; Vekrellis et al., 2011; Lashuel et al., 2013). PD is by far the most prevalent LBD that is characterized by the degeneration of the dopaminergic neurons in the *substantia nigra pars compacta* (SNpc), however, selective vulnerability of the dopaminergic neurons is not well known (Braak and Braak, 2000). Nevertheless, there is a growing evidence that supports aSyn oligomerization and fibrillation as a leading cause of PD development (Conway et al., 1998; Narhi et al., 1999; Tsigelny et al., 2012). Which species of aSyn are toxic has been widely debated and evidence links either fibrillary forms (Trojanowski and Lee, 1998) or intermediate soluble oligomer aSyn species (Conway et al., 2000) as being the most toxic. Specific aSyn mutations that favor aSyn oligomerization instead of fibrillization have been linked to increased toxicity. This is most likely due to higher affinity to associate with membranes (Karpinar et al., 2009; Winner et al., 2011; Rockenstein et al., 2014), impact receptor activation (Diogenes et al., 2012), mitochondrial function (Luth et al., 2014), SNARE complex assembly and subsequent dopamine release (Choi et al., 2013).

Accordingly, synaptic dysfunction due to small aSyn aggregate accumulation at the synapses as a reason for the early symptoms of PD and related synucleinopathies is quite plausible (Kramer and Schulz-Schaeffer, 2007; Schulz-Schaeffer, 2010). Likely, the overt neuronal loss of dopaminergic neurons is preceded by the disturbances in the synapse, where loss of function (Collier et al., 2016; Dettmer et al., 2016) or gain of toxicity (Tsigelny et al., 2012) of aSyn could elicit dual toxic effects due to aSyn accumulation into the aggregates that lack functional properties. However, consensus about the exact nature of aSyn toxicity has not been reached (Benskey et al., 2016; Collier et al., 2016; Villar-Pique et al., 2016).

2.2 Ubiquitin-proteasome system and autophagy-lysosomal pathway

The UPS and the ALP are the main protein degradation pathways that are responsible for the removal of misfolded and damaged proteins as well as protein aggregates [Fig. 1] (Rubinsztein, 2006). The UPS is responsible for the degradation of the majority of the proteins, approximately 80-90%, including short lived and damaged substrates (Rock et al., 1994). Then again, autophagy is mostly responsible for the degradation of long-lived, aggregated proteins and organelles (Lilienbaum, 2013). These degradation systems work in tandem to not only degrade proteins into polypeptides, but also to maintain

the energy equilibrium during starvation. Besides, aforementioned pathways are involved in the control of protein quality (Lilienbaum, 2013).

Many, if not all, of the neurodegenerative proteinopathies and their toxic effects can be at least in part attributed to the damaged or hampered protein degradation pathways (Rubinsztein, 2006), and aSyn linked pathology is not an exception. Aggregation of aSyn is accompanied by autophagic, proteasomal, and lysosomal alterations. Even though it is not fully understood how aSyn clearance is divided among different degradation pathways there are factors that contribute to the partition of aSyn clearance. The most studied changes affecting aSyn clearance are the folding state, post-translational modifications, localization, oligomer forms, and solubility (Martinez-Vicente and Vila, 2013). Nevertheless, ageing could be considered the greatest risk of PD development as all the cellular mechanisms that are affected in the normal ageing are affected in PD, including aberrations in the UPS and ALP. The only difference is the rate of the deterioration of protein degradation systems (Collier et al., 2011). In the subsequent chapters, I will briefly discuss machinery regulating the UPS and ALP, and how these pathways are involved in aSyn processing both during the basal state and during the pathological formation of aSyn inclusions and aggregates.

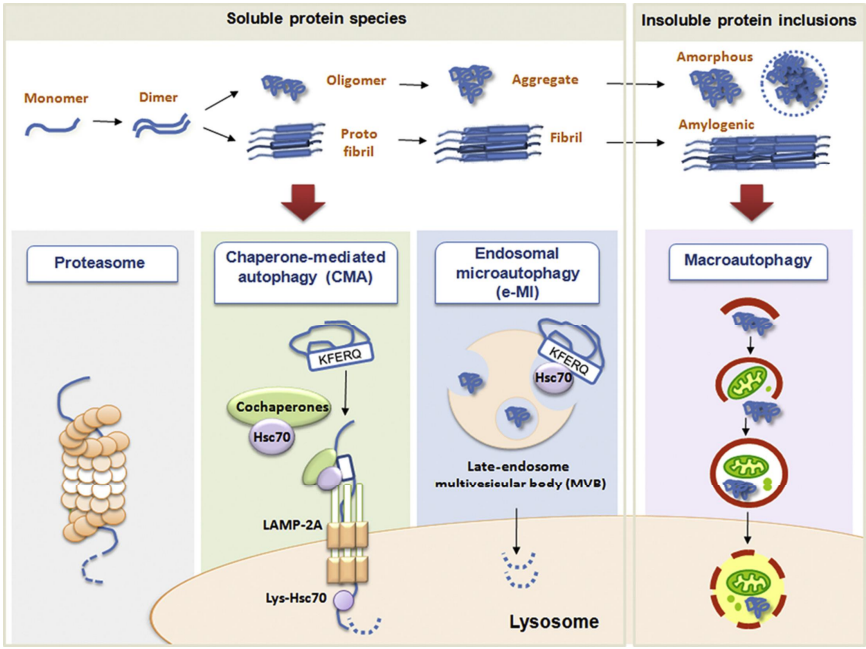

Figure. 1 Schematic representation of proteasomal system and autophagy role in the degradation of aggregation prone proteins. aSyn under physiological conditions is in a monomeric state, however, dimerization and subsequent formation of oligomers and protofibrils, aggregates, fibrils and insoluble amorphous and amylogenic inclusions can occur. Different parts of the protein degradation system are responsible for the proteolysis of these protein species. Methods in Enzymology, Vol. 588, Tan and Wong, Kinetics of Protein Aggregates Disposal by Aggrephagy, Pages 245-281., copyright (2017), with permission from Elsevier.

2.2.1 Role on the proteasomal system in protein degradation

The UPS functions by covalently binding ubiquitin with proteins that are aimed for degradation. Ubiquitin is linked to the lysine residues of the substrate by ubiquitin activating (E1), conjugating (E2), and ligating (E3) enzymes (Hershko et al., 1983), and this process is repeated multiple times to create a polyubiquitin chain (Chau et al., 1989). If the polyubiquitinated substrate is intended for the 26S proteasomal degradation, then ubiquitin is covalently bound by a K48 residue. These K48 chains are recognized as a canonical signal that sequesters mostly short-lived proteins for 26S proteasomal degradation (Chau et al., 1989; Xu et al., 2009). Polyubiquitylated proteins are then degraded by the 26S proteasomes (Fig. 2A), which is a large protease complex that consists of a proteolytic core (20S) and two 19S regulatory units (called PA700 in mammals). The entrance of the 20S unit can be opened up by an array of proteasomal regulatory complexes: PA28, PA200, and PA700 that confer the conformational changes to the 20S subunit (Rechsteiner and Hill, 2005; Stadtmueller and Hill, 2011). Only PA700 is able to remove the polyubiquitin conjugates from the protein prior to degradation (Lim and Tan, 2007).

However, ubiquitin has seven lysine residues, and modifications at either of these residues are targeting proteins for a different fate that not necessarily means degradation (Pickart and Fushman, 2004). A fairly recent study has shown that all ubiquitin modifications at lysine residues apart from K63 can at least partially send proteins for the 26S degradation as shown by mass-spectrometry analyses after the proteasomal inhibitor treatment (Xu et al., 2009). Additionally, it has been shown that a single K48 substitution is lethal in yeast (Finley et al., 1994), while substitution of up to four of the lysine residues other than K48 in yeast can produce aberrant yet viable cells (Xu et al., 2009). Nevertheless, ubiquitination is not necessarily required for proteasomal degradation (Liu et al., 2003). It has become apparent that both 26S and 20S can degrade different pools of the same protein in a non-selective manner by either 20S or 26S, however (Fig. 2B), the primary requirement of ubiquitin-independent degradation is the presence of an unstructured region in the substrate (Liu et al., 2003; Asher et al., 2005).

2.2.2 aSyn processing by proteasomal system

It has been a long-held notion that for a protein to be degraded via 26S the proteasome substrate has to be conjugated with at least 4 ubiquitin molecules (Hicke, 2001). Around at the same time, it was demonstrated that *in vitro* native aSyn is degraded by purified 20S proteasomes. Besides, proteasomal inhibition in neuroblastoma cells did not increase accumulation of the ubiquitinated aSyn forms (Tofaris et al., 2001). While the most abundant forms of aSyn in LBs are monoubiquitinated and to a lesser extent biubiquitinated, approximately 10% of the total aSyn in LBs is unmodified (Hasegawa et al., 2002; Tofaris et al., 2003; Anderson et al., 2006). Liu et al.

(2003) later showed that latent 20S proteasomes are able to digest substrates with natively disordered regions. This observation provided compelling evidence that aSyn does not exclusively require ubiquitination to be targeted for UPS degradation.

Several E3 ligases are able to ubiquitinate aSyn (Chung et al., 2001; Liani et al., 2004; Shin et al., 2005; Mulherkar et al., 2009; Tofaris et al., 2011). Recent evidence in cell free conditions have showed that monoubiquitinated aSyn is degraded by 26S proteasomes (Shabek et al., 2012) but the extent of the degradation is dependent on the ubiquitin ligation site on aSyn. Notably, the N-terminal lysine ubiquitination was shown to correlate with increased aSyn degradation by proteasomes, while modification at the middle of aSyn did not increase the protein degradation (Abeywardana et al., 2013). Interestingly, the monoubiquitinated aSyn has been shown to exhibit differences in the rate of aSyn aggregate formation (Meier et al., 2012). aSyn monoubiquitinated at lysine residues (K12, K21, and K23) has been shown to be present in LBs (Anderson et al., 2006) and show similar fibril formation capacity to that of native aSyn protein or decreased fibril formation rate and aggregation in to small aggregates if modified at K12 and K21 (Meier et al., 2012).

Perhaps the best-known ligase associated with aSyn is parkin. Its deficiency has been associated with the accumulation of a rare form of O-glycosylated aSyn in parkin-deficient PD patient brains. A particular aSyn modification was shown to be a substrate for the parkin ligase while native aSyn is not ligated by parkin (Shimura et al., 2001). Interestingly, O-glycosylated aSyn was not detected in the transfected human embryonic kidney (HEK-293) or neuroblastoma SH-SY5Y cells and thus could be a specific modification present only in the parkin-deficient PD patient brains (Chung et al., 2001). It was not surprising that the first reported familial mutation that was linked to the UPS was in Parkinson protein 2, E3 ubiquitin protein ligase gene (*PRKN2* or *PARKIN*). This familial mutation causes juvenile PD (Kitada et al., 1998), and later many other gene mutations in *PRKN2* gene (Khan et al., 2003), and for example, a gene coding for ubiquitin C-terminal hydrolase isozyme L1 was linked to early onset PD (Leroy et al., 1998).

So far, a set of different ligases have been shown to ligate aSyn and the monoubiquitination of aSyn has been detected at seven different lysine residues of aSyn (Nonaka et al., 2005; Rott et al., 2008). For example, E3 ubiquitin-ligases SHIA1 and SHIA2 (seven in absentia homolog) are able to ubiquitinate native aSyn *in vitro* (Liani et al., 2004). The effect was corroborated by two independent research groups in cell models (Lee et al., 2008a; Rott et al., 2008). Moreover, SIAH binds and ubiquitinates aSyn binding protein, synphilin-1 (Liani et al., 2004). Synphilin-1 is a major component of LBs (Wakabayashi et al., 2000) and can as well be ubiquitinated by parkin. Notably, overexpression of both aSyn and synphilin-1 is required for the LB-like inclusions to be ubiquitinated by parkin (Chung et al., 2001).

While aforementioned ligases are associated with native aSyn modification, E6 associated protein has been shown to sequester aSyn oligomer forms (Mulherkar et al., 2009) and Hsp70-interacting protein preferentially recognizes and mediates degradation of toxic oligomers (Tetzlaff et al., 2008) either via proteasomal or lysosomal degradation (Shin et al., 2005). Additionally, E3 ubiquitin-protein ligase is involved in the ubiquitination of aSyn but due to the modification occurring on the K-63 residue it is believed that aSyn is targeted to lysosomal degradation (Tofaris et al., 2011).

Not only aSyn ubiquitination enzymes are conferring aSyn toxicity but it has also emerged that alteration in deubiquitinase USP9X levels modulates aSyn monoubiquitination levels. USP9X activity retains aSyn in cells, thus pointing to the more favorable degradation of monoubiquitinated aSyn via proteasomes as opposed to the lysosomal pathway. Upon proteasomal impairment, USP9X decreases monoubiquitinated aSyn and subsequent inclusion formation (Rott et al., 2011). It is supported by the observation that SIAH-1-mediated aSyn ubiquitination promotes aggregation and toxicity (Lee et al., 2008a). Another deubiquitinase, ubiquitin specific peptidase 8 (USP8), has been implicated in the pathology of aSyn processing, as it has been shown that increased activity of USP8 retains cellular aSyn (Alexopoulou et al., 2016). To add another layer of complexity to aSyn ubiquitination, the ubiquitin-related conjugating system of small ubiquitin-like modifiers (SUMO) has been shown to act as an aSyn ubiquitination inhibitor. PIAS2 (protein inhibitor of activated STAT 2) was shown to inhibit aSyn ubiquitination by both SIAH-2 and E3 ubiquitin-protein ligase ligases. Besides, accumulation of SUMOylated proteins have been detected in PD and LBD brains (Rott et al., 2017).

2.2.3 aSyn aggregation and its role on the proteasomal system

Ubiquitinated protein inclusions have been observed in an array of neurodegenerative diseases including LBD (Lowe et al., 1988). Additionally, primary dopaminergic tyrosine hydroxylase positive (TH+) cells confer high vulnerability to UPS alterations, and parkin overexpression was demonstrated to at least partially rescue dopaminergic neurons from A53T aSyn overexpression and proteasomal inhibition (Petrucelli et al., 2002). Loss of proteasomal subunits and impaired proteasomal activity in sporadic PD patients are almost exclusively restricted to the substantia nigra [SN] (McNaught et al., 2002; St. P. McNaught et al., 2003). While Chu et al. (2009) have shown that 20S proteasome staining intensity in nigral neurons are decreased only in the neurons harboring inclusions.

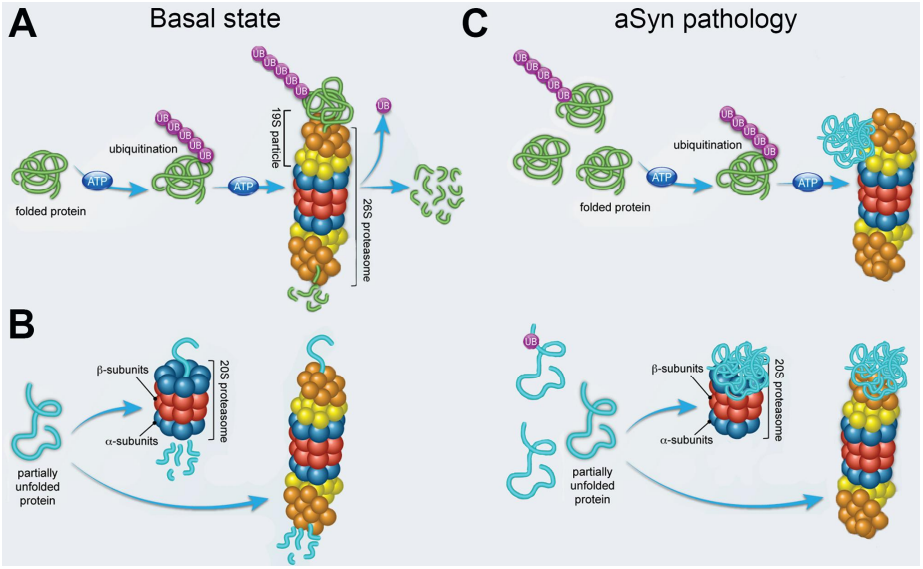

Figure. 2 Representation of the proteasomal degradation pathway under the physiological conditions and in case of synucleinoapathies. (**A**) the 26S proteasomal degradation pathway processes short-lived, damaged proteins. This ATP-dependent process requires substrate conjugation with a ubiquitin chain in order to be recognized and degraded by the 26S proteasome. (**B**) 26S and 20S proteasomal degradation is possible independently of ATP and ubiquitin conjugation for proteins that contain an unstructured region. (**C**) aSyn aggregates and fibrils can directly bind proteasomes and inhibit protein degradation. Adapted from: Ben-Nissan G, Sharon M (2014) Regulating the 20S Proteasome Ubiquitin-Independent Degradation Pathway, Biomolecules 4(3):862-884. Distributed under the Creative Commons Attribution License (CC BY 3.0).

Inclusion formation *in vivo* is enhanced by the pharmacological inhibition of proteasomes. Proteasomal inhibitor injections into the medial forebrain bundle results in widespread proteasomal inhibition in the SN and subsequent accumulation of LB like inclusions and motor impairment in mice (Xie et al., 2010). A similar effect can be achieved by conditionally deleting the 26S protease regulatory subunit 4 without affecting the activity of 20S proteasomes. In the affected brain areas, researchers reported LB-like accumulation, substantial neuronal degeneration, and motor deficits characteristic of PD (Bedford et al., 2008). When considering the familial PD form, *SNCA* triplication, the Singleton et al. (2003) report shows an extensive LB formation in the affected individuals, thus at least indirectly pointing to the increased and pathological aSyn ubiquitination.

aSyn overexpression models in cells (Tanaka et al., 2001; Petrucelli et al., 2002) and in animals (Chen et al., 2006b) have shown that aSyn accumulation has an inhibitory effect on proteasomes (Fig. 2C). Interestingly, the familial form of A53T aSyn mutant is more toxic to the UPS (Stefanis et al., 2001) as it is degraded slower than native aSyn (Bennett et al., 1999). Soluble aSyn oligomers and insoluble filaments have been shown to inhibit chymotrypsin-like activity of 20S proteasomes with β-amyloid like structures being

important for the inhibitory activity (Lindersson et al., 2004). In another study, aSyn aggregates have been shown to bind and inhibit 26S ubiquitin-dependent and ubiquitin-independent protein degradation in HEK-293 cells (Snyder et al., 2003). A recent study by Thibaudeau et al. (2018) has yielded a common UPS inhibitory feature shared by oligomers related to PD, AD, and Huntington's disease where soluble oligomers were shown to inhibit the 20S subunit by an allosteric stabilization of the closed gate conformation of the 20S core enzyme. In the particular study, the aforementioned disease oligomer fractions that could inhibit the 20S subunit were immunoreactive against an oligomer specific antibody (A11) that has been described in detail by Kayed et al. (2003). This inhibitory effect was achieved by impairing a HbYX motif that is required for the binding and activation of the 20S subunit by many of the proteasomal regulators (Thibaudeau et al., 2018). Emmanouilidou et al. (2010) had earlier demonstrated that intermediate aSyn oligomer species can inhibit 26S proteasomal activity and that this inhibitory effect was lost when pharmacological dissociation of aSyn oligomers was performed.

2.3 Autophagy-lysosomal pathway

There are three major types of the ALP: macroautophagy, microautophagy, and chaperone-mediated autophagy (CMA). Among them, macroautophagy is responsible for degradation of majority of the proteins, especially during starvation (Mizushima et al., 2002). Even though substrate recognition differs among these three autophagy types, lysosomal degradation is an important feature shared by them all. Neurons are especially reliant on the proper autophagic function. The brain is very often the most affected organ as deleterious mutations in genes linked to the ALP and lysosomal disorders are often reported in neurodegenerative disorders (Nixon, 2013). In the subsequent chapters, I will briefly discuss all three autophagy types and how each of them is involved in aSyn degradation and pathology.

2.3.1 Chaperone-mediated autophagy (CMA) core machinery

CMA (Fig. 3A) is initiated when heat shock cognate 71 kDa protein (Hsc70) recognizes specific amino acid sequences on damaged proteins and chaperones designated proteins to the lysosome (Chiang et al., 1989). Hsc70 and the substrate binds to the lysosome membrane protein type 2A (Lamp2a) receptor that is located on the lysosomal membrane (Cuervo and Dice, 1996), thereafter the substrate is unfolded, most likely by Hsc70 (Salvador et al., 2000). For a substrate to be degraded, Hsc70 disassembles from the substrate in an ATP-dependent manner. Then, the substrate-Lamp2a complex binds more Lamp2a molecules to create a multimer-Lamp2a complex, as monomeric Lamp2a lacks the ability to translocate the substrate across the lysosomal membrane (Bandyopadhyay et al., 2008). Importantly, binding to

Lamp2a is the time limiting step in the CMA (Cuervo and Dice, 1996). CMA is considered to be the main catabolic pathway for oxidized, misfolded, damaged, and aggregation prone proteins and is severely impaired during ageing (Kiffin et al., 2004).

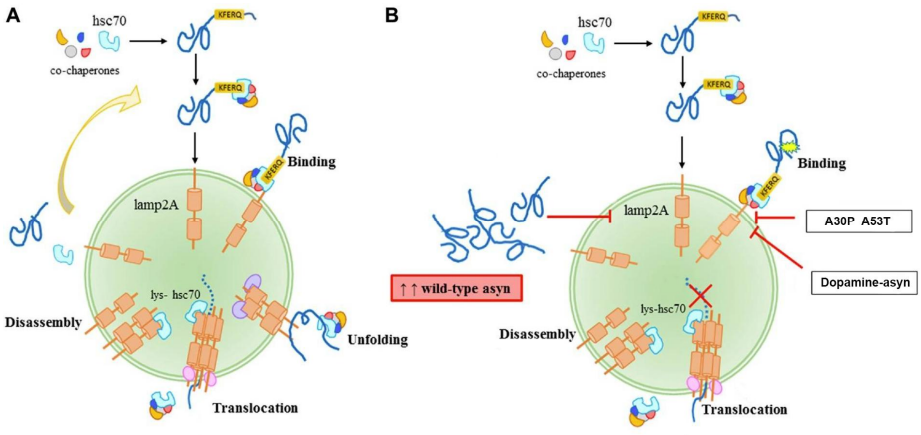

Figure. 3 CMA under physiological conditions and in case of the aSyn accumulation and PD. (**A**) CMA mediates wild-type aSyn degradation under basal conditions. (**B**) CMA mediated aSyn degradation is impaired in synucleinopathies. Increased amount of wild-type aSyn can block CMA due to excess of substrate. Familial aSyn forms (A30P and A53T), as well as post-translational modifications (aSyn dopamine modification), have been shown to inhibit Lamp2a protein due to high binding affinity that blocks degradation of native Lamp2a substrate. Adapted from: Sala G, Marinig D, Arosio A and Ferrarese C (2016) Role of Chaperone-Mediated Autophagy Dysfunctions in the Pathogenesis of Parkinson's Disease. Front. Mol. Neurosci. 9:157.Distributed under the Creative Commons Attribution License (CC BY 4.0).

2.3.2 Role of CMA in aSyn clearance

Native aSyn contains KFERQ CMA recognition motif that, during basal conditions, directs aSyn for CMA dependent degradation (Cuervo et al., 2004). Even though primary aSyn degradation in the ALP pathway functions via CMA pathway upon stressful stimuli, excessive aSyn protein burden can be directed to macroautophagy dependent aSyn degradation (Xilouri et al., 2009). This seminal work highlighted the impact of aSyn on the CMA rate-limiting step: aSyn binding to Lamp2a. Notably, familial forms of aSyn, A30P and A53T, were shown to associate with lysosomal membrane receptor Lamp2a (Fig. 3B) without being translocated into the lysosome, thus in effect working as an inhibitor of Lamp2a receptors (Cuervo et al., 2004). *In vivo*, co-overexpression of wild-type (wt) aSyn and Lamp2a in the rat nigrostriatal tract has been show to ameliorate aSyn protein load, and decrease phosphorylated and sodium dodecyl sulfate (SDS) soluble aSyn levels. Noticeably, the diffuse distribution pattern of aSyn observed after aSyn overexpression was lost when aSyn was co-expressed together with Lamp2a. This study showed that increasing CMA activity by manipulating the rate-limiting step in CMA

mediated flux of wt aSyn most likely due to decrease in total monomeric aSyn levels (Fig. 3B) as well as by decreasing CMA-related protein accumulation due to CMA-inhibitory aSyn oligomer/post-translational modifications (Xilouri et al., 2013). Inversely, downregulation of Lamp2a with virus vectors expressing short hairpin RNAs targeting Lamp2a resulted in accumulation of aSyn puncta and substantial dopaminergic neuron loss in SNpc (Xilouri et al., 2016).

These observations would be in line with previous reports, of post-translationally modified aSyn (phosphorylated, ubiquitinated, nitrated, and oxidized) having a decreased degradation rate via CMA (Fig. 3B). Importantly, while the above-mentioned aSyn modifications are less susceptible for CMA degradation, dopamine modified aSyn was demonstrated to act similarly to mutated aSyn and inhibit other CMA-related protein degradation. Consequently, dopaminergic neuron vulnerability could be partially attributed to cellular presence of dopamine (Martinez-Vicente et al., 2008). Dopamine modified aSyn was shortly thereafter shown to have an altered conformation with the C- and N-terminal portions of aSyn positioned in close proximity that led to decreased fibrillation (Outeiro et al., 2009). These conformational changes could lead to the shift in aSyn favoring oligomeric species formation as opposed to fibrils. Nevertheless, oligomer species-related toxicity was not observed in the SH-SY5Y neuroblastoma cell line after 24-hour treatment, but it could not be excluded that in a more physiological setting aggregates could be potentially harmful (Yamakawa et al., 2010). Although aSyn's inhibitory effect on the CMA is partially ablated by upregulation of the bulk autophagy under basal conditions, this effect cannot be entirely reversed under oxidative stress conditions. Lamp2a downregulation confers increased sensitivity to oxidative stress (Massey et al., 2006) and at least in SH-SY5Y cells macroautophagy has been shown to exacerbate neuronal cell loss after CMA inhibition. However, this neuronal cell loss most likely correlates with an increase in autolysosome formation. In the case where autophagosome formation exceeds lysosomal capacity to degrade autophagosomes, cargo accumulation in the aforementioned autophagosomes has been suggested as a possible cause of neuronal toxicity after CMA inhibition (Xilouri et al., 2009).

Interestingly, aSyn accumulation and ensuing blockage of CMA leads to decreased binding between protein myocyte enhancer factor 2D (MEF2D) and Hsc70. MEF2D is an essential transcription factor for neuronal survival and upon CMA inhibition the inactive form of it accumulates in the cytosol. PD brains contain increased levels of the inactive protein that is not capable to bind DNA and sustain neuronal survival signals (Yang et al., 2009). Additionally, in the case of PD pathology, Lamp2a and Hsc70 levels are decreased in *post-mortem* PD brains (Alvarez-Erviti et al., 2010). Increased aSyn levels and decreased Hsc70 protein levels in early sporadic PD patients correlate with ablated Lamp2a protein levels and aberrations linked to the CMA protein degradation proceed those seen in late PD (Murphy et al., 2015). Additionally, researchers have reported an increase in microtubule-associated protein 1 light chain 3 (LC3II) levels (Alvarez-Erviti et al., 2010), however, in

this case interpretation of induced autophagy in PD patients' *post-mortem* brains should be taken with caution. Increase in LC3II levels alone without verification of other autophagy markers and structure of autophagosomes could as well be an indicator of the cumulative inhibition in bulk autophagy and lysosomal dysfunction (Spencer et al., 2009).

2.3.3 Macroautophagy core machinery

In literature, macroautophagy and autophagy are used synonymously and hereafter in the text will be referred to as autophagy. Under physiological conditions basal autophagy is low, however, under stress and external stimuli cells can upregulate autophagy very fast. Autophagy is mainly initiated through inhibition of the mammalian target of rapamycin (mTOR) signaling pathway, although the autophagic flux can also be activated via indirect activation of the vacuolar protein sorting 34 (VPS34)-beclin1 complex which is independent of mTOR (He and Klionsky, 2009; He and Levine, 2010). Autophagy is an important ALP that is responsible for bulk degradation of cytoplasmic and aggregated proteins. Autophagic degradation is initiated by the formation of an isolation membrane that engulfs a portion of the cytoplasm around the substrate. After the completion of a double-layer autophagosome, the outer membrane of the newly formed vesicle is fused to the lysosome. This process is considered non-selective as it degrades proteins, their aggregates, and organelles (Mizushima et al., 2002). However, the initial idea that autophagy is non-selective can be attributed only to a small fraction of cellular processes arising from the studies with starved yeast cells. Mammalian or yeast cells that are under duress of stress, caused by nutrient shortage, consequently recycle cellular components to compensate for the lack of nutrients. In this specific example, it is believed that autophagy is somewhat non-selective. Nevertheless, autophagy is essential for the homeostatic processes within the cell, and non-starved cells will non-selectively degrade components of the cytosol, including damaged mitochondria, peroxisomes, invading pathogens, as well as protein aggregates (Zaffagnini and Martens, 2016). Selectivity of the autophagic processes was proven with the discovery of the autophagy receptors, for example, p62 (sequestosome 1/ubiquitin-binding protein p62) and NBR1 (next to BRCA1 gene 1 protein). p62 and NBR1 have been shown to preferentially sequester aSyn aggregates for autophagy-dependent degradation and are able to recognize both ubiquitinated substrates and cargo recognition elements on the inner side of the autophagosome LC3II (Watanabe et al., 2012; Shaid et al., 2013).

The autophagy core machinery is mediated by approximately 36 autophagy-related (Atg) proteins that have largely been identified via yeast studies. Three core protein complexes and their subsequent interactions can be used to describe initiation and formation of autophagy (Fig. 4). Initiation of bulk autophagy requires assembly of ULK1 (unc-51-like kinase 1) complex consisting of ULK1/2 (Atg1 in yeast), Atg13, FIP200 (focal adhesion kinase

family interacting protein of 200 kDa; Atg17 in yeast), and ATG101 that is exclusively found in eukaryotic cells. After autophagy activation, ULK1/2 complex translocates to the pre-autophagosomal structure (site of autophagosome formation) in the yeast or omegasome/cradle in mammals where it recruits a second (VPS34) core complex. VPS34 consists of phosphoinositide 3-kinase catalytical subunit Vps34 that in turn forms a complex with the protein kinase Vps15 and beclin1 (Atg6 in yeast). Subsequently, Vps34 forms an autophagy specific complex with Barkor (beclin 1-associated autophagy-related key regulator; ATG14).

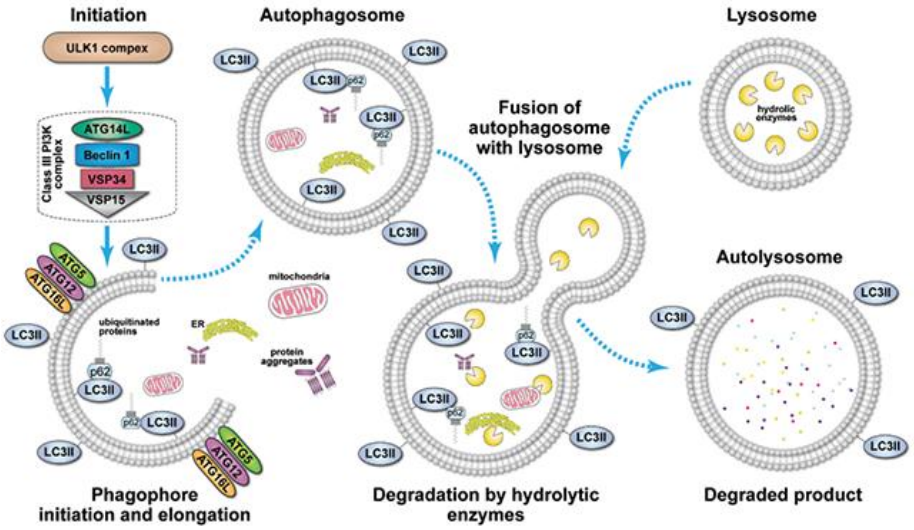

Figure. 4 Initiation of bulk autophagy starts by assembly of ULK1 after input from various kinase pathways and environmental cues. ULK1 translocates to an omegasome or pre-autophagosomal structure and recruits the VPS34 core complex. The Atg12-Atg5-Atg16L1 and LC3II conjugation systems promote the elongation of the phagophore and closure of the autophagosome. Autophagy receptors p62 sequester ubiquitinated proteins and binds to the lipidated LC3II at the inner phagophore side. After closure of autophagosome, it fuses with a lysosome. The newly formed autolysosome contains hydrolytic enzymes from lysosome that degrades autophagy cargo. Adapted from: Ndoye A and Weeraratna AT (2016) Autophagy- An emerging target for melanoma therapy. F1000Research, 5(F1000 Faculty Rev):1888. Distributed under the Creative Commons Attribution License (CC BY 4.0).

Formation of the phosphoinositol 3-phosphate (PI3P) signals other PI3P-binding proteins that are responsible for the formation and expansion of the pre-autophagosomal structure into the fully enclosed autophagosome. Even though this process is not fully understood, it requires a third core complex recruitment that acts in a similar manner as a ubiquitin E3 ligation system. The Atg12-Atg5-Atg16L1 conjugation system is required for the conjugation of the LC3II (Atg8 family) to phosphatidylethanolamine. LC3II proteins are believed to be responsible for recognition of the cargo and regulatory proteins,

autophagosome closure, and fusion with lysosome (Otomo et al., 2013; Hurley and Schulman, 2014; Suzuki et al., 2017; Zachari and Ganley, 2017).

Importantly, only autophagy is capable of targeting and removing large, insoluble protein inclusions. In autophagy deficient systems, neurodegeneration and severe neuronal pathology is observed. Essential autophagy gene (Atg5 and Atg7) deletions leads to cytosolic incisions of ubiquitinated proteins and motor impairments (Hara et al., 2006; Komatsu et al., 2006; Tan and Wong, 2017).

2.3.4 Macroautophagy's role in the processing and degradation of aSyn

Proof that aSyn is degraded not only by the UPS but also by ALP pathway came from D. Rubinsztein's lab. They were able to show that a common autophagy inducer, rapamycin, is able to increase the clearance of both wt and common familial PD variants of aSyn (Webb et al., 2003). In previous chapters it was briefly described that autophagy is likely a compensatory mechanism after CMA machinery becomes incapacitated and that autophagy confers increase in neuronal toxicity (Xilouri et al., 2009). Nevertheless, the signaling pathway responsible for the activation of autophagy has been suggested as an important factor in determining protective or harmful effects of autophagy on the aSyn degradation process. Particularly, Vps34-beclin1 dependent activation has been linked to cell survival after aSyn accumulation. Overexpression of beclin1 has been shown to promote cell survival after aSyn overexpression due to increased lysosomal activity (Spencer et al., 2009). There is indication that increase in aSyn protein levels negatively regulates very early stages of autophagy by inhibiting pre-autophagosomal structure formation (Fig. 4). Namely, an essential autophagy protein, Atg9, colocalizes with the trans-Golgi network and LC3II-positive vesicles. When autophagy is induced, the amount of Atg9 shifts from the trans-Golgi network and predominantly are seen together with LC3II that is indicative of autophagosome formation. However, in case of increased aSyn protein levels Atg9 transfer is not initiated (Winslow et al., 2010).

Even with all of the advancements in the ALP and UPS fields autophagy's role in aSyn degradation is unclear. It is indicative that autophagy is an important pathway for aSyn degradation (Webb et al., 2003; Vogiatzi et al., 2008) while other reports have been contesting this role (Cuervo et al., 2004). *In vivo* approaches with transgenic animals and the paraquat-toxin model have given some hints of CMA involvement in aSyn degradation when cells are presented with increased aSyn protein burden (Mak et al., 2010). ALP inhibition in wt mouse does not seem to contribute to the induction of aSyn clearance via autophagy, while transgenic human wt aSyn-expressing animals after ALP inhibition had an increased accumulation of aSyn inclusions. The authors suggested that only upon increased aSyn protein accumulation the UPS cannot cope with aSyn burden and ALP is activated (Ebrahimi-Fakhari et

al., 2011). Indeed, upon cell treatment with bafilomycin A1, that blocks fusion of autophagosomes and lysosomes, aSyn is more readily accumulated near lysosomes while a milder effect was observed with 3-methyladenine, an inhibitor that more specifically inhibits only macroautophagy (Klucken et al., 2012).

Additionally, inhibition of the autolysosome formation by bafilomycin A1 is accompanied by an increase in p62. Interestingly, immediately after aSyn fibril addition to the HEK-293 cells aSyn positive inclusions were observed in the autophagosome lumen. It was suggested that due to autophagosome co-localization with LBs in the brains of LBD patients it is likely that not only aSyn aggregates but also higher order inclusions can undergo degradation via autophagy (Watanabe et al., 2012). Opposite effects were shown in a more recent work. Similarly, preformed aSyn fibrils were added to HEK-293 cells or primary neuronal cultures, however in this case HEK-293 cells were expressing aSyn. Formed aSyn aggregates were not degraded by autophagy, but rather impaired autophagosome maturation and led to the accumulation of aforementioned autophagosomes (Tanik et al., 2013).

Studies with p62-deficient aSyn transgenic mice have produced an additional role for p62 in aSyn pathology. p62-deficient animals showed increased accumulation of LB-like inclusions and it was found that another autophagy receptor, NBR1, is upregulated. aSyn aggregates observed in p62-deficient animals exhibited a higher degree of phosphorylation (Tanji et al., 2015). Increased levels of NBR1 has been correlated with increased LB-like inclusion formation. NBR1/p62 could potentially have an antagonistic role in the formation of aSyn aggregates (Odagiri et al., 2012). Interestingly, in another proteinopathy (sporadic inclusion body myositis) NBR1 related protein degradation was shown to be inhibited by the phosphorylation event of glycogen synthase kinase 3β. This in turn inhibited protein aggregation and retained ubiquitinated NBR1 substrate in the cells (Nicot et al., 2014).

Consequently, it has been proposed that in case of increased aSyn levels the main degradation pathway could be autophagy, however CMA involvement cannot be excluded (Ebrahimi-Fakhari et al., 2011). *In vitro* studies with autophagy inhibition by 3-methyladenine or knockdown of beclin1 or Atg5 has been shown to correlate with increased levels of aSyn oligomer formation that were specifically recognized by A11 oligomer antibody. Autophagy favors removal of larger aSyn aggregates (Yu et al., 2009), additionally, the bafilomycin A1 sensitive pathway seems to be important in aSyn aggregate removal. Increased toxicity after bafilomycin A1 treatment correlated with decreased aSyn aggregation. This points to aSyn aggregation as a detoxifying mechanism at least in the context of autophagic degradation. However, additive toxic effect of aSyn and bafilomycin A1 co-treatment cannot be excluded (Klucken et al., 2012).

2.4 aSyn phosphorylation role in aSyn aggregation and degradation

Phosphorylation at serine-129 (p-S129) is the predominant modification of aSyn in LBs (Anderson et al., 2006), as dramatic accumulation of this particular modification has been reported in brain samples with different forms of synucleinopathies (Kahle et al., 2000a; Fujiwara et al., 2002) and similar pathology has been reproduced *in vivo* in different PD animal models (Neumann et al., 2002; Yamada et al., 2004). Under physiological conditions in rat brain, aSyn phosphorylation is below 4% and aSyn is rapidly dephosphorylated *post-mortem* (Fujiwara et al., 2002). Stress causes rapid aSyn dephosphorylation in the striatum while the observed effect is diminished in aged animals. It is possible that phosphorylation of aSyn can mediate synaptic plasticity upon acute stress (Hirai et al., 2004). Recently, a report has shown that p-S129 aSyn levels are naturally increased in the SN region of healthy human brains (Muntane et al., 2012). Additionally, aSyn phosphorylation has been implicated in the regulation of dopamine transporter activity, membrane bound aSyn was shown to increase dopamine transporter capacity to uptake dopamine. This finding uncouples the idea that phosphorylation of aSyn is the toxic event only in the aggregate formation stage (Hara et al., 2013). aSyn membrane bound capacity has been shown to decrease in the case of p-S129 (Azeredo da Silveira et al., 2009; Visanji et al., 2011; Kuwahara et al., 2012) thus aSyn phosphorylation could be the cue that physiologically cycles aSyn between membrane bound cytosolic fractions (Hara et al., 2013). Consequently, aSyn phosphorylation likely plays an important physiological role in aSyn functions; at the same time upon disruption in cell homeostasis it could potentially mediate aSyn aggregation, inclusion formation, and dopaminergic cell death (Tenreiro et al., 2014a; Oueslati, 2016).

Inhibition of the proteasomal system increases aSyn accumulation, especially the amount of phosphorylated aSyn in the SN (Bentea et al., 2015) that is coupled with increase in kinase activity and aSyn phosphorylation upon proteasomal inhibition (Chau et al., 2009). There are indications that phosphorylated aSyn is more favorably targeted for the proteasomal system and degradation in an ubiquitin-independent manner. However, p-S129 aSyn half-life is much shorter than that of the native aSyn, an indication that the modification could potentially be used as a signal for rapid aSyn processing and removal from cells at least under basal conditions (Machiya et al., 2010).

In a yeast model, an aSyn phosphorylation resistant mutant failed to activate autophagy (Tenreiro et al., 2014b). A recent link between polo-like kinase 2 (PLK2) and aSyn degradation has been implicated in targeted aSyn degradation. PLK2 was shown to phosphorylate aSyn and increase aSyn autophagic degradation. Importantly, a Ser-129 phosphorylation event as well as PLK2/aSyn complex formation was required for aSyn degradation and subsequent neuronal survival (Oueslati et al., 2013). aSyn-PLK2 complex is

stabilized by the phosphorylation event but actual complex degradation is mediated by PLK2 polyubiquitination that allows this complex to be selectively recognized by macroautophagy receptors. Polo-like kinase 3 (PLK3) was shown to form a similar complex with aSyn and could represent a novel and selective aSyn degradation pathway (Dahmene et al., 2017).

2.5 Overview of prolyl oligopeptidase (PREP)

PREP (POP, PO, or PEP) is a serine protease (EC 3.4.21.26) that is ubiquitously expressed throughout the body with the highest protein levels in brain, kidney, testis, and thymus (Goossens et al., 1996; Myohanen et al., 2008). In the brain, the highest PREP protein expression and activity is seen in cortical and nigrostriatal tissues (Irazusta et al., 2002; Myöhänen et al., 2007) with almost exclusive localization in the neuronal cells (Rossner et al., 2005). mRNA levels of PREP are the highest during cellular differentiation and neuronal migration, but gradually decrease into adulthood (Agirregoitia et al., 2010). However, during ageing PREP mRNA levels dramatically increase (Jiang et al., 2001). Additionally, decreased (Ichai et al., 1994; Mantle et al., 1996b) and increased (Aoyagi et al., 1990) PREP activity have been reported in AD *post-mortem* brains. While PREP and β-amyloid deposit colocalization has been demonstrated in the brains of a senescence accelerated mouse (Fukunari et al., 1994), as well as in AD patients *post-mortem* brain samples (Hannula et al., 2013). Moreover, it has been shown that PREP activity is decreased in PD, LBD, and Huntington's disease (Mantle et al., 1996b).

PREP was first identified as an oxytocin-cleaving enzyme from human uterine tissue (Walter et al., 1971) and later it was shown that PREP cleaves at the C-terminal side of the proline (Koida and Walter, 1976). Initial crystallography studies with PREP demonstrated that PREP is a rigid structure composed of a catalytical and a β-propeller domain (Fulop et al., 1998; Fulop et al., 2000). Eukaryotic PREP has restrictive requirements for its substrate, anything larger than approximately 3 kDa (30 amino acids) cannot be cleaved by PREP (Moriyama et al., 1988) due to the position of the catalytical pocket between the catalytical and β-propeller domains (Fulop et al., 1998). It is believed that the substrate gets to the catalytical pocket from the side opening between the catalytical and β-propeller domain (Szeltner et al., 2004; Juhász et al., 2005), and that flexible loop structures that are located near the putative entry site to the catalytical site are essential for gating peptide access (Szeltner et al., 2013). In the recent years, equilibrium between closed and open PREP conformation has been demonstrated. Notably, PREP inhibition shifts protein conformation to the closed monomer (Lopez et al., 2016) however, eukaryotic PREP has never been crystalized without catalytical stabilization.

Some of the most studied PREP substrates are neuropeptides: substance P, arginine-vasopressin (Toide et al., 1995), and thyrotropin-releasing hormone [TRH] (Shinoda et al., 1995; Bellemere et al., 2005). Nevertheless, PREP has been shown to hydrolyze a large set of peptides *in vitro*, see review by Garcia-Horsman et al. (2007) for further information. Apart from hydrolytic activity, PREP has been implicated in the regulation of the inositol cycle in *Dictyostelium Discoideum* (Williams et al., 1999), and in neuronal and glial cell lines (Schulz et al., 2002). PREP can form direct protein interactions with growth associated protein 43 (GAP-43) independent of PREP enzymatic activity (Di Daniel et al., 2009) and with glyceraldehyde 3-phosphate dehydrogenase [GAPDH] (Matsuda et al., 2013). A possible role for PREP in the cellular trafficking and axonal transport has also been suggested due to PREP's colocalization with tubulin (Schulz et al., 2005). Recently it was suggested that substrate binding and enzymatic activity of PREP could be secondary processes and that PREP primarily functions through peptide gated direct interactions (Mannisto and Garcia-Horsman, 2017).

2.5.1 PREP's role in aSyn aggregation

PREP was initially thought to bind and hydrolyze a small fragment of the proline rich C-terminal part of aSyn (Brandt et al., 2005; Brandt et al., 2008). However, PREP is not able to cleave proteins that exceed 3000 Da (Moriyama et al., 1988). Eukaryotic PREP selectivity to the substrate size has been attributed to the restricted movement of the catalytical site and an unusual β-propeller domain that is positioned above the catalytical domain and limits proteins that have more than ~30 amino acid residues from accessing the catalytical pocket (Fulop et al., 1998; Fulop et al., 2000). Brandt et al. (2008) further demonstrated that intact, recombinantly purified aSyn is not cleaved by PREP but the rate of aSyn aggregation is increased in the presence of PREP. Notably, aSyn aggregation was abolished by a small molecule catalytical PREP inhibitor and in the presence of catalytically inactive PREP. It has been postulated that this increase in aSyn aggregation is most likely due to PREP stabilizing the aSyn conformation that favors nucleation and has little effect on aSyn aggregate propagation (Lambeir, 2011). Shortly thereafter, the effect of PREP inhibition on aSyn was shown to reduce high molecular weight aggregates and SDS-insoluble aSyn forms in cell lines overexpressing both wt and familial forms of aSyn. An interesting observation from the study was that PREP inhibition visibly reduced the co-localization between PREP and aSyn staining that prompted an idea that protein-protein interaction could be the mechanism that facilitates aSyn aggregation (Myohanen et al., 2012). Savolainen et al. (2015) proved that aSyn aggregation is indeed linked to direct protein-protein interaction with PREP. Furthermore, the inhibition of PREP does not dissociate the protein interaction but on the contrary stabilizes the aSyn-PREP complex. PREP inhibitors change protein conformation and

creates more tightly packed PREP that most likely does not have the ability to induce aSyn dimerization but is still able to bind aSyn (Savolainen et al., 2015).

However, decrease of aSyn immunostaining in transgenic aSyn mouse brains after a short, five-day treatment with PREP inhibitor, KYP-2047, could not be explained by dissociation between PREP and aSyn. It was suggested that PREP inhibition, apart from decreasing aSyn aggregation has a role in aSyn clearance (Myohanen et al., 2012). Shortly thereafter, it was demonstrated that PREP inhibition indeed increases aSyn clearance, notably by activating the macroautophagy pathway (Savolainen et al., 2014). Interestingly, the increase in LC3II, which is an indicator of increased autophagosome formation, was elevated in transgenic mice treated with a PREP inhibitor after five-day treatment but the difference was gone after four weeks of treatment. This observation, together with the decreased aSyn immunostaining after four weeks, hints that PREP inactivation is sufficient to clear the aggregates without excessive activation of the autophagy pathway (Savolainen et al., 2014).

Findings and observations described in this literature review regarding PREP and aSyn aggregation has been the foundation of this thesis work and in part serves to delineate some of the molecular mechanisms that govern pathological aSyn accumulation.

3 AIMS OF THE STUDY

Therapies targeted at aSyn clearance and reduction in the rate of aSyn aggregation are just a few of the strategies for the development of the new PD therapies that has a potential to rescue dopaminergic neurons. The findings that PREP is a direct interaction partner of aSyn, as well as negative regulator of autophagy, garnered interest in establishing the role of PREP inhibition as a potential drug therapy for neurodegenerative disorders. However, mechanisms of this dual effect of PREP inhibition on aSyn clearance and aggregation is not understood. Consequently, therapeutic possibilities of PREP inhibitors are limited unless cellular mechanisms that mediate autophagy induction and PREP's role on aSyn aggregation can be explained. The aim of this study was to establish PREP's role in autophagy regulation and in the aSyn aggregation process and to investigate the impact of chronic PREP inhibition on viral overexpression of aSyn.

The specific aims of the study were:

I. To study aSyn aggregation process and toxicity after restoration of PREP in PREP knockout cells and mouse nigrostriatal tract.

II. To establish the impact of long-term PREP inhibition by KYP-2047 on the motor performance, dopaminergic cell survival, and aSyn aggregation process in aSyn adeno-associated virus (AAV) mouse PD model.

III. To characterize PREP involvement in signaling pathways that lead to negative autophagy regulation and potential of PREP inhibition to alter these pathways.

4 MATERIALS AND MAIN METHODS

4.1 Reagents

Reagents were purchased from Sigma if not specified otherwise. The PREP inhibitor, KYP-2047 (4-phenylbutanoyl-l-prolyl-2(S)-cyanopyrrolidine), was synthesized in the School of Pharmacy, University of Eastern Finland (Jarho et al., 2004). KYP-2047 was dissolved in 0.2 % dimethyl sulfoxide (DMSO) in 0.9 % saline solution for intra-ventricular osmotic mini-pump administration (Study II). For cell culture work, 1 μM KYP-2047 working contention with 0.1% DMSO was used (Study I and III) if not specified otherwise.

4.2 Viral vectors and plasmids

AAV driven by chicken β-actin promoter (CBA) was acquired from the Michael J. Fox Foundation. All constructs used in the studies carry human open reading frame. AAV2-CBA-aSyn ($1.5x10^{13}$ vg/mL) and AAV2-CBA-eGFP (enhanced green fluorescent protein; 8.1 x 10^{12} vg/ml) viral vectors were constructed, produced, and titered by Vector Core at the University of North Carolina. AAV1-EF1α-PREP (AAV-PREP) viral vector and pAAV1-EF1α-PREP (#59967, Addgene), pAAV1-EF1α-S554A-PREP (S554A-PREP; #59968; Addgene), and AAV1-EF1a-V5-aSyn (#60057, Addgene) plasmids were obtained from the National Institute of Drug Abuse (Dr. Brandon Harvey, Intramural Research Program). Clustered Regularly Interspaced Short Palindromic Repeats (CRISPR) with associated protein 9 (CRISPR-cas9) method was used for PREP deletion (Study I and III) with pSpCas9n(BB)-2A-Puro (PX462) V2.0 plasmid, a gift from Feng Zhang (#62987, Addgene). PX462 was digested with BbsI restriction enzyme (R0539S, NEB) and ligated separately for Guide A (5'atggcacagtaatctt) and Guide B (5'cttgagcagtgtccca) with Ligate-IT Ligation Kit (#K1422; ThermoFisher Scientific). Guides were targeting 3rd exon of PREP.

For study III, pCMV3-PPP2Ac-C-FLAG (HG10420-CF), pCMV3-N-FLAG-PPP2Ac (HG10420-NF), pCMV3-PTPA (protein phosphatase 2 phosphatase activator; HG12287-UT), and pCMV3-N-FLAG-PTPA (HG12287-NF) were purchased from Sino-Biological. pAAV-EF1a control vector 50 bp insert was created by annealing complementary oligonucleotides. pAAV-EF1a-FLAG(C)-PME1 (protein phosphatase methylesterase 1) and pAAV-EF1a-PME1-FLAG(N) inserts were amplified from pUC19-PPME1 (HG29687-U; Sino-Biological) with overhangs containing either N- or C-terminal FLAG sequence. pAAV1-EF1α-hPREP backbone was digested with KpnI-HF (R3142; NEB) and EcoRV-HF (R3195; NEB) and recombined with all of the aforementioned inserts using an In-Fusion HD cloning kit (639645; Clontech).

For study III, cDNA of PREP, S554A-PREP, PP2A catalytical subunit (PP2Ac), PME1, and PTPA for protein-fragment complementation assay (PCA) were cloned in a pcDNA3.1/zeo backbone containing humanized *G. princeps* PCA fragments [GLuc] (Nykanen et al., 2012). PREP-GLuc-2N and S554A-PREP-GLuc-2N have been described previously (Savolainen et al., 2015). GLuc-N2 PREP constructs and empty GLuc-1N plasmid (backbone) was digested with EcoRI-HF (R3101; NEB) and KpnI-HF (NEB) restriction enzymes and ligated with Ligate-IT Ligation Kit (ThermoFisher Scientific) to create PREP-GLuc-1N and PREP(S554A)-GLuc-1N plasmids. PP2Ac (HG10420-CF; Sino-Biological), PME1 (Sino-Biological), and PTPA (HG12287-UT; Sino-Biological) cDNA was PCR amplified. Inserts were recombined with EcoRI-HF (NEB) and KpnI-HF (NEB) digested GLuc-1N, Gluc-2N, GLuc-1C, and GLuc-2C backbone using In-Fusion cloning kit (Clontech). Additionally, pcDNA3.1-PP2Ac and pcDNA3.1-PME1 were created by recombining PCR amplified fragments in GLuc-N1 backbone digested with HindIII-HF (R3104; NEB) and EcoRI (NEB) as described above but in this case, the GLuc fragment was removed from the construct. Identity of all constructs was confirmed by DNA sequencing. The pcDNA3-tau plasmid (0N4R) has been described previously by Brunello et al. (2016) and was a gift from Henri Huttunen's lab.

4.3 Animals

For study II, male C57BL/6J mice (7–9 weeks old; Envigo) were used. For study I and III, PREPko mice (Deltagene Inc.) and wt littermates were back crossed in C57BL/6JRccHsd genetic background (Envigo; 5–10 back crossings; 7–9 weeks old). Animals were housed under standard laboratory conditions in individually ventilated cages (Mouse IVC Green Line, Techniplast) with bedding and nesting material and aspen brick (aspen chips, strips, and bricks; Tapvei). Mice had access to chow food (Teklad 2016, Envigo) and filtered and irradiated water *ad libitum*. After surgical procedures, animals were housed individually for the duration of the experiment. The experiments were performed according to European Communities Council Directive 86/609/EEC and were approved by the Finnish National Animal Experiment Board (ESAVI-198-04.10.07; ESAVI-441-04.10.07-2017). Outline of study I and II can be seen in Fig. 5.

4.4 Surgical procedures

Mice were anesthetized with isoflurane (4% induction, 1.5–2.0% maintenance) and the recombinant AAV vectors were injected above mouse SN in a stereotaxic operation. AAV expression pattern and impact on behavior had been tested in study II and Julku et al. (2018). To target the SN, viral

vectors were given as single injection (volume 1 µL (Study I and II) or 2 µL co-injection (Study I), rate 0.2 µL/min) into the left hemisphere, 3.1 mm anterior and 1.2 mm lateral to bregma, and 4.2 mm below the dura (Paxinos and Franklin, 1997). In study II, a cannula (Alzet Brain Infusion Kit 3, Durect) attached to a minipump was implanted in the left hemisphere at 0.7 mm anterior and 1.4 mm lateral to bregma, and was lowered 2.5 mm deep to lateral ventricle according to Hof et al. (2000).

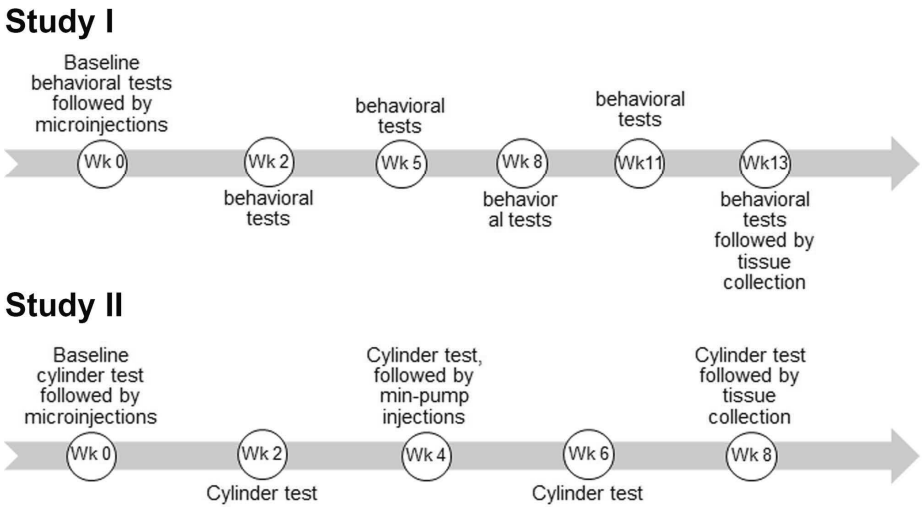

Figure. 5 Experimental outline for Study I and II. In **study I**, unilateral AAV microinjection of aSyn or combination of aSyn and PREP was delivered to SNpc of wt and PREPko mice. Cylinder test and locomotor activity was measured at baseline (week 0; wk 0) followed by stereotaxic surgery. Animal behavior was measured at 2, 5, 8, 11, and 13 weeks. In s**tudy II**, wt animals received unilateral aSyn or GFP AAV microinjection. Motor behavior was measured prior to surgeries (wk 0), at 2, 4, 6, and 8 weeks. After behavioral tests on week 4, cannula attached to the minipump was implanted intracranially. Minipump contained PREP inhibitor, KYP-2047.

4.5 Tissue processing

Mice intended for immunohistochemistry (IHC) analysis were deeply anesthetized with sodium pentobarbital (150 mg/kg) and transcardially perfused with phosphate-buffered saline (PBS) and 4% paraformaldehyde (PFA). Brains were post-fixed for 24 h in 4% PFA at 4°C and transferred to a solution of 10% sucrose in PBS overnight at 4°C. On the next day, tissue was transferred to 30% sucrose solution in PBS. Brains were frozen on dry ice and were kept at -80 °C until sectioning. Frozen brain sections were sectioned as 30 µm free-floating sections on a cryostat (Leica CM3050) and kept in a cryoprotectant solution. Mice tissue intended for Western blot (WB) assays in study III were transcardially perfused with ice-cold PBS. Thereafter, brains were frozen in isopentene on dry ice and kept at -80°C until further analyses.

4.6 Behavioral experiments

4.6.1 Cylinder test

(1) Cylinder test was used to measure motor asymmetry in spontaneous forelimb preference after unilateral microinjections (Study I and II). Baseline (BL) paw preference score was acquired before stereotaxic surgery and every 2-3 weeks after the surgery. Shortly, mouse was filmed for 5 minutes. However, if number of individual rearing episodes that resulted in mouse touching cylinder wall were less than 20, mouse was filmed for additional time. Data was analyzed by the formula $\frac{Contralateral+0.5*Both}{Ipsilateral+Contralateral+Both} * 100$; where 'Both' paws were defined as touches where the animal landed both of the forepaws on the cylinder wall at the same time after the rearing. No habituation of the animals to the testing cylinder was allowed before video recording.

4.6.2 Horizontal and vertical locomotor activity

For study I, mice were released in the corner of an open field arena for the duration of 2 h (Med Associates) and activity was recorded at the same time of the day for all of the animals. Total distance (locomotor activity) and vertical activity were analyzed. Data was collected in 5 min intervals and activity was recorded for 120 min (light intensity 150 lx). Data was analyzed with Activity Monitor v 7.06 software.

4.7 Immunohistochemistry procedures

4.7.1 Immunohistochemistry

IHC was performed for detection of total aSyn (Study I and II), p-S129 aSyn (Study II), oligomer-specific aSyn (Study I and II) and TH (Study I and II). Briefly, the endogenous peroxidase activity was inactivated with 10% methanol and 3% hydrogen peroxide (H_2O_2) solution in PBS (pH 7.4) for 10 min, and non-specific binding was blocked with 10% normal serum in PBS containing 0.5% Triton-X-100. The sections were incubated overnight at room temperature with sheep anti-aSyn antibody (1:500, ab6162, Abcam), rabbit anti-p-S129 aSyn primary antibody (1:250, ab59264, Abcam), mouse anti-human aSyn oligomer-specific primary antibody (1:200, AS132718, Agrisera) and rabbit anti-TH primary antibody (1:2000, AB152, Millipore). Thereafter, sections were incubated with secondary antibodies for 2 h; donkey anti-sheep for aSyn (1:500, ab6900, Abcam), goat anti-rabbit for p-S129 aSyn (1:500, #31460, ThermoFisher Scientific), goat anti-mouse for oligomer-specific aSyn (1:300, #31430, ThermoFisher Scientific). Biotin conjugated goat anti-rabbit

secondary antibody was used for TH (1:500, BA1000, Vector Laboratories) and the signal was enhanced with the avidin–biotin complex-method (Standard Vectastain ABC kit, Vector Laboratories). The antigen–antibody complexes were identified following incubation with 0.05% 3,3′-diaminobenzidine and 0.03% H_2O_2 solution. Finally, the sections were transferred to glass slides, dehydrated in alcohol series, and mounted with Depex (BDH).

4.7.2 Proteinase K treatment

Proteinase K (PK) protocol to remove soluble proteins from sections was performed in Study I and II. Shortly, sections were mounted onto gelatin-coated slides and dried overnight at 55°C. Sections were wetted with Tris-buffered saline with 0.05% Tween-20 (TBS-T) and digested with 10 µg/ml PK (#V3021, Promega) in TBS-T for 10 min at 55°C. Thereafter, the sections were post-fixed with 4% PFA for 10 min and processed for aSyn oligomer-specific immunostaining with the primary and secondary antibody concentrations as in 4.7.1 IHC section.

4.7.3 Microscopy and stereology

Optical density (OD) analyses for TH and aSyn (Study I and II) from striatum and SN were imaged with 3DHISTECH slide scanner (3DHISTECH Ltd.) and three coronal sections from each mouse were processed for further analyses with Pannoramic Viewer (Version 1.15.3, 3DHISTECH Ltd.). Images were converted to grayscale and inverted, line analyses tools for striatum or freehand for SN in ImageJ (1.48b; NIH) were used to measure the OD of immunoreactivity. To correct the effect of TH background staining, correction values were obtained from the corpus callosum of each section and subtracted from the OD values of the striatum. p-S129 aSyn immunohistochemical sections were imaged and average particle area and numbers per section were quantified using Image-Pro Plus software (Media Cybernetics, Inc.), four representative SN sections per brain were used. High magnification images were acquired with Qimaging 2000R camera (Qimaging) attached to an Olympus BX51 microscope with Olympus Microscope Objective Lens UPlanApo 20x/0.5 and100x/1.35 oil iris and processed with Adobe Photoshop CS6 (Version 13.0 x64).

The number of TH+ cells in SNpc or aSyn oligomer-specific particles from SN were estimated using the optical fractionator method (Study I and II). The TH+ and aSyn oligomer particles were analyzed with a Stereo Investigator platform (MicroBright-Field) attached to an Olympus BX51 microscope (Olympus Optical). From each animal, three representative sections for TH+ cells or four sections for aSyn oligomers were selected for quantitative analysis. Each reference space was outlined at low magnification (4x), and cells were counted using a high magnification (60x, UPlanApo 60x/1.4 oil

immersion) objective. Grid size was 100 x 80 µm and 120 x 120 µm respectively, the counting frames were 60 x 60 µm. Injected and non-injected SNpc were counted for TH and injected side for aSyn particle numbers as no aSyn staining was detected in the control side. The coefficient of error was between 0.05 and 0.10 (Schmitz and Hof, 2005). Results were expressed as the mean cell number per section and all stereological estimations were blinded.

4.8 Cell experiments and *in vitro* assays

4.8.1 Cell Cultures

HEK-293 (Study I and III) and SH-SY5Y human neuroblastoma cells (Study III) and their respective PREPko cell lines generated in these backgrounds were used in experiments. HEK-293 and SH-SY5Y PREPko cells were generated using PX462 plasmids (See 4.2 Viral vectors and plasmids). HEK-293 cells and HEK-293 PREPko cells were cultured in full Eagle's medium (DMEM; #D6429, Sigma) with an additional 10% (v/v) fetal bovine serum (FBS; #16000-044, ThermoFisher Scientific), 1% (v/v) L-glutamine-penicillin-streptomycin solution (15140122; ThermoFisher Scientific). HEK-293 PREPko cells were cultured in 20% (v/v) FBS (ThermoFisher Scientific). SH-SY5Y and SH-SY5Y PREPko cell lines were cultured with Dulbecco's modified eagle medium (DMEM-Glutamax; #31966021; ThermoFisher Scientific) containing 15% FBS (ThermoFisher Scientific) for wt and 30% FBS for SH-SY5Y PREPko cells, 1% non-essential amino acids (NEAA; #11140050; ThermoFisher Scientific) and 50 µg/ml Gentamycin (15750-045; ThermoFisher Scientific). Human breast adenocarcinoma (MCF-7) cells were cultured in MEBM medium (mammary epithelial cell growth medium; Kit Catalog #CC-3150, Lonza) supplemented with BPE, hEGF, insulin, hydrocortisone, and GA-1000 from the kit. Additionally, cholera toxin (1 ng/ml, Sigma) was added to the complete medium while 0.005 mg/ml transferrin (Sigma) was supplemented prior to use. Cells were kept at 37 °C and 5% CO2, water-saturated air.

4.8.2 Cell sample preparation and induction of aSyn aggregation

Transfections of plasmid DNA was done with Lipofectamine 3000 (L3000015; ThermoFisher Scientific) according to the manufacturer's instructions. If not specified otherwise, cells were lysed in ice cold modified RIPA buffer (50 mM Tris HCl pH 7.4, 1% NP-40, 0.25% sodium deoxycholate, 150 mM NaCl) supplemented with Halt Phosphatase (#87786, ThermoFisher Scientific) and Protease Inhibitor cocktail (#78430, ThermoFisher Scientific). Protein concentration was measured by bicinchoninic acid method (BCA; Pierce BCA Protein Assay Kit, #23225, ThermoFisher Scientific).

For aSyn aggregation (Study I), cells were transfected with aSyn, GFP, aSyn + GFP or aSyn + PREP. In oxidative stress groups 24 hours after plasmid transfection, the aggregation process of aSyn was induced by adding 100 mM H_2O_2 and 10 mM $FeCl_2$ in cell culturing medium, adapted from Myohanen et al. (2012). Non-stressed cells after transfection were grown for 72 hours. Thereafter, cells were fractioned in TBS for soluble aSyn, in Triton X-100 for membrane-bound aSyn, and in SDS buffer for SDS-soluble and insoluble aSyn (Fagerqvist et al., 2013). The protein amounts from Triton X-100 and SDS-fractions were correlated to total protein amounts (Ponceau S Staining).

4.8.3 Gel electrophoresis and protein immunoblots

Detailed description of the sample preparation protocols for WB can be found in original publications (Study I and III). Shortly, prior to WB, protein concentration was measured by BCA method. Standard SDS-PAGE techniques were used and ~30 µg sample was loaded to 12% (#4561044; Bio-Rad) or 4-20% Mini-Protean TGX gels (#4561094; Bio-Rad). Gels were transferred by Trans-Blot Turbo Transfer System (#1704150; Bio-Rad) onto Trans-Blot Turbo Midi PVDF (#1704157; Bio-Rad) or nitrocellulose (#1704159; Bio-Rad) membranes. Membranes were incubated at 4 °C overnight in 5% skim milk or 5% BSA in Tris-buffered saline with 0.05% Tween-20 (TBS-T). List of primary antibodies and respective concentrations can be found in Table 1. After overnight incubation, the membranes were washed and incubated with appropriate HRP-conjugated secondary antibodies for 2 h in room temperature, goat anti-mouse HRP (#31430; ThermoFisher Scientific); goat-anti rabbit (#31463; ThermoFisher Scientific). The membranes containing co-immunoprecipitation (coIP) samples were incubated with Clean-Blot IP Detection Reagent (#21230, ThermoFisher Scientific) in 5% skim milk. The images were captured using the C-Digit imaging system (Licor) [Study I and III] or ChemiDoc XRS+ (Bio-Rad) [Study III]. ImageJ was used for analyzing bands, and the OD values were calculated by comparing the OD value to the corresponding β-actin OD values.

4.8.4 Co-immunoprecipitation (coIP)

For study III, cells were lysed in washing buffer (20 mM Tris, pH 7.5, 150 mM NaCl, 1 mM EDTA, 1 mM EGTA, 1% Triton X-100 and 2.5 mM sodium pyrophosphate) supplemented with protease inhibitor cocktail. Samples were sonicated 3x1sec and centrifuged at 16,000 g for 15 min. 10 µL of agarose with anti-FLAG M2 antibody (#2220; Sigma) was used per immunoprecipitation reaction. PREP inhibitor or DMSO was added directly to the samples and samples were incubated for 2 h in washing buffer at 4 °C with gentle agitation. FLAG fusion proteins were eluted from the agarose beads with FLAG peptide (300 µg/mL; #F3290; Sigma) in Tris-buffered saline for 30 min. SDS-buffer

was added and lysate was boiled for 3 min at 95 °C, thereafter samples were processed for WB.

Table 1 Full list of antibodies used for WB and immunocytochemistry (ICC)

Antigen	Species	Manufacturer	Product #	Dilution
B55alpha(2G9), PPP2R2A	Mouse	AbCam	ab213945	1:2000
B55alpha, PPP2R2A	Rabbit	AbCam	ab197194	1:2000
Bcl-2	Rabbit	Abcam	ab59348	1:500
Bcl-2 phoshpo S70	Rabbit	Cell Signalling	2827S	1:500
Bcl-xL	Rabbit	AbCam	ab32370	1:1000
Bcl-xL phospho S62	Rabbit	AbCam	ab180849	1:1000
Beclin phospho-T119	Rabbit	Millipore	ABC118	1:500
Beclin1	Rabbit	AbCam	ab62557	1:2000
DAPK	Rabbit	Sigma	D1319	1:1000
DAPK phospho-S308	Mouse	Sigma	D4941	1:1000
FLAG	Rabbit	Sigma	F7425	1:2000
GAPDH	Mouse	Millipore	MAB374	1:2000
JNK1+JNK2	Rabbit	AbCam	ab85139	1:1000
JNK1+JNK2+JNK3 phospho- 85+Y185+Y223)	Rabbit	AbCam	ab76572	1:1000
LC3B	Rabbit	Sigma	L7543	1:1000
Oxidative stress defense cocktail	Rabbit	AbCam	ab179843	1:250
PME1	Rabbit	AbCam	ab86409	1:500 WB/ 1:200 (ICC)
PP2A phospho-T307	Rabbit	ThermoFisher	PA5-36874	1:500
PP2AC(α+β); Clone Y119	Rabbit	AbCam	ab32141	1:2000 WB/ 1:400 (ICC)
PREP	Rabbit	AbCam	ab58988	1:1000
PTPA	Mouse	AbCam	ab129244	1:1000 WB/ 1:400 (ICC)
SQSTM1/p62	Mouse	Abcam	ab56416	1:5000
αSyn	Sheep	Abcam	ab6162	1:1000
αSyn phospho-S129	Rabbit	Abcam	ab51253	1:500
β-actin	Rabbit	Abcam	ab8227	1:2000
Tau-5	Mouse	Abcam	ab80579	1:4000
Tau S262	Rabbit	Abcam	ab64193	1:1000

4.8.5 Immunocytochemistry (ICC)

ICC to detect changes in co-localization between PP2Ac and PME1, and PP2Ac and PTPA after PREP inhibition or deletion was performed as described in (Myohanen et al., 2012). Briefly, wt or PREPko HEK-293 cells

were plated over glass coverslips in a 12-well plate and allowed to attach overnight. Thereafter, HEK-293 cells were treated for 4 h with KYP-2047 and fixed with 4% PFA. Unspecific binding was blocked with 10% normal goat serum (S-1000, Vector Laboratories) for 30 min and thereafter cells were incubated with primary antibodies against PP2Ac, PME1, and PTPA (see Table 1 for details) overnight at 4 °C. The following secondary antibodies were used to incubate cells 1 h in room temperature: for mouse PP2Ac, anti-mouse AlexaFluor488 (dilution 1:400; ab150113, Abcam); for rabbit PP2Ac, anti-rabbit AlexaFluor 488 (dilution 1:400; ab150077, Abcam); for mouse PTPA, anti-mouse AlexaFluor 568 (dilution 1:400; ab175473, Abcam); for rabbit PME-1, anti-rabbit AlexaFluor 568 (dilution 1:400; ab175471, Abcam). Cells were mounted with Vectashield containing DAPI (H-1200, Vector Laboratories). Imaging was performed using Leica TCS SP5 confocal microscope (Leica).

4.8.6 Cell viability and reactive oxygen species measurements

For cell viability (Study I), cells were transfected with aSyn, GFP, and aSyn + PREP and incubated for 24 h. After cell exposure to oxidative stress, cell viability was measured using mitochondrial oxidoreductase activity assay 3-(4,5-dimethylthiazol-2-yl)-2,5-diphenyl-tetrazolium bromide (MTT). 100 µL of MTT solution (5 µg/µL) was added to the cells and incubated in cell culture conditions for 2 h. Cell culture media was replaced with 200 µL DMSO. The absorbance was measured at 550 nm with absorbance at 650 nm subtracted as background. Reactive oxygen species (ROS) were measured using 2',7'-dichlorofluorescin diacetate (DCFDA) Cellular ROS Detection Assay Kit (ab113851, Abcam) after induction of oxidative stress (Study I). DCFDA treatment was performed according to the manufacturer's instructions. Fluorescence signal for excitation (495 nm) and emission (529 nm) was read with the Wallac 1420 Victor fluorescence plate reader (PerkinElmer). Signal was adjusted to the total protein amount.

4.8.7 aSyn ELISA from cell culture supernatant

aSyn levels in cell culture medium of wt and PREPko HEK-293 cells were measured after cell transfection either with aSyn or aSyn + PREP plasmids and induction of aSyn aggregation (Study I). Human aSyn ELISA Kit (ab210973, Abcam) was used according to the manufacturer's instruction. Fluorescence was red at 450 nm with the Wallac 1420 Victor fluorescence plate reader (PerkinElmer). aSyn amount in medium was adjusted to the total protein levels.

4.8.8 Proteasomal activity

Proteasomal 20S activity assay is based on proteolysis of 7-amino-4-methylcoumarin (AMC) conjugated peptide. For chymotrypsin-like 20S proteasomal activity (Study I) measurements were conducted as previously described by Ebrahimi-Fakhari et al. (2011). In brief, cells were lysed in 20S activity buffer and incubated for 1 h at 37 °C with Suc-Leu-Leu-Val-Tyr-AMC substrate (#I-1395, Bachem). The fluorescence excitation (360 nm) and emission wavelengths (460 nm) were read with the Wallac 1420 Victor fluorescence plate reader (PerkinElmer). The velocity of the reaction was calculated as nM AMC per minute per μg of protein.

4.8.9 Protein-fragment complementation assay (PCA)

The PCA was performed as previously described by (Nykanen et al., 2012). Wt and PREPko HEK-293 cells were plated on Poly-L-lysine coated white walled 96-well plates (25,000 cells/well; #6005070, PerkinElmer) and after 24 h they were transfected with PCA reporter constructs (100 ng of plasmid DNA/well). 48 h after transfection, the cells were washed with PBS and phenol red free DMEM (#21063-029, ThermoFisher Scientific) was added to the cells (without serum and antibiotics). The cells were allowed to settle for 1 h. If inhibitors were tested, they were added to the cells in phenol red free DMEM and the cells were treated for 4 h prior to measurement. A GLuc-PCA signal was detected by injecting 25 μl of native coelenterazine (Nanolight Technology) to the cells (final concentration 20 μM) and measuring the luminescence signal with Varioskan Flash multiplate reader (ThermoFisher Scientific).

4.8.10 Thymidine incorporation assay

Wt and PREPko HEK-293 cells and MCF7 cells were plated on 24-well plates (100,000 cells/well) and the following day they were exposed to the KYP-2047 for 24 h. For the last 6 h of treatment [methyl-^{3}H] thymidine (PerkinElmer) was added in the incubation medium at 1 μCi/ml. After incubation, the cells were washed with ice-cold PBS and free unbound thymidine was precipitated with 5 % trichloroacetic acid and discarded. Finally, the cells were lysed with 0.1 M NaOH. Supermix scintillation cocktail (Perkin Elmer) was added and the counts were measured (5 min per well) with 1450 Microbeta TriLux scintillation counter (PerkinElmer).

4.8.11 Tau aggregation

Briefly, HEK-293 cells were transfected with tau 0N4R plasmid. The next day the cells were treated with okadaic acid (OA, 10 nM), and okadaic acid in combination with KYP-2047 (10 μM) in cell culture medium for 48 h. Cells

were lysed with extraction buffer (10 mM Tris-HCl, 1mM EDTA, 150 mM NaCl, 1% Triton X-100, 0.25% Nonidet P-40, pH = 6.8) supplemented with protease and phosphatase inhibitors. Lysates were incubated on ice for 20 min and centrifuged (20,000 g, 1 h, 4°C). The supernatant (soluble fraction) was collected while the pellet (insoluble fraction) was dissolved with SDS-buffer and sonicated (4 x 3s). Levels of tau were studied using WB. The insoluble fractions were separated on Mini-Protean TGX Stain-free gels (#4568094, Bio-rad) and the level of protein on each sample was determined by detecting the proteins on the gel and on the membrane with the stain-free protocol of Chemidoc XRS (Bio-rad).

4.9 Data analyses

Statistical analyses were performed with SPSS 22/24 (Study I and II) for repeated measures behavioral analyses and two-way interactions. GraphPad PRISM (studies I, II, and III) software was used for student's t-test, one-way analysis of variance (ANOVA) with Tukey's post hoc test, two-way ANOVA or repeated measures ANOVA with Tukey's post hoc test. In all cases, values of $p < 0.05$ were considered to be significant. Data is presented as mean ± SEM.

5 RESULTS

5.1 PREP inhibition and deletion influences aSyn caused motor behavior in viral aSyn overexpression mouse model (I and II)

PREP's role on aSyn aggregation and ensuing motor behavior was investigated in Study I and II. In Study I, PREPko animals or wt littermates received microinjection of either aSyn viral vector or combination of aSyn and PREP viral vectors to see aSyn aggregation and spreading in the nigrostriatal tract in the absence of PREP protein. In Study II, aSyn was overexpressed in wt mouse nigral tissue and motor behavior was analyzed before and after chronic 1-month long inhibition of PREP catalytical activity by a small-molecule inhibitor, KYP-2047.

Findings of the experiments are summarized in Fig. 6. In study I, statistically significant interaction between PREPko animal groups on total traveled distance was seen (Fig. 6A; $F_{(5,75)} = 4.174$, $p = 0.002$, two-way ANOVA), while wt animal groups did not differ. Already at the 5-week time point, PREPko animals injected with aSyn + PREP had a significant reduction in total traveled distance and this effect extended until the termination of experiments at the 13-week time point ($p = 0.014$) when compared to aSyn-only injected PREPko mice. Similarly to locomotor activity, statistically significant interaction on vertical activity was observed only between PREPko animal groups (Fig. 6B; $F_{(5,75)} = 2.539$, $p = 0.036$, two-way ANOVA). From 5-week time point (Fig. 6B; $p = 0.02$) to the termination of the experiment ($p = 0.041$) aSyn + PREP injected PREPko animals exhibited reduced vertical locomotion. PREPko animals exhibited higher BL horizontal locomotor activity compared to wt littermates (Fig. 6A; $t_{(31)} = 1.091$, $p = 0.000031$, student's t-test).

Cylinder test in study I and II, measured unilateral misbalance caused by aSyn viral vector injections. In study I, significant change of paw preference in wt animals but not in PREPko mice (Fig. 6C; $F_{(5,150)} = 5.453$, $p = 0.001$, two-way ANOVA) was seen over the course of the experiment starting at the 2-week time point ($p < 0.0005$) and for the duration of the study (Fig. 6C; $p = 0.007$, 13-week time point). Similar effect in paw misbalance after aSyn viral vector injection was seen in Study II, aSyn-injected animals exhibited motor misbalance when compared to GFP-injected littermates (Fig. 6D; $F_{(1,31)} = 16,873$, $p = 0.000271$, two-way ANOVA). After KYP-2047 treatment was initiated, behavioral scores of aSyn-injected, KYP-2047 treated animals improved to those observed in GFP-injected animals (Fig. 6D; $p = 0.025$). aSyn-injected, vehicle (DMSO) treated mice motor behavior did not improve and at the 6-week time point aSyn-DMSO and aSyn-KYP-2047 group had a

significant difference (p = 0.006) in their paw use, and the KYP-2047 effect extended to 8-week time point for the remaining animals (p = 0.048).

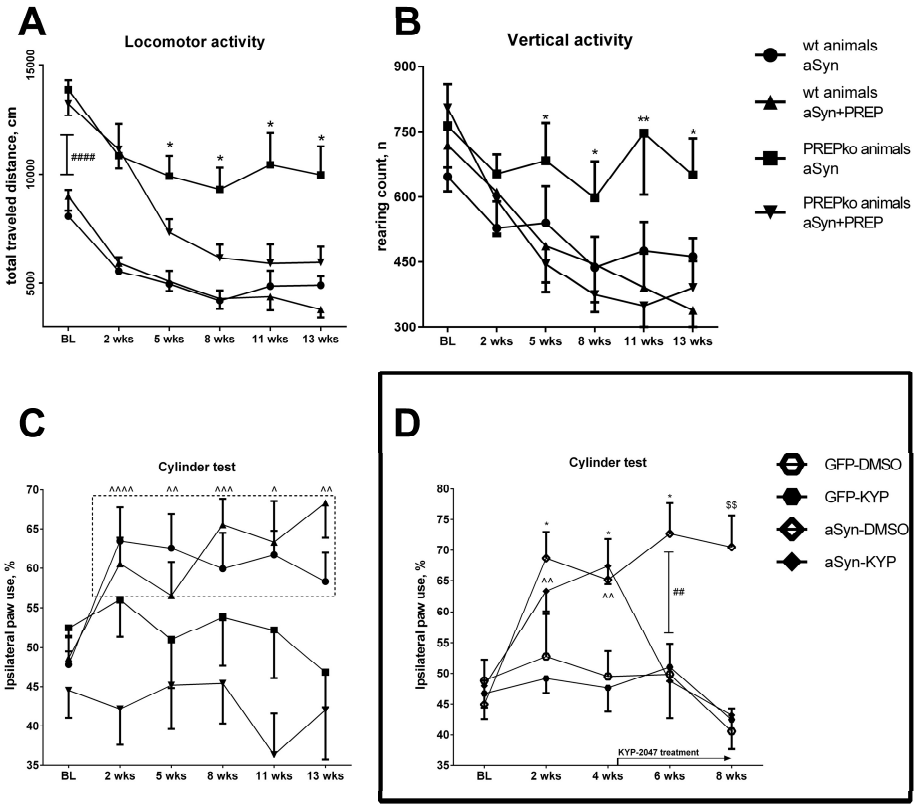

Figure. 6 Unilaterally injected AAV-aSyn virus vector impact on wt and PREPko mouse behavior. (**A**) Total traveled distance was significantly different between PREPko animal groups starting at the 5-week time point until the end of the experiments. BL locomotor activity was higher in PREPko animal groups compared to wt (n = 7–10). (**B**) Vertical activity was statistically different between PREPko animal groups starting from the 5-week time point (n = 7–10). (**C**) In cylinder test, increased ipsilateral paw use after unilateral aSyn viral vector injection was seen in wt animal groups (n = 15–17). Bars represent mean ± SEM. *p < 0.05, **p < 0.01, PREPko aSyn vs. PREPko aSyn + PREP; ####p < 0.0005, wt vs. PREPko; ^p < 0.05, ^^p < 0.01, ^^^p < 0.001, ^^^^p < 0.0005, wt animal BL vs. post-injection measurements. Two-way ANOVA; student's t-test for BL locomotor activity. (**D**) aSyn viral vector injection increased ipsilateral paw use. KYP-2047 treatment (aSyn-KYP) rescued motor misbalance (week-6 and week-8). Error bars represent means ± SEM. *p < 0.05, aSyn-DMSO versus GFP-DMSO; ^^p < 0.01, aSyn-KYP versus GFP-KYP; $^{\#\#}$p < 0.01, aSyn-DMSO versus aSyn-KYP; $^{\$\$}$p < 0.01, aSyn-DMSO versus aSyn-KYP, GFP-DMSO, and GFP-KYP; two-way ANOVA.

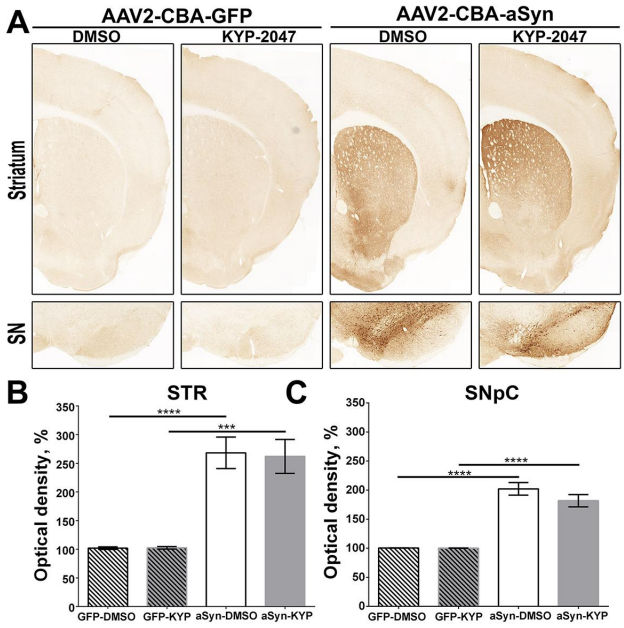

Figure. 7 Total aSyn immunoreactivity in striatum and SN after GFP and aSyn viral vector microinjections. (**A**) aSyn immunoreactivity was increased 8 weeks after unilateral aSyn but not GFP viral vector microinjections. (**B–C**) Significant increase in total aSyn OD was observed in striatum and SNpc in aSyn viral vector injected groups. KYP-2047 treatment (aSyn-KYP) did not have an effect on total aSyn amounts compared to vehicle (aSyn-DMSO) treatment (**A–C**). n = 7–9 in each group. Error bars represent means ± SEM. ***p < 0.001, ****p < 0.0001 (one-way ANOVA).

5.2 Effect of PREP deletion and inhibition on aSyn and TH distribution in wt and PREPko animals (I and II)

Total aSyn optical density distribution pattern among aSyn-injected animals was similar in studies I and II. Significant changes were seen only between aSyn and GFP-injected animal groups in Study II (Fig. 7A-C; in striatum, $p < 0.0001$; SN, $p < 0.0001$, one-way ANOVA). Therefore, total aSyn oligomer-specific staining was quantified by stereological investigation. In study I, differences between PREPko animals and wt groups in total oligomer aSyn counts was not observed (Fig. 8A-B). However, when PK treatment was performed prior to aSyn oligomer-specific staining, differences were observed between animal phenotype and viral vector injections (Fig. 8C, A; $F_{(1, 16)} = 6.413$, $p = 0.022$, two-way ANOVA). Interestingly, in study I, aSyn + PREP injected PREPko mice had less PK-resistant aSyn oligomers than aSyn injected PREPko animals (Fig. 8C) with visually lighter and more diffuse PK-resistant aSyn oligomer pattern (Fig. 8A). The ratio between the number of PK-resistant aSyn and total aSyn oligomer particles was matched for individual animals (Fig. 8D) and interaction was observed between viral vectors and animal phenotype ($F_{(1,16)} = 5.847$, $p = 0.028$, two-way ANOVA). PK-resistant and total

aSyn oligomer ratio in the PREPko animal group with aSyn + PREP injection was decreased while the opposite effect was seen between wt animal groups. Moreover, the PREPko animal group with aSyn + PREP injections had the smallest area of the p-S129 aSyn staining (Fig. 8E) and it was visually more diffuse (Fig. 8A).

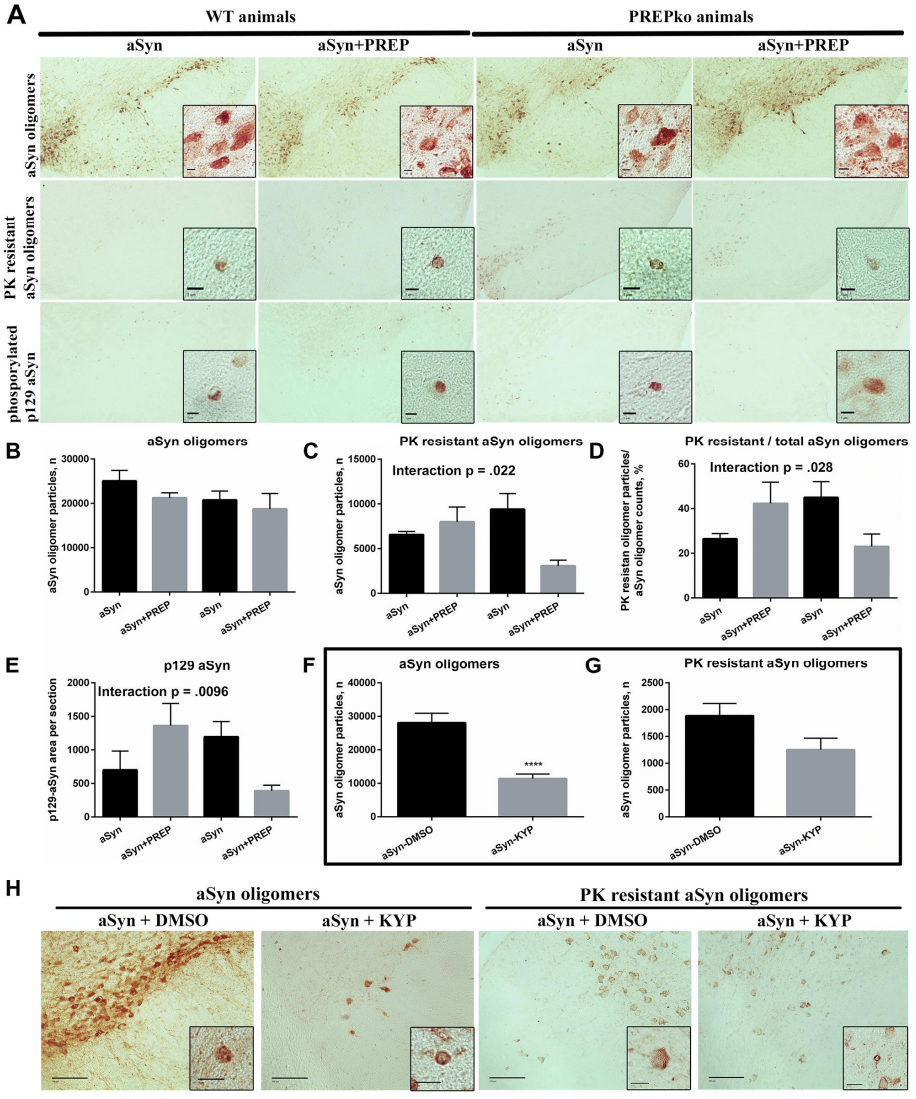

Figure. 8 aSyn oligomer-specific particles in SN. (**A**) Representative images of aSyn and PK-resistant oligomers and p-S129 aSyn staining in SN brain sections. More diffuse staining in total aSyn, PK-resistant aSyn oligomers and p-S129 aSyn is seen in aSyn + PREP injected PREPko animals. Scale bar 5 µm. (**B**) Oligomer-specific particle stereological counts were not different between the animal groups (n = 7–8). (**C**) A statistically decreased number of PK-resistant oligomers was seen in the PREPko aSyn + PREP animal group (n = 4–6). (**D**) Ratio between PK-resistant oligomers and total aSyn oligomer count was reduced in aSyn + PREP injected PREPko animal group (n = 4–6). (**E**) p-S129 aSyn stained area showed a significant interaction between groups [n = 5] (two-way ANOVA). (**F**) aSyn oligomer numbers were decreased in aSyn-injected, KYP-2047 treated (aSyn-KYP) group compared to vehicle treatment (aSyn-DMSO). (**G**) aSyn PK-resistant particle count did not show significant differences between aSyn-injected groups. (**H**) Strong immunostaining of aSyn oligomers was seen in the aSyn-DMSO group while aSyn-KYP-2047 group showed reduced aSyn oligomer-staining in PK soluble and resistant samples (n = 9). Bars represent means ± SEM. ****p < 0.0001 (student's t-test). Scale bars: 100 µm; insets, 15 µm.

Our research group had previously reported changes in the aSyn amount after KYP-2047 treatment (Myohanen et al., 2012; Dokleja et al., 2014; Savolainen et al., 2014). Similarly in study II, KYP-2047 treatment caused a significant decrease in the total aSyn oligomer-specific particles (Fig. 8F, H; p < 0.0001). Corresponding KYP-2047 treated sections showed less bright inclusions and staining of aSyn oligomer immunoreactivity (Fig. 8H). PK-resistant aSyn oligomer-specific particle counts between the KYP-2047-treated group and the vehicle-treated group was not statistically significant (Fig. 8G; p = 0.0736). Nevertheless, the PK-resistant aSyn oligomer-specific particle counts in SN was approximately one-tenth of all detected oligomer particles in both vehicle and KYP-2047-treated aSyn injected mouse groups (Fig. 8F-G).

In studies I and II, TH OD in SN and striatum as well, as dopaminergic neuron loss in SNpc was quantified. In study I, effect on TH+ cell loss was not seen between viral vector injection and phenotype but due to the significant main effect for viral vectors additional analyses were performed to compare aSyn and aSyn + PREP injected groups. aSyn + PREP injected animals had more pronounced TH+ cell loss (Fig. 9A, D; p = 0.0097). TH OD analyses did not show a clear loss of TH+ fibers in either the striatum or the SNpc (Fig. 9A-C). PREP inhibitor treatment in study II did not alter TH+ cell count between the groups (Fig. 9G; p = 0.0593). Nevertheless, mild TH+ cell loss was seen in the vehicle-treated aSyn group. TH immunoreactivity in striatum between vehicle-treated groups (Fig. 9E) and between vehicle-treated aSyn group and both GFP groups in SNpc (Fig. 9F) was seen.

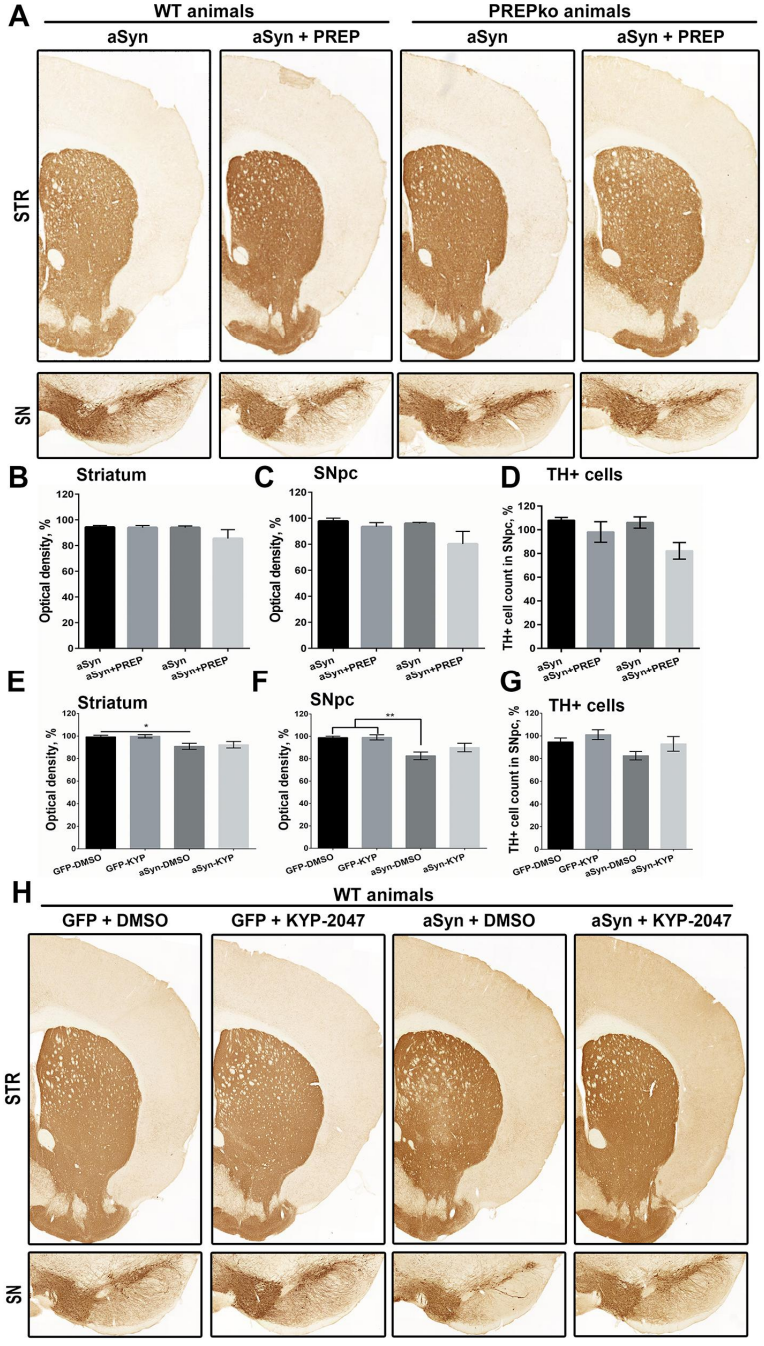
A
WT animals
PREPko animals
aSyn
aSyn + PREP
aSyn
aSyn + PREP
STR
SN
B
Striatum
Optical density, %
C
SNpc
Optical density, %
D
TH+ cells
TH+ cell count in SNpc, %
aSyn
aSyn+PREP
E
Striatum
Optical density, %
F
SNpc
Optical density, %
G
TH+ cells
TH+ cell count in SNpc, %
GFP-DMSO
GFP-KYP
aSyn-DMSO
aSyn-KYP
H
WT animals
GFP + DMSO
GFP + KYP-2047
aSyn + DMSO
aSyn + KYP-2047
STR
SN

Figure. 9 Mild changes in TH+ cell counts and TH+ OD after aSyn injection. (**A**) Representative brain sections of TH staining from striatal and nigral brain areas (study I). (**B-C**) TH OD analyses did not show changes in striatum and SN (study I). (**D**) Significant TH+ cell decrease was observed between aSyn and aSyn + PREP injected animal groups (study I). (**E-F**) aSyn-DMSO had significantly reduced TH+ staining in striatum (vs. GFP-DMSO) and in SNpc (vs. GFP groups). Significance was not observed in the aSyn-KYP-2047 case (study II). (**G**) TH+ cell stereology did not show a statistical significance between groups ($p = 0.0593$; study II). (**H**) Representative images of TH+ staining in striatum and SN 8 weeks after GFP and aSyn viral vector injections (study II). Bars represent means ± SEM, *$p < 0.05$; **$p < 0.01$; one-way ANOVA.

5.3 aSyn distribution from wt and PREPko HEK-293 cells in soluble, membrane bound, and insoluble fractions

In study I, the aSyn aggregation pattern in wt and PREPko HEK-293 cells after oxidative stress treatment was studied by WB. aSyn was separated between soluble (TBS), membrane bound (TrX), and insoluble aSyn (SDS) fractions (Fig. 10A-F). Additionally, autophagy marker levels were measured after aSyn plasmid transfection and oxidative stress (Fig. 10G-I). WB images can be found in the respective publication and supplementary material (Study I). In PREPko cells, a moderate difference was seen in TBS-soluble p-S129 aSyn between aSyn and aSyn + PREP transfected groups (Fig. 10A). Membrane bound p-S129 aSyn level after aSyn + PREP transfection both in wt (Fig. 10B) and PREPko cells (Fig. 10B) were significantly decreased. Additionally, a significant increase in p-S129 aSyn levels was observed after oxidative stress only in PREPko cells (Fig. 10B). SDS-soluble p-S129 aSyn levels were significantly decreased by stress in wt (Fig. 10C) and PREPko cells (Fig. 10C).

In the TBS fraction, oxidative stress decreased aSyn level in wt cells (Fig. 10D) while TrX-soluble aSyn fraction was lowered in aSyn + PREP group for both phenotypes (Fig. 10E). aSyn in SDS-fractions was decreased after oxidative stress (Fig. 10F), additionally, aSyn + PREP transfection reduced SDS-soluble aSyn levels even further (Fig. 10F) in wt cells. A similar effect was seen in PREPko cells (Fig. 10F).

The baseline p62 levels, a protein accumulation marker, in PREPko cells were approximately 50% lower than in wt cells (Fig. 10H). p62 was significantly elevated by stress and transfections (Fig. 10H) in PREPko cells. Autophagy regulators, such as beclin1 levels, did not show changes (Fig. 10G) and autophagosome marker, LC3BII levels, were mildly affected by aSyn and aSyn + PREP transfections in wt cells (Fig. 10I).

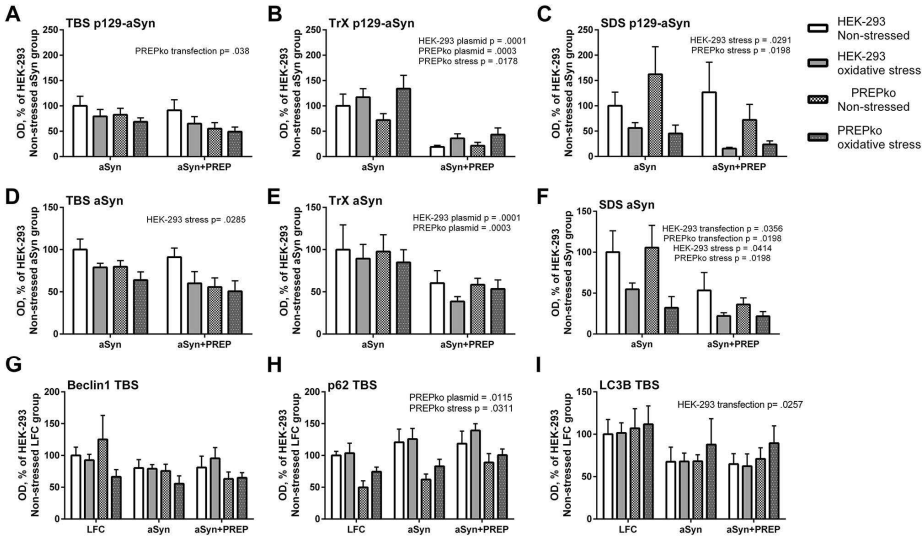

Figure. 10 PREP's role in the aSyn distribution between soluble (TBS), membrane bound (TrX), and insoluble (SDS) fractions and changes in autophagy markers. Cells were transfected with aSyn or aSyn + PREP and treated with oxidative stress for 48 hrs. (**A**) p-S129 aSyn was reduced in PREPko cells after aSyn + PREP transection. (**B**) Combination of aSyn + PREP considerably reduced TrX soluble p-S129 aSyn level. (**C**) Oxidative stress reduced the levels of SDS-soluble p-S129 aSyn in both cell lines. (**D**) Oxidative stress reduced aSyn levels in HEK-293 cells. (**E**) aSyn + PREP transfections reduced aSyn levels compared to aSyn transfected groups. (**F**) A significant reduction of aSyn was seen after oxidative stress in both cell lines. aSyn + PREP transfection lowered the SDS-aSyn levels. (**G**) No effect was observed in beclin1 levels between cell lines or treatments. (**H**) Stress and plasmid transfection had a significant effect on the PREPko cell p62 levels. (**I**) Slight decrease of LC3BII levels was seen after transfections in HEK-293 cells. Bars represent mean ± SEM, two-way ANOVA.

5.4 Cellular response to oxidative stress is altered in PREPko cells

A set of oxidative and cellular toxicity tests were performed to characterize PREPko cell response in the presence of protein overload and oxidative stress (Study I). First, MTT assay was performed after cell transfection (aSyn or aSyn + PREP) and oxidative stress induction. Oxidative stress caused cytotoxicity in HEK-293 (Fig. 11C; $F_{(1,23)} = 183.9$, $p < 0.0005$) and PREPko oxidative stress groups (Fig. 11D; $F_{(1,23)} = 28.10$, $p < 0.0005$, two-way ANOVA), however, overall cell death in PREPko cells exposed to stress was lower than in wt cells. All transfections had an effect on wt cell viability (Fig. 11C; $F_{(1,23)} = 28.10$, $p < 0.0005$, Univariate analyses), aSyn + PREP group compared to all other groups ($p = 0.025$ vs. aSyn, $p = 0.007$ vs. GFP and $p < 0.0005$ vs control group) as well as between control group and aSyn group ($p = 0.035$). The plasmid transfection effect in PREPko cells was only observed between negative control and aSyn + PREP groups ($p = 0.02$) (Fig. 11D; $F_{(3,23)} = 4.271$, $p = 0.015$, two-way ANOVA).

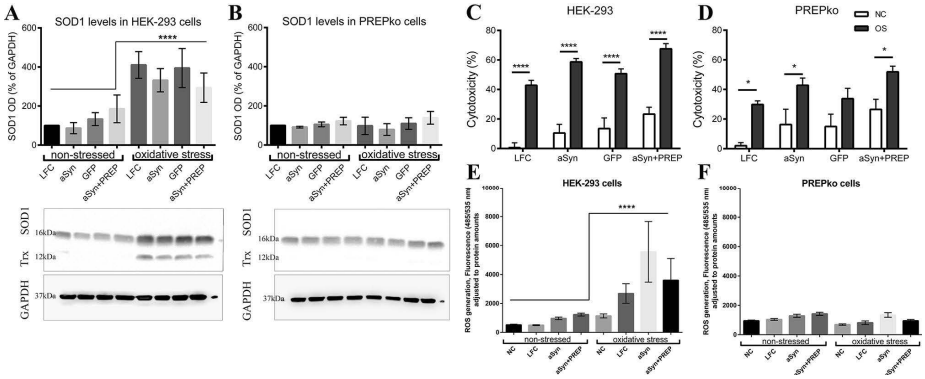

Figure. 11 PREPko cells show reduced cell death and response to stress. (**A**) Superoxide dismutase 1 (SOD1) protein levels were upregulated in the HEK-293 oxidative stress groups compared to the non-stressed groups. (**B**) No differences in SOD1 protein levels were detected between PREPko groups. (**A-B**) Representative images of WB bands for SOD1 and thioredoxin (Trx) in HEK-293 and PREPko cells in the presence and absence of oxidative stress. (**C**) MTT assay showed significant stress dependent effect in all HEK-293 oxidative stress (OS) groups. The aSyn + PREP transfected groups showed the highest cytotoxicity while the aSyn transfected cell group had significantly reduced cell numbers only compared to control group. (**D**) OS effect in PREPko cells was less pronounced. aSyn + PREP transfected group had increased cytotoxicity compared to control group. (**E**) ROS were statistically increased in the HEK-293 cells after oxidative stress treatment. (**F**) Oxidative stress did not upregulate ROS in PREPko cells. Two-way ANOVA. Bars represent mean ± SEM. *$p < 0.05$, **$p < 0.01$, ****$p < 0.0005$.

ROS were measured in wt and PREPko cells using DCFDA. The fluorescence signal was significantly increased between wt cell oxidative stress conditions (Fig. 11E; $p < 0.0005$) as well as compared to PREPko cell oxidative stress groups (Fig. 11F; $p < 0.0005$). However, differences in ROS production was not observed between PREPko cell groups (Fig. 11F). Similarly, WB was used to measure oxidative stress markers, superoxide dismutase 1 (SOD1) and thioredoxin, in HEK-293 wt and PREPko cells. SOD1 protein levels were increased in the wt cell oxidative stress groups compared to the non-stressed wt cells (Fig. 11A; $p < 0.0005$) and PREPko cell oxidative stress group (Fig. 11A-B; $p < 0.0005$). We did not observe increased levels of SOD1 or thioredoxin in PREPko cells in the presence of oxidative stress (Fig. 11B).

5.5 PREP deletion causes changes in cellular protein degradation pathways and aSyn recycling

PREP inhibition has been previously shown to induce autophagic flux and increases aSyn clearance both *in vitro* and *in vivo* (Savolainen et al., 2014). In study I, autophagic and proteasomal activity effects on aSyn degradation were measured. In wt cells, oxidative stress and plasmid transfections reduced proteasomal activity (Fig. 12A; $F_{(4,36)} = 16.58$, $p < 0.0001$, two-way ANOVA), with the non-stressed control group having significantly higher proteasomal activity. The oxidative stress conditioned aSyn + PREP group had the most

decreased S20 proteasomal activity in wt cells (Fig. 12A), where it was significantly lower compared to the rest of the oxidative stress groups (vs. control group ($p = 0.0029$), GFP group ($p = 0.008$), and aSyn group [$p = 0.013$]).

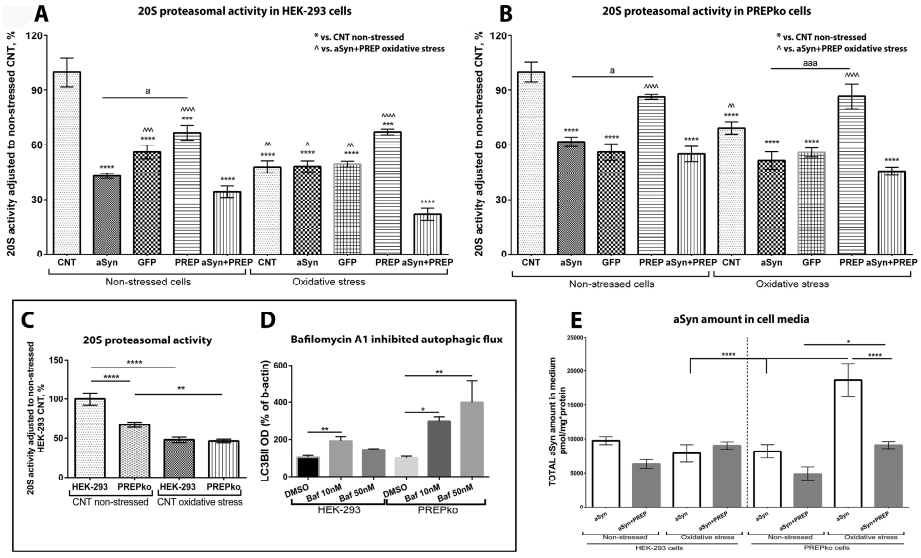

Figure. 12 PREPko cells show altered proteasomal and autophagic activity, and aSyn distribution in response to oxidative stress and aSyn overexpression. (**A**) HEK-293 cells transfected with aSyn + PREP showed the largest decrease in the proteasomal activity, however, in non-stressed conditions, aSyn and aSyn + PREP groups were not statistically different. (**B**) PREPko cells were less responsive to transfections. There were no differences between GFP, aSyn, and aSyn + PREP transfected cells. (**C**) Basal S20-proteasome activity was decreased in PREPko cells while no differences were observed between cell types in the presence of oxidative stress (two-way ANOVA). (**D**) PREPko cells showed increased LC3BII accumulation after bafilomycin A1 (Baf) treatment. 4 h incubation with Baf (10 nM) showed increased autophagosome accumulation as assessed by LB3BII in wt and PREPko cells, but in PREPko cells there was significantly elevated LC3BII levels after Baf (50 nM) treatment. $^{a,*,\wedge}p < 0.05$, $^{**,\wedge\wedge}p < 0.01$, $^{***,\wedge\wedge\wedge,aaa}p < 0.001$, $^{****,\wedge\wedge\wedge\wedge}p < 0.0005$ (one-way ANOVA). (**E**) PREPko cells in stress condition had increased levels of extracellular aSyn in the aSyn transfected group compared to non-stressed PREPko cells or stressed wt cells with aSyn transfection. Restoring PREP to PREPko cells with aSyn reduced extracellular aSyn to control levels. Bars represent mean ± SEM, $^{*}p < 0.025$, $^{****}p < 0.0005$, three-way ANOVA.

PREPko cells have decreased proteasomal activity compared to the wt cells at the BL level ($p < 0.0005$) while differences between cell types were not observed in the presence of oxidative stress (Fig. 12C; $F_{(1,28)} = 12.842$, $p < 0.001$, two-way ANOVA). Similar to wt cells, PREPko cell 20S-proteasomal activity changed significantly between stress and plasmid transfection conditions (Fig. 12B; $F_{(4,36)} = 5.480$, $p = 0.0015$, two-way ANOVA). The non-stressed control group had statistically higher 20S-proteasomal activity compared to all the groups except the PREP transfected groups (Fig. 12B). In PREPko cells, aSyn + PREP groups were statistically different only to non-

stressed control and PREP transfected groups ($p < 0.0005$), and oxidative stress control ($p = 0.005$) group. When aSyn and PREP transfected groups were compared, a statistical difference was observed between non-stressed ($p = 0.015$) and oxidative stress ($p = 0.0001$) groups that indicated that in PREPko cells overexpression of PREP alone does not significantly decrease 20S-proteasomal activity.

Accumulation of autophagosomes was observed in wt and PREPko cells after 4 h bafilomycin A1 (10 and 50 nM) treatment (Fig. 12D). HEK-293 wt cells showed a 2-fold increase ($p = 0.0031$) in autophagosomes with 10 nM bafilomycin A1 treatment ($F_{(2,9)} = 11.02$, $p = 0.0038$, one-way ANOVA). Concentration-dependent accumulation of autophagosomes was seen in PREPko cells ($F_{(2,9)} = 10.15$, $p = 0.0038$) with a 3-fold increase at 10 nM ($p = 0.046$) and a 4-fold increase at 50 nM ($p = 0.0055$) concentration of bafilomycin A1, suggesting that PREPko cells have increased autophagic flux (Fig. 12D).

We measured aSyn levels in cell medium after we noticed that some of the data from WB showed an apparent decrease of total aSyn in membrane bound and insoluble fractions (Fig. 10). After aSyn transfection and oxidative stress treatment there was a significant increase in aSyn protein levels in PREPko cell media compared to wt cells (Fig. 12E; $p < 0.0005$). PREPko cells showed a significant oxidative stress-related increase of secreted aSyn ($p < 0.0005$) between aSyn and aSyn + PREP transfected PREPko cells (Fig. 12E; $p = 0.021$).

5.6 PREP deletion and inhibition affects beclin1/bcl2 complex phosphorylation by activating upstream kinase pathways responsible for autophagy activation (study III)

Our group has previously demonstrated that PREP inhibition by KYP-2047 induces autophagy and is one of the mechanisms responsible of aSyn clearance (Savolainen et al., 2014). Additionally, data from study I showed that PREPko cells have induced autophagy and altered 20S proteasome activity. In study III (schematic representation Fig. 17C), we characterized the network starting from beclin1 since in a previous publication (Savolainen et al., 2014), PREP inhibition caused changes in beclin1 levels. Particular p-beclin1 phosphorylation event is indicative of beclin1 activation due to dissociation of inhibitory beclin1-bcl2/bcl-xL (B-cell lymphoma 2 /B-cell lymphoma-extra large) complex (Zalckvar et al., 2009b), and phosphorylation of bcl2 (Ser-70) or bcl-xL (Ser-62) residues is associated with reduced binding to, and subsequent activation of, beclin1 (Wei et al., 2008; Pattingre et al., 2009). Indeed, we saw an increased phosphorylation of beclin1 (Thr-119; p-beclin1) after 4 h KYP-2047 treatment (Fig. 13A; $p = 0.008$) in HEK-293 cells. Additionally, increase in bcl2 protein levels were observed (Fig. 13A; p =

0.0403). When PREP was deleted in HEK-293 cells, we saw an upregulated beclin1 ($p = 0.0071$), p-beclin1 ($p = 0.0101$), and phosphorylated bcl2 (Ser-70; $p < 0.0001$), and decreased bcl2 ($p < 0.0001$) levels in PREPko cells compared to the corresponding wt cells (Fig. 13B). In PREPko mouse cortical tissue samples, bcl-xL protein levels were lowered ($p = 0.0429$) and phosphorylated bcl-xL (Ser-62) was upregulated (Fig. 13B; $p = 0.0223$). To test if opposite changes would occur with PREP overexpression, we overexpressed PREP in HEK-293 cells. In wt cells, PREP overexpression caused a significant decrease in p-beclin1 levels compared to control ($p= 0.0003$) or catalytically inactive S554A-PREP ($p = 0.0198$) transfected groups (Fig. 13C), however bcl2 protein levels were decreased as well ($p= 0.0005$).

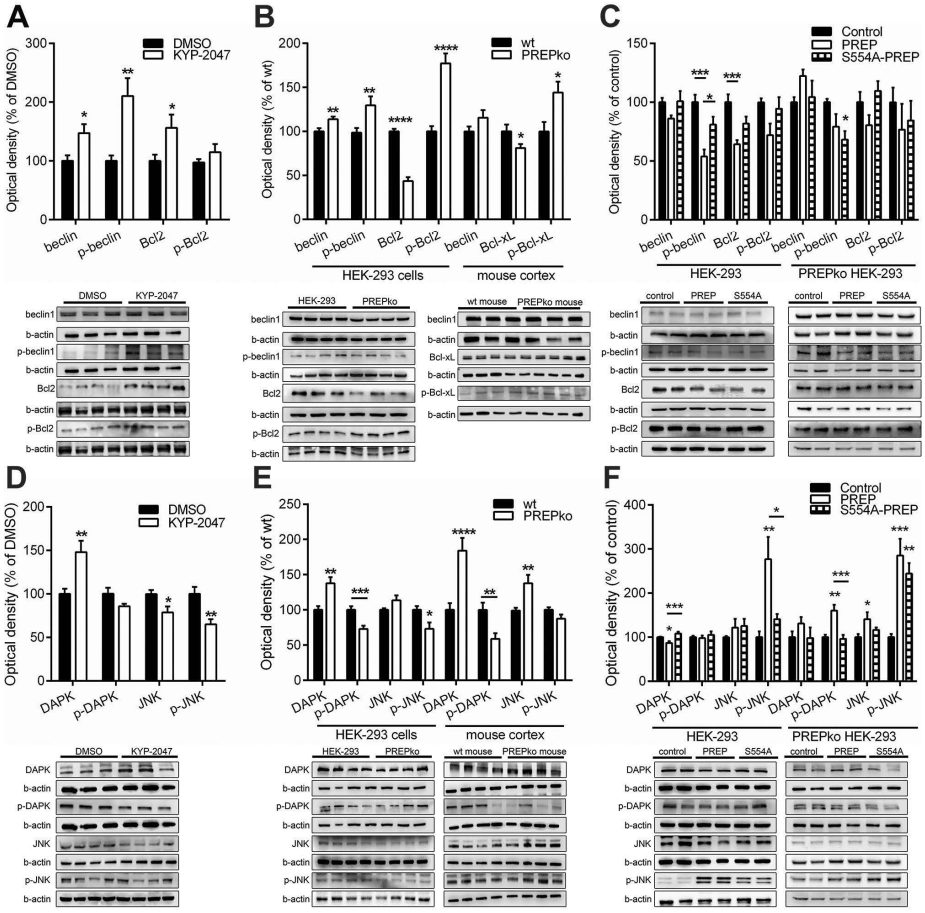

Figure. 13 PREP inhibition or deletion alters PP2A downstream kinase pathways, and beclin1 and bcl2 phosphorylation. (**A**) Beclin1 and bcl2 protein levels and beclin1 Thr-119 phosphorylation (p-beclin1) was increased after 4 h PREP inhibition in HEK-293 cells. (**B**) PREPko cells had upregulated beclin1 and p-beclin1 levels. Bcl2 levels in PREPko cells or Bcl-xL levels in PREPko mouse cortex were decreased while their corresponding phosphorylated forms were increased. (**C**) Wt cells after PREP overexpression had decreased p-beclin1 and bcl2 protein levels, while in PREPko cells a minor decrease in b-beclin1 was seen. (**D**) 4 h PREP inhibition increased DAPK protein levels, and decreased JNK1 protein levels and p-JNK1 (Tyr185) phosphorylation. (**E**) PREPko cells and mice have increased DAPK protein levels and decreased S-308 DAPK phosphorylation (p-DAPK). JNK1 levels were increased in PREPko mice while p-JNK1 was decreased in PREPko cells. (**F**) PREP overexpression or restoration increase p-JNK1 levels. In PREPko cells, p-DAPK was upregulated. Bars represent mean ± SEM, *p < 0.05; **p < 0.01; ***p < 0.001; ****p < 0.0001, student's t-test and ANOVA.

Death-associated protein kinase (DAPK) has been shown to induce autophagy by phosphorylating beclin1 (Zalckvar et al., 2009a; Zalckvar et al., 2009b) while c-Jun N-terminal kinase 1 (JNK1) has been shown to phosphorylate bcl2/bcl-xL at multiple sites (Wei et al., 2008). After 4 h KYP-2047 incubation, DAPK and JNK1 protein levels, Ser-308 phosphorylation site on DAPK (p-DAPK), and Tyr-185 phosphorylation site on JNK1 (p-JNK1) were analyzed by WB (Fig. 13D). PREP inhibition significantly elevated DAPK protein levels ($p = 0.0037$) but had little effect on p-DAPK while both JNK1 ($p= 0.0179$) and p-JNK1 ($p = 0.0031$) levels were decreased. Similar changes were seen in PREPko cells and mouse cortex, where increase in DAPK protein levels (Fig. 13D; cells, $p = 0.0015$; mouse, $p < 0.0001$) and decrease in p-DAPK (Fig. 13D; cells, $p = 0.0003$; mouse, $p = 0.0052$) was detected. Additionally, decrease in p-JNK1 was seen in PREPko cells ($p = 0.0187$) while increase in JNK protein levels ($p= 0.0071$) was seen in PREPko mice cortical tissue samples. Interestingly, PREP overexpression slightly downregulated DAPK protein levels (Fig. 13F) compared to both control ($p = 0.0283$) and S554A-PREP ($p = 0.0005$) groups while p-JNK1 was significantly increased (Fig. 13F) in PREP group ($p = 0052$ vs. control; $p = 0.0217$ vs. S554A-PREP). Restoration of PREP in PREPko cells increased p-DAPK levels only in PREPko group (Fig. 13F; vs. control $p = 0.0014$, vs. S554A-PREP $p = 0.0008$). The effect on p-JNK1 levels in PREPko cells was similar to that observed in wt cells, PREP restoration increased p-JNK1 levels compare to control ($p = 0.002$) but the phosphorylation level in S554A-PREP group was similarly increased compared to control group ($p = 0.0023$) pointing to differences between PREP catalytical activity and protein conformation changes (Fig. 13F).

5.7 PP2A complex regulates downstream kinase activation after PREP inhibition or deletion (study III)

DAPK and JNK1 dephosphorylation is controlled by protein phosphatase 2A (PP2A) that is the main phosphatase in mammalian cells (Fig. 17B-C). Therefore, we wanted to study the effects of PREP inhibition on PP2A. We observed decrease in PP2Ac's phosphorylation levels after 4 h PREP inhibition

(p = 0.005) or FTY720, a known PP2Ac activator (Chen et al., 1992; Cristobal et al., 2011) [0.5 μM; p = 0.0018] treatment (Fig. 14A), indicating increased activity of PP2A. PP2Ac protein levels were slightly increased in KYP-2047 treated group (Fig. 14A; p = 0.0319). When we treated cells with a PP2Ac inhibitor, okadaic acid (OA) [Fig. 14B; 50 nM], or combination of OA and KYP-2047, only OA treated cells had significantly increased phosphorylated Tyr-307 PP2Ac (p-PP2Ac; p = 0.0263) levels. PP2A complex activation correlates with PP2Ac dephosphorylation [Fig. 17A] (Chen et al., 1992) and increased phosphorylation of PP2Ac is especially evident in acute myeloid leukemia (Cristobal et al., 2011).

Interestingly, in PREPko cells p-PP2Ac phosphorylation levels were significantly decreased (Fig. 14C; p < 0.0001) while in PREPko mice cortex the total PP2Ac protein levels are upregulated (p = 0.0031). However, when PREP or S554A-PREP was overexpressed changes were seen only in wt HEK-293 cells (Fig. 14D). The PREP transfected group had significantly decreased PP2Ac levels (Fig. 14D; vs. control, p < 0.0001; vs. S554A-PREP, p = 0.0016) while p-PP2Ac phosphorylation was decreased in PREP (p= 0.0377) and S554A-PREP (p= 0.0377) groups compared to control.

Changes in PP2Ac phosphorylation and protein levels prompted us to investigate whether PREP modifications could have an effect on PP2A subunits, and if PREP could regulate PP2Ac's activity by modifying its endogenous regulators. Interestingly, PP2A 55 kDa regulatory subunit B alpha (B55α) protein levels after 4 h PREP inhibition were decreased (Fig. 15C; p =0.0016), however in PREPko cells (Fig. 15D; p = 0.003) and PREPko mice cortical tissue (Fig. 15C; p = 0.0351) the levels were increased. When PREP was overexpressed, decrease in B55α was seen only in wt HEK-293 cells compared to control (p = 0.0162) and S554A-PREP (p = 0.0016) transfected samples (Fig. 15F). After 4 h KYP-2047 treatment, the levels of an endogenous inhibitor, PME1, protein levels were decreased (Fig. 15C; p = 0.0419), but not in PREPko cells or animals (Fig. 15D). However, in PREPko cells, PREP restoration significantly increased PME1 levels compared to the control group (Fig. 15E; p = 0.0026). Another PP2Ac regulator that changed due the PREP modifications, was PTPA that was significantly lowered by PREP overexpression (Fig. 15E; vs. control, p = 0.0138; vs. S554A-PREP, p = 0.0313) in wt cells as well as in PREPko cells (Fig. 15E; p = 0.0253). However, levels were not changed after PREP inhibition in PREPko cells or animal cortex (Fig. 15C-D).

Thereafter we tested if PREP could be interacting with PP2Ac complex subunits or regulatory proteins. PCA was used to screen for putative interaction partners. Surprisingly, a luminescence signal indicating a direct interaction between PREP-PP2Ac, PREP-PME1, and PREP-PTPA (Fig. 14H) was seen. When cells were treated with 10 μM KYP-2047, the signal intensity was significantly increased for PREP-PME1 (Fig. 14H; p = 0.0391). When PREP or S554A-PREP complex formation with the aforementioned proteins

was tested, signal intensity was increased between S554A-PREP-PME1 and S554A-PREP-PP2Ac complex (Fig. 14I).

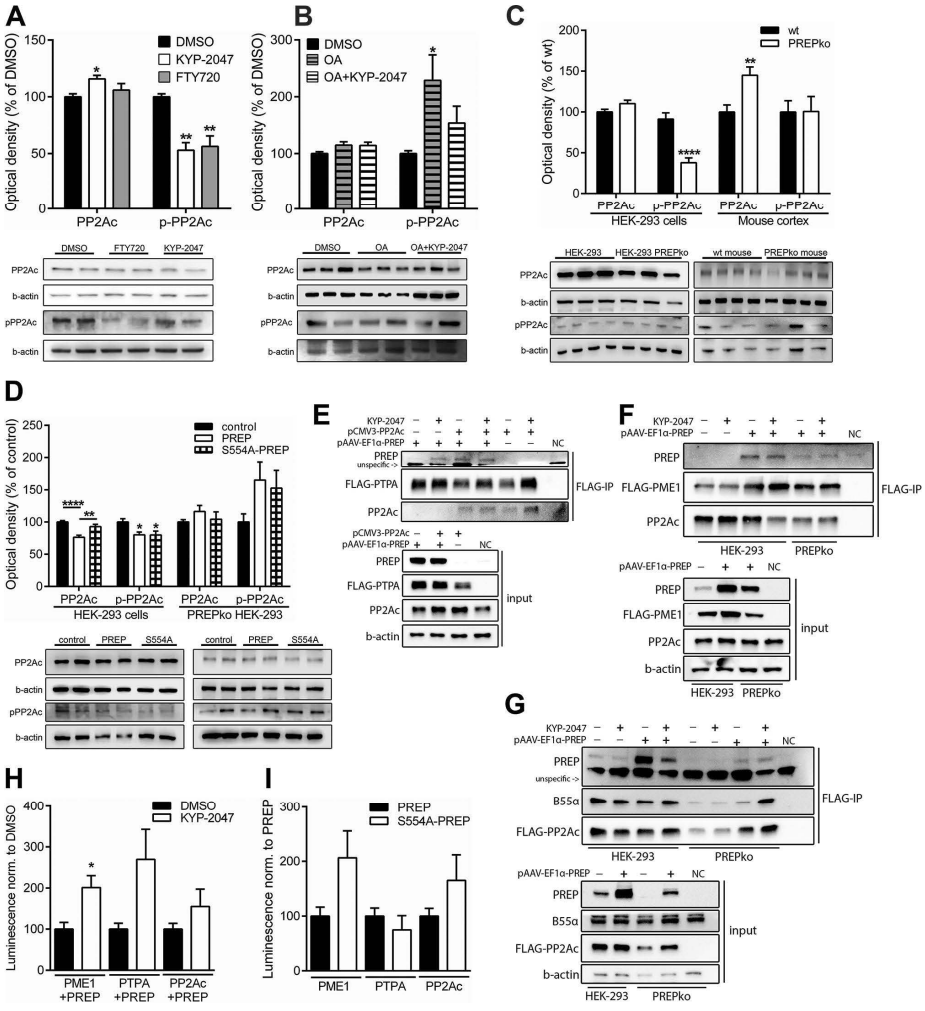

Figure. 14 PREP is a novel PP2A complex interacting protein that after inhibition or deletion dephosphorylates PP2Ac at Tyr-307. (**A-B**) PP2Ac and p-PP2Ac protein levels were altered after HEK-293 cells were treated 4 h with KYP-2047 (1 μM), FTY720 (0.5 μM), OA (50 nM), and combination of OA and KYP-2047. (**C**) p-PP2Ac levels are significantly decreased in HEK-293 PREPko cells while in PREPko animals PP2Ac protein levels are upregulated. (**D**) PREP overexpression in HEK-293 cells decreased PP2Ac levels and its phosphorylation. (**E-G**) FLAG-PTPA, FLAG-PME1, and FLAG-PP2Ac immunoprecipitate PREP. B55α pulldown in PREPko cells was reduced but could be restored by overexpressing PREP. (**H-I**) Luminescence signal was detected between GLuc fused PREP or S554A-PREP and GLuc-PME1, GLuc-PTPA plasmids in HEK-293 PREPko cells. Luminescence signal between proteins increased after 4 h incubation with KYP-2047 (10 μM). Bars represent mean ± SEM, *p < 0.05; **p < 0.01; ****p < 0.0001, student's t-test and ANOVA.

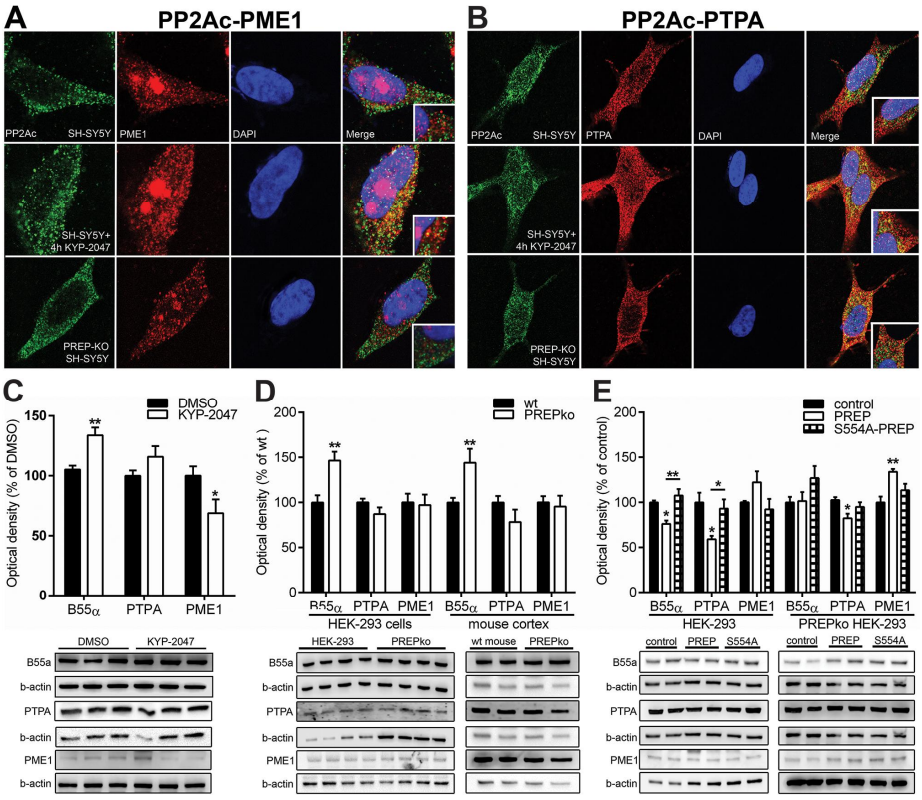

Figure. 15 PREP inhibition or deletion affects B55α, PTPA, and PME1 protein levels and their colocalization with PP2Ac. ICC was performed in SH-SY5Y wt (incubated with either DMSO or KYP-2047) or PREPko cells. (**A**) PP2Ac (in green) and PME1 (red) (**B**) PP2Ac (in green) and PTPA (red). Scale bars: 5 μm. (**C**) HEK-293 cells treated 4 h with KYP-2047 showed increased B55α and decreased PME1 protein levels. (**D**) B55α levels were increased in PREPko cell and mice cortical tissue samples. (**E**) PREP overexpression in wt cells decreased B55α and PTPA levels, while in PREPko cells PREP restoration reduced PTPA and increased PME1 protein levels. Bars represent mean ± SEM, *p < 0.05; **p < 0.01, student's t-test and ANOVA.

We attempted to coIP PREP with FLAG-PTPA, FLAG-PME1, and FLAG-PP2Ac (Fig. 14E-G). FLAG-PTPA immunoprecipitated PREP, and moreover, PREP coIP was more pronounced when KYP-2047 was added to the incubation buffer or when PP2Ac was overexpressed in addition to PREP and FLAG-PTPA (Fig. 14E). We were able to immunoprecipitate PREP with FLAG-PME1 (Fig. 14F) and FLAG-PP2Ac (Fig. 14G) but KYP-2047 had no effect on the interaction. However, when B55α levels were measured from the same samples, FLAG-PP2Ac in PREPko cell fractions did not immunoprecipitate B55α, and only after PREP restoration B55α pulldown slightly increased. Interestingly, B55α levels were restored to those observed in wt cells after PREP overexpression and KYP-2047 addition to the incubation buffer (Fig. 14G).

These results were supported by immunocytochemistry showing that the PP2Ac-PME1 interaction was increased with KYP-2047 treatment (Fig. 15A). Complete loss of PREP affected PP2Ac-PME1 complex formation differently than catalytical inhibition, most of the PME1 and PP2Ac staining was lost in PREPko cell nuclei while PP2Ac puncta were smaller in cytosol (Fig. 15A). Similar but less pronounced colocalization was seen between PP2Ac-PTPA complex after PREP inhibition or deletion (Fig. 15B).

5.8 Impact of PREP inhibition and deletion on PP2A-mediated disease models (study III)

Downregulation of PP2A activity has been connected to tau hyperphosphorylation in AD (Sontag and Sontag, 2014), and to uncontrolled cell proliferation in various cancers (Ruvolo, 2016). Since elevated PREP activities have been reported in these conditions (Sakaguchi et al., 2011; Hannula et al., 2013; Larrinaga et al., 2014; Suzuki et al., 2014; Tanaka et al., 2017), we wanted to test if PREP inhibitors have beneficial effects on cellular models of these diseases. HEK-293 cells were transfected with 0N4R tau and its aggregation was initiated with OA. Thereafter, two total tau antibodies were used to measure tau aggregation in HEK-293 cells with tau overexpression after OA+KYP-2047 treatment (Fig. 16IA-C). When we used an antibody that has been raised against a peptide close to the Ser-262 phosphorylation site, in the soluble fraction tau levels were significantly upregulated in both OA (Fig. 16A; vs. KYP-2047 treated group; $p = 0.0007$) and OA+KYP-2047 (Fig. 16A; vs. KYP-2047 treated group; $p = 0.0137$) groups. In the insoluble fraction, the OA+KYP-2047 treated group had reduced tau aggregation (Fig. 16A). Total tau antibody (Tau5) showed increased tau levels in the soluble cell fraction in the OA+KYP-2047 treated group (Fig. 16B; vs. KYP-2047 treated group; $p = 0.0108$) but similar to S262-Tau, the insoluble fraction had significantly increased tau protein levels only in the OA treated group (Fig. 16B; vs. KYP-2047 treated group; $p = 0.0102$).

Additionally, to assess PREP's impact on other cellular processes regulated by PP2A, we measured cell proliferation. HEK-293 PREPko cell proliferation levels were significantly reduced compared to wt cells (Fig. 16D; $p = 0.0002$). However, when wt cells were incubated with KYP-2047, we saw only minor changes in the proliferation rate (Fig. 16E). Though when we treated breast cancer cell line (MCF7, Fig. 16F), that is reported to have an increased expression of PP2A inhibitory protein SET and reduced PP2A activity (Rincon et al., 2015), we observed reduced proliferation rate of the MCF7 cells with 10 μM KYP-2047 treatment (vs. DMSO $p = 0.404$).

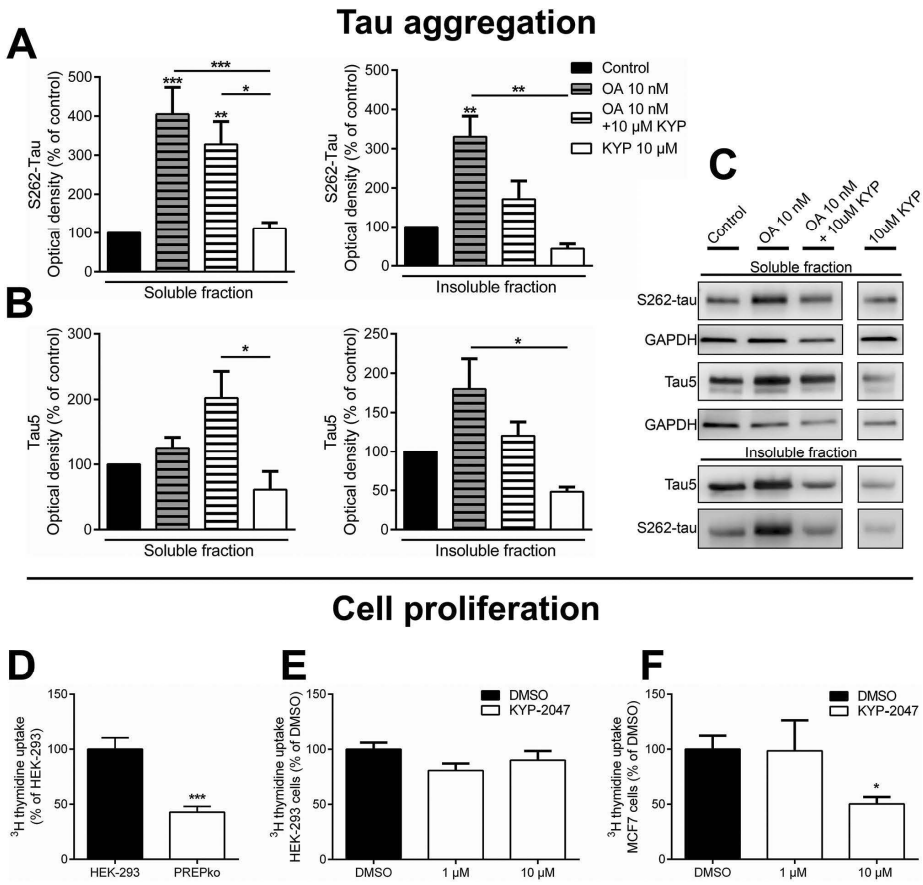

Figure. 16 PREP deletion and inhibition decreases OA caused tau aggregation and cell proliferation in a cancer cell line. HEK-293 cells were treated with OA (10 nM) and combination of OA and KYP-2047 (10 μM) for 48 h and tau protein distribution between the soluble and insoluble fractions was measured with (**A**) total tau5 and (**B**) S262-tau antibodies. OA and KYP-2047 treated samples had decreased aggregate levels in insoluble fractions. (**C**) Representative WB images for figures **A** and **B**, full bands in study III's supplementary material. Cell proliferation rate was measured by [methyl-^{3}H] thymidine incorporation from (**D**) HEK-293 wt and PREPko cells, (**E**) HEK-293 cells treated with KYP-2047, and (**F**) MCF7 cells treated with KYP-2047 for 24h. PREPko cells and MCF7 cells after KYP-2047 treatment showed decreased proliferation rate. Bars represent mean ± SEM, *p < 0.05; **p < 0.01; ***p < 0.001; ****p < 0.0001; student's t-test and ANOVA.

6 DISCUSSION

6.1 Methodological considerations

PREP has been implicated in the pathology of AD and PD as the colocalization of PREP has been reported with aSyn in PD patient SN and with β-amyloid plaques and tau protein in AD patient *post-mortem* brains (Hannula et al., 2013). Several studies have reported changes in PREP enzyme activity in these diseases (Mantle et al., 1996a; Laitinen et al., 2001) and during aging (Jiang et al., 2001). Earlier studies have demonstrated a beneficial effect of PREP inhibition on aSyn aggregation *in vitro* (Brandt et al., 2008), in cell models (Myohanen et al., 2012; Dokleja et al., 2014), and in transgenic animal brains (Myohanen et al., 2012; Savolainen et al., 2014). Additionally, reports on PREP protein-protein interactions indicate that PREP's non-hydrolytic functions could be catalytical activity independent (Di Daniel et al., 2009; Savolainen et al., 2015). For example, the abnormal neuronal growth cone morphology that is seen in PREPko mice can be restored to the wt animal phenotype after overexpression of catalytically inactive PREP (Di Daniel et al., 2009). Similarly, PREP binding to aSyn is PREP activity independent (Savolainen et al., 2015). Comprehensive research has been done on aSyn aggregation after PREP catalytical inhibition. However, there has not been any data on aSyn aggregation in the absence of PREP in cells or animals. Aforementioned reports indicate that addressing PREP modulation with only PREP inhibitors might not be sufficient to elucidate PREP's role on aSyn aggregation.

In this work, the aSyn AAV vector overexpression model was chosen because aSyn AAV vectors have high efficiency to transfect neurons in the SNpc. After AAV delivery, histopathological changes develop over a relatively short time [4 to 8 weeks] (Kirik and Björklund, 2003) compared to transgenic animal models where initial symptoms develop slowly (9-12 months). In a prior PREP inhibitor study, even though PREP inhibition increased aSyn clearance and reduced aSyn immunoreactivity in a transgenic mouse line, clear motor changes were not seen (Savolainen et al., 2014). Unilateral aSyn overexpression presents an opportunity to evaluate loss of TH+ cells, appearance of motor deterioration that in turn would present an opportunity for PREP inhibitor intervention. After aSyn overexpression, initial spontaneous motor asymmetry in the cylinder test is largely caused by impaired dopamine release while total striatal dopamine content remains steady and TH+ cell loss is not seen (Lam et al., 2011; Gaugler et al., 2012). Consequently, the aSyn viral vector model is suitable for evaluation of drugs that have potential to reduce aSyn mediated synaptic toxicity when dopaminergic cell loss is still not apparent.

6.2 aSyn toxicity is altered in the absence of PREP (I)

In study I, it was demonstrated that PREPko animals are less sensitive to aSyn overexpression. Restoration of PREP together with aSyn overexpression resulted in a more pronounced drop in locomotor activity in aSyn + PREP injected animals, pointing to increased toxicity. In cylinder test, PREPko animals irrespective of viral vector injections did not exhibit motor misbalance that could be explained by increased extracellular levels of dopamine and delayed dopamine reuptake by dopamine transporter in PREPko mice striatum (Julku et al., 2018). aSyn + PREP injected animals had less TH+ cells in SN as opposed to aSyn injected animals and this could be either the synergic increase in aSyn toxicity due to PREP overexpression or due to an increased load of viral vector particles that were injected in the aSyn + PREP animal groups. However, cell data would support the prior reason of PREP potentiating aSyn toxicity, as aSyn + PREP transfected groups exhibited the highest cell death. Additionally, PREPko mice that had PREP restored in their nigrostriatal tract did not exhibit any toxicity (Julku et al., 2018).

aSyn aggregation was quantified by stereology but no apparent changes were seen in oligomer numbers between wt and PREPko animals. Nevertheless, PK-resistant aSyn oligomers were significantly reduced in PREPko mice injected with aSyn + PREP and the same observation held true for the p-S129 aSyn. This could indicate that PREPko mice injected with aSyn+ PREP have more soluble oligomer aSyn species that are thought to be more toxic (Karpinar et al., 2009; Winner et al., 2011), while reduced aSyn p-S129 levels also corroborated this observation due to the fact that most of the aSyn in, for example, LBs is phosphorylated. However, whether p-S129 aSyn is an indicator of toxicity is not comprehensively understood (Oueslati, 2016).

Experiments with PREPko cells indicated that lack of PREP could ameliorate aSyn toxicity due to increased autophagic flux, at the same time cells showed reduced 20S proteasomal activity at basal conditions. Increase in autophagic flux is similar between PREP inhibition and deletion. However, in transgenic mice PREP inhibition was showed to increase 20S proteasomal activity to the wt mice levels (Savolainen et al., 2014), but in study I, the overexpression of PREP in PREPko cells barely reduced 20S proteasomal activity. This could be an indication that PREPko cells have developed compensatory mechanisms that allow them to cope with protein overload.

Additionally, PREPko animals do not respond to the lipopolysaccharide (LPS)-induced microglial activation pointing to direct involvement of PREP in neuroinflammation (Hofling et al., 2016). PREP is not present in glial cells of the healthy brain, however during inflammation PREP expression in microglial cells rapidly increases (Penttinen et al., 2011). aSyn is a known inducer of microglial activation (Rocha et al., 2018) and aSyn aggregates are able to potentiate neurotoxicity via glial activation. After aSyn aggregate engulfment, activated microglia rapidly starts producing ROS via NADPH oxidase (nicotinamide adenine dinucleotide phosphate oxidase) associated

pathways (Zhang et al., 2005). While PREP inhibitor, KYP-2047, is capable of reducing TNFα (tumor necrosis factor alpha) levels and exhibit neuroprotection after microglial stimulation with LPS and IFNγ (interferon gamma) in neuronal co-cultures (Natunen et al., 2018). Interestingly, IFNγ and aSyn stimulated microglial supernatant toxicity in SH-SY5Y cells could be abolished by PREP inhibition (Klegeris et al., 2008). Even though study I did not address the possible role of microglial activation as a mechanism of reduced aSyn toxicity, it could provide an explanation for PREPko animal resistance to aSyn toxicity (Hofling et al., 2016).

6.3 PREP inhibition decreases aSyn oligomer particle numbers and improves motor behavior in the aSyn virus vector overexpression mouse model (II)

Since none of the earlier reports of PREP inhibition on aSyn aggregation showed behavioral changes, the main purpose of study II was to establish whether aSyn-caused motor deficits can be rescued by PREP inhibition. Consequently, study II was aimed at establishing the aSyn viral vector overexpression mouse model that would have motor misbalance after aSyn overexpression in nigrostriatal tract in order to administer KYP-2047 after motor deterioration would have become apparent. The main findings in study II were that chronic intraventricular KYP-2047 delivery restores aSyn-caused unilateral motor misbalance to the levels of control animals. This effect was likely mediated through decreased PK soluble aSyn aggregate formation in SN. While PREP inhibition had little effect on total aSyn protein levels, thus further supporting the impact of PREP on formation of aSyn oligomers as shown in study I. Additionally, TH+ stereology showed decreased neuron loss in the KYP-2047 treated animal group compared to controls pointing to increased neuronal survival after KYP-2047 treatment was initiated. There has been contradictory information on dopaminergic cell loss in aSyn viral vector based mouse models in the literature (St Martin et al., 2007; Lee et al., 2012; Oliveras-Salva et al., 2013), and the idea that aSyn overexpression can cause motor impairment without dopaminergic cell loss has been under debate (Lee et al., 2012).

Similarly, in study I, TH+ cell loss was mild but caused a behavioral response, probably due to the decreased extracellular dopamine in striatum. However, our findings did not fully support the idea that PD-phenotype in the aSyn overexpression model is dependent on dopaminergic cell loss. It is possible that mouse endogenous aSyn protects cells from human aSyn overexpression as suggested by Luk et al. (2016). To support this, aSyn virus vector injections have been more toxic in rats (Kirik et al., 2002; Yamada et al., 2004), and in a recent paper, aSyn viral vector overexpression in rat SN showed a direct impact on nigrostriatal projection degeneration and loss of unilateral vesicular monoamine transporter 2 (VMAT2). This indicates that

aSyn aggregation in early stages of PD pathology initiate motor symptoms via disruption in dopamine homeostasis and aberrations in synaptic transmission independently of cell loss (Phan et al., 2017).

Even though study II did not directly address this issue it could be extrapolated that earlier findings of KYP-2047-induced autophagic aSyn degradation and reduced aSyn dimerization could have contributed to the reduced aSyn oligomerization and improved motor behavior (Savolainen et al., 2014; Savolainen et al., 2015). Particularly, the reduced PK soluble aSyn species in the presence of KYP-2047 point to PREP's role in the early stages of aSyn aggregation and especially in dimerization of aSyn that has been previously suggested from *in vitro* studies (Lambeir, 2011; Savolainen et al., 2015). Moreover, since PK-resistant aSyn inclusions were not decreased as effectively as soluble forms after KYP-2047 treatment, this suggests that this might be related to the protein degradation pathway's ability to degrade these inclusions after they have already been formed. There are no reports about autophagy's ability to degrade *in vivo* formed insoluble aSyn aggregates, and at least insoluble preformed fibrils are not degraded by autophagy (Tanik et al., 2013).

Whether LBs and higher order aSyn aggregates are the main cause of the neuronal toxicity is highly debated. Large aggregates could act as a protective mechanism that sequesters soluble toxic oligomer species (Roberts and Brown, 2015; Brundin et al., 2017; Peng et al., 2018). There are reports showing that soluble oligomers rich in β-structure are highly toxic species (Cremades et al., 2012), and this supports the use of PREP inhibition to reduce aSyn toxicity in synucleinopathies.

6.4 PREP and PP2A complex interaction and activity is modulated by KYP-2047 (III)

From the discovery of PREP as a proline cleaving peptidase in the early seventies (Walter et al., 1971) up until a decade ago, PREP research has focused mainly on its peptidase activity (Garcia-Horsman et al., 2007). However, *in vitro* substrates for PREP could not be verified in the *in vivo* studies, and fairly recently, PREP has been demonstrated to form direct protein interactions independently of its catalytical activity with growth-associated protein GAP-43, GAPDH, and aSyn (Di Daniel et al., 2009; Matsuda et al., 2013; Savolainen et al., 2015). In relation to aSyn, it was demonstrated that PREP increases aSyn aggregation *in vitro* but this process could be reversed by PREP catalytical inhibition (Brandt et al., 2008). Later on it was shown that PREP inhibition does not dissociate PREP and aSyn complex and that PREP conformational changes upon PREP inhibition prevented aSyn dimerization (Savolainen et al., 2015). Due to these observations, it was suggested that PREP might act as a regulatory protein through peptide-gated protein interactions where PREP enzymatic activity has a secondary importance (Mannisto and Garcia-

Horsman, 2017). Although PREP has been reported to participate in various physiological and pathological processes, such as cell proliferation and maturation (Agirregoitia et al., 2007; Moreno-Baylach et al., 2011), cellular signaling (Harwood, 2011), protein processing (Tenorio-Laranga et al., 2012), and several others, the primary physiological role for PREP has not been found.

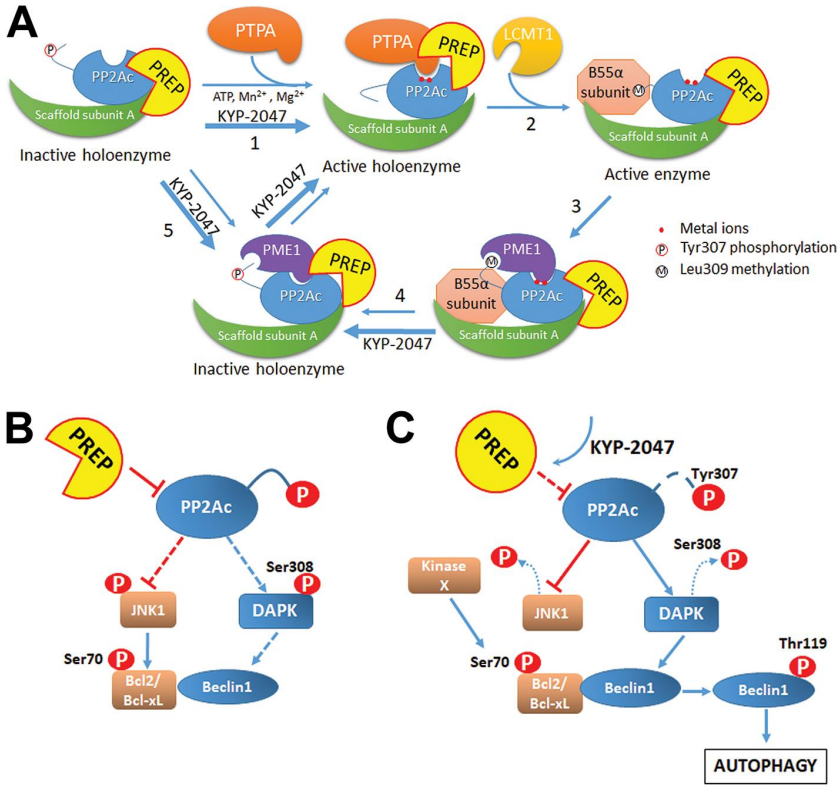

Figure. 17 Schematic representation of PREP role in PP2A complex and downstream kinase pathway activation. (**A**) PP2Ac forms a complex with scaffold subunit A and PREP; phosphorylation of PP2Ac renders it inactive. **1**. After PP2Ac is dephosphorylated, PTPA in the presence of ATP and metal ions activates PP2Ac catalytical pocket; **2**. Leucine carboxyl methyltransferase 1 (LCMT1) binds to the PP2Ac and methylates Leu-309. Methylated PP2Ac allows binding of B55α; **3**. PME1 binds PP2A complex and demethylates PP2Ac; **4**. B55α and metal ions dissociate from the catalytical pocket rendering PP2A inactive (stable); **5**. PME1 can bind inactive PP2A holoenzyme. KYP-2047 increases binding and recycling time between active/inactive PP2A complexes. (**B**) PREP negatively affects PP2A activity by reducing PP2Ac autodephosphorylation. (**C**) KYP-2047 changes PREP binding to the PP2A and facilitates PP2Ac dephosphorylation. PP2A dephosphorylates DAPK and JNK1 inactivating JNK1 and activating DAPK. DAPK phosphorylates beclin1 while unknown kinase (kinase X) pathway phosphorylates bcl2/bcl-xL. Phosphorylation of beclin1/bcl2/bcl-xL dissociates complex and activates autophagy.

In this study, we showed that PREP regulates PP2A – the main serine/threonine phosphatase in mammalian cells – via direct protein-protein interactions (schematic representation in Fig. 17A). Our studies show that

PREP catalytical activity is not essential for PP2A complex binding, supporting the hypothesis that peptidase activity is not the main cellular function of PREP. However, divergence in downstream kinase pathways after PREP or catalytically inactive S554A-PREP overexpression point to protein conformation and/or PREP enzymatic activity as a prerequisite for the full PP2A activation. Previous PREP-aSyn interaction studies have demonstrated that interaction between aSyn and S554A-PREP is stronger than the binding between the PREP-aSyn complex, however the S554A-PREP interaction could not be altered with PREP inhibitors (Savolainen et al., 2015), giving additional strength to catalytically active PREP conformation being an important factor in PREP protein-protein interactions.

Study III's data indicates that PREP could exist in different PP2A protein complexes, as PREP was immunoprecipitated with PME1, PTPA, and PP2Ac. Increased luminescence signal was seen between PREP and PME1 after KYP-2047 treatment and this suggests that inhibited PREP conformer more actively interacts with PME1. Additionally, PP2Ac and PME1 colocalization data indicated that after KYP-2047 treatment proximity of PP2Ac-PME1 is increased. PP2Ac is the only known PME1 substrate (Lee et al., 1996; Yabe et al., 2018) and PME1 binding to PP2Ac is necessary for its demethylation, but at the same time, PME1 inactivates PP2Ac by evicting metal ions from the catalytical pocket of PP2Ac (Xing et al., 2008). Moreover, PME1 acts as a regulator of PP2Ac stability and protects it from ubiquitination and proteasomal degradation (Yabe et al., 2015). However, in pathological conditions PME1 has been reported to act as a PP2A inhibitor, as increased PME1 protein levels have been reported in cancer (Wandzioch et al., 2014). Then again, PME1 bound inactive PP2A complex can be reactivated by PTPA (Fellner et al., 2003; Longin et al., 2004; Hombauer et al., 2007), and PTPA can indirectly control PP2Ac phosphorylation levels by mediating protein tyrosine phosphatase 1B protein and mRNA levels, thus leading to the decrease in PP2Ac phosphorylation (Luo et al., 2013). In study III, colocalization of PP2Ac and PTPA after KYP-2047 inhibition was increased; this PTPA proximity could be an indicator of PP2A complex reactivation and this was supported by decreased Tyr-307 phosphorylation of PP2Ac and corresponding changes in the kinase network (see below). KYP-2047 treatment, PREPko cell and animal data points to a scenario where PREP inhibition initially inactivates PP2A complex by increasing PP2Ac-PME1 complex assembly and protects it from degradation. At the same time, PREP inhibition increases PTPA and PP2Ac proximity that allows for a rapid PP2A complex activation (Fig. 17A).

As stated above, decreased PP2Ac phosphorylation in PREPko systems and after KYP-2047 treatment indicated that PP2Ac is activated (Chen et al., 1992; Liu et al., 2008). Increased PP2A activity was additionally validated by PP2A downstream kinase pathway activation: we saw activating dephosphorylation in Ser-308 in DAPK, inhibiting dephosphorylation in JNK Tyr-185, and corresponding changes in beclin1 Thr-119 phosphorylation and Bcl2/Bcl-xL

levels. This leads to dissociation of Beclin1-Bcl-2/Bcl-xL complexes and initiation of autophagosome formation after PREP inhibition or deletion. Additionally, we screened changes in phosphorylation rates of PP2A-regulated kinases such as Akt, mTORC1, and S6K and saw decreased phosphorylation after PREP inhibition and in PREPko systems that further supports the importance of PREP as a PP2A regulator (see manuscript III). This was further supported by our findings on decreased tau aggregation and cell proliferation after PREP inhibition or deletion. The role of PREP as a PP2A regulator can explain several earlier findings of PREP and its inhibition or deletion. For example, PREP inhibition has been shown to reduce cancer cell proliferation through arrest in G_0/G_1 cell cycle without any effect on non-tumorigenic control cells (Sakaguchi et al., 2011; Larrinaga et al., 2014; Suzuki et al., 2014; Tanaka et al., 2017). Additionally, it would explain reports of PREP involvement in the phosphoinositide metabolism (Williams et al., 1999; Williams et al., 2002) due to lithium impact on PP2A activity (Tsuji et al., 2003; Chen et al., 2006a). PREPko mice brain and body size (Hofling et al., 2016) could be partially attributed to the increased activity of PP2A (Dickey and Strack, 2011; Naetar et al., 2014). Moreover, PP2A activity has been shown to be important in adaptive endotoxin tolerance. Cells repeatedly exposed to LPS show increase in PP2A activity (Sun et al., 2015). In PREPko animals, LPS administration does not induce microglia activation (Hofling et al., 2016).

An initial report by Savolainen et al. (2014) proposed that PREP is a negative regulator of autophagy. However, in light of the results presented in the thesis it is more likely that the beneficial effects that were observed after PREP inhibition in study II or reduced aSyn toxicity in PREPko animals in study I stem from PP2A modulation. Currently, it is not possible to say whether a PREP and aSyn protein-protein interaction is linked to the PP2A activity. There is indication that aSyn can directly modulate PP2A activity (Qu et al., 2018). Activation of PP2A, similarly, has been suggested for the treatment of PD and AD (Park et al., 2016). For example, eicosanoyl-5-hydroxytryptamide (EHT) has been shown to reduce aSyn phosphorylation and aggregation by preventing dephosphorylation of PP2A in an aSyn transgenic mouse model (Lee et al., 2011). While in an AD mouse model, sodium selenite, a PP2A activator, was shown to reduce tau phosphorylation (Corcoran et al., 2010; van Eersel et al., 2010). Additionally, PP2A is an important drug target for cancer therapy as PP2A downregulation is a common cancer resistance mechanism (Chen et al., 1992; Cristobal et al., 2011; Kauko et al., 2018). For example, PP2A activation in a co-treatment with kinase inhibitors has been suggested as a potentially lethal therapy for hard to treat cancers as it would sensitize cancer cells to kinase inhibitors (Westermarck, 2018). Evidence of a PREP and PP2A interaction still does not address important questions about which PP2A complexes are activating autophagy after PREP inhibition and whether activation of other PP2A downstream pathways would contribute to unwanted side effects.

7 CONCLUSIONS

The aim of this study was to investigate the role of PREP deletion or inhibition on aSyn inclusion formation and clearance both in cells and *in vivo*, and mechanisms orchestrating these processes. In this work, the approach of viral vector overexpression was chosen as the main source of aSyn accumulation and aggregation *in vivo*. Findings in this work validate data from earlier PREP inhibitor studies in transgenic aSyn animal models and suggest an explanation to the long held debate about PREP's physiological role in cells. Moreover, the molecular mechanisms underlying PREP activity in cells suggest that PREP inhibition could not only be a novel strategy in treating synucleinopathies but also could be implemented in other neurodegenerative disorders as well as cancer. The main findings from the studies are:

I PREP enhances aSyn-mediated toxicity in cells and *in vivo* after PREP restoration in PREPko cells and mice nigrostriatal tract. However, PREPko cell data points to cellular adaptation processes such as increased autophagy, changed proteasomal activity, and aSyn secretion that mitigate aSyn overexpression-caused toxicity when PREP is restored to the PREPko cells and animals.

II Chronic PREP inhibition in mouse aSyn viral vector overexpression PD model reduced aSyn oligomer formation without affecting total aSyn amount. Moreover, KYP-2047 treatment was sufficient to abolish unilateral motor misbalance associated with unilateral aSyn toxicity.

III PREP deletion and inhibition affects PP2A complex activity through direct protein-protein interaction. This interaction can be modulated by PREP inhibition that increases PP2A activity and upregulates e.g., autophagy-inducing proteins. This offers several novel possibilities for PREP modulation in drug discovery, and may explain earlier reports about PREP, including its impacts on cell proliferation, changes in its activity during ontogenesis, ageing, tumors, and neurodegeneration, and suggested functions as a regulator for cellular signaling. Consequently, PREP's main physiological function could be regulation of PP2A.

Preclinical implications discussed in this thesis point to PREP inhibition as a feasible target therapy not only for PD but also for other neurodegenerative diseases and possibly cancer. However, before further conclusions can be drawn, different PREP inhibitors should be tested in the preclinical settings.

REFERENCES

Abeliovich A, Schmitz Y, Fariñas I, Choi-Lundberg D, Ho W-H, Castillo PE, Shinsky N, Verdugo JMG, Armanini M, Ryan A, Hynes M, Phillips H, Sulzer D, Rosenthal A (2000) Mice Lacking α-Synuclein Display Functional Deficits in the Nigrostriatal Dopamine System. Neuron 25:239-252.

Abeywardana T, Lin YH, Rott R, Engelender S, Pratt MR (2013) Site-specific differences in proteasome-dependent degradation of monoubiquitinated alpha-synuclein. Chem Biol 20:1207-1213.

Agirregoitia N, Casis L, Gil J, Ruiz F, Irazusta J (2007) Ontogeny of prolyl endopeptidase and pyroglutamyl peptidase I in rat tissues. Regul Pept 139:52-58.

Agirregoitia N, Bizet P, Agirregoitia E, Boutelet I, Peralta L, Vaudry H, Jegou S (2010) Prolyl endopeptidase mRNA expression in the central nervous system during rat development. J Chem Neuroanat 40:53-62.

Alexopoulou Z, Lang J, Perrett RM, Elschami M, Hurry ME, Kim HT, Mazaraki D, Szabo A, Kessler BM, Goldberg AL, Ansorge O, Fulga TA, Tofaris GK (2016) Deubiquitinase Usp8 regulates alpha-synuclein clearance and modifies its toxicity in Lewy body disease. Proc Natl Acad Sci U S A 113:E4688-4697.

Alvarez-Erviti L, Rodriguez-Oroz MC, Cooper JM, Caballero C, Ferrer I, Obeso JA, Schapira AH (2010) Chaperone-mediated autophagy markers in Parkinson disease brains. Arch Neurol 67:1464-1472.

Anderson JP, Walker DE, Goldstein JM, de Laat R, Banducci K, Caccavello RJ, Barbour R, Huang J, Kling K, Lee M (2006) Phosphorylation of Ser-129 is the dominant pathological modification of alpha-synuclein in familial and sporadic Lewy body disease. J Biol Chem 281.

Aoyagi T, Wada T, Nagai M, Kojima F, Harada S, Takeuchi T, Takahashi H, Hirokawa K, Tsumita T (1990) Deficiency of kallikrein-like enzyme activities in cerebral tissue of patients with alzheimer's disease. Experientia 46:94-97.

Asher G, Tsvetkov P, Kahana C, Shaul Y (2005) A mechanism of ubiquitin-independent proteasomal degradation of the tumor suppressors p53 and p73. Genes Dev 19:316-321.

Azeredo da Silveira S, Schneider BL, Cifuentes-Diaz C, Sage D, Abbas-Terki T, Iwatsubo T, Unser M, Aebischer P (2009) Phosphorylation does not prompt, nor prevent, the formation of alpha-synuclein toxic species in a rat model of Parkinson's disease. Hum Mol Genet 18:872-887.

Bandyopadhyay U, Kaushik S, Varticovski L, Cuervo AM (2008) The chaperone-mediated autophagy receptor organizes in dynamic protein complexes at the lysosomal membrane. Mol Cell Biol 28:5747-5763.

Barker RA, Williams-Gray CH (2016) Review: The spectrum of clinical features seen with alpha synuclein pathology. Neuropathol Appl Neurobiol 42:6-19.

Bedford L, Hay D, Devoy A, Paine S, Powe DG, Seth R, Gray T, Topham I, Fone K, Rezvani N, Mee M, Soane T, Layfield R, Sheppard PW, Ebendal T, Usoskin D, Lowe J, Mayer RJ (2008) Depletion of 26S proteasomes in mouse brain neurons causes neurodegeneration and Lewy-like inclusions resembling human pale bodies. J Neurosci 28:8189-8198.

Beitz JM (2014) Parkinson's disease: a review. Front Biosci (Schol Ed) 6:65-74.

Bellemere G, Vaudry H, Morain P, Jegou S (2005) Effect of prolyl endopeptidase inhibition on arginine-vasopressin and thyrotrophin-releasing hormone catabolism in the rat brain. J Neuroendocrinol 17:306-313.

Bennett MC, Bishop JF, Leng Y, Chock PB, Chase TN, Mouradian MM (1999) Degradation of alpha-synuclein by proteasome. J Biol Chem 274:33855-33858.

Benskey MJ, Perez RG, Manfredsson FP (2016) The contribution of alpha synuclein to neuronal survival and function - Implications for Parkinson's disease. J Neurochem 137:331-359.

Bentea E, Van der Perren A, Van Liefferinge J, El Arfani A, Albertini G, Demuyser T, Merckx E, Michotte Y, Smolders I, Baekelandt V, Massie A (2015) Nigral proteasome inhibition in mice leads to motor and non-motor deficits and increased expression of Ser129 phosphorylated alpha-synuclein. Front Behav Neurosci 9:68.

Braak H, Braak E (2000) Pathoanatomy of Parkinson's disease. J Neurol 247 Suppl 2:II3-10.

Brandt I, Vriendt KD, Devreese B, Beeumen JV, Dongen WV, Augustyns K, Meester ID, Scharpé S, Lambeir A-M (2005) Search for substrates for prolyl oligopeptidase in porcine brain. Peptides 26:2536-2546.

Brandt I, Gerard M, Sergeant K, Devreese B, Baekelandt V, Augustyns K, Scharpe S, Engelborghs Y, Lambeir AM (2008) Prolyl oligopeptidase stimulates the aggregation of alpha-synuclein. Peptides 29:1472-1478.

Brundin P, Dave KD, Kordower JH (2017) Therapeutic approaches to target alpha-synuclein pathology. Exp Neurol 298:225-235.

Brunello CA, Yan X, Huttunen HJ (2016) Internalized Tau sensitizes cells to stress by promoting formation and stability of stress granules. Sci Rep 6:30498.

Burre J, Sharma M, Tsetsenis T, Buchman V, Etherton MR, Sudhof TC (2010) Alpha-synuclein promotes SNARE-complex assembly in vivo and in vitro. Science 329:1663-1667.

Chandra S, Fornai F, Kwon HB, Yazdani U, Atasoy D, Liu X, Hammer RE, Battaglia G, German DC, Castillo PE, Sudhof TC (2004) Double-knockout mice for alpha- and beta-synucleins: effect on synaptic functions. Proc Natl Acad Sci U S A 101:14966-14971.

Chartier-Harlin M, Kachergus J, Roumier C, Mouroux V, Douay X, Lincoln S, Levecque C, Larvor L, Andrieux J, Hulihan M (2004) Alpha-synuclein locus duplication as a cause of familial Parkinson's disease. Lancet 364.

Chau KY, Ching HL, Schapira AH, Cooper JM (2009) Relationship between alpha synuclein phosphorylation, proteasomal inhibition and cell death: relevance to Parkinson's disease pathogenesis. J Neurochem 110:1005-1013.

Chau V, Tobias J, Bachmair A, Marriott D, Ecker D, Gonda D, Varshavsky A (1989) A multiubiquitin chain is confined to specific lysine in a targeted short-lived protein. Science 243:1576-1583.

Chen CL, Lin CF, Chiang CW, Jan MS, Lin YS (2006a) Lithium inhibits ceramide- and etoposide-induced protein phosphatase 2A methylation, Bcl-2 dephosphorylation, caspase-2 activation, and apoptosis. Mol Pharmacol 70:510-517.

Chen J, Martin BL, Brautigan DL (1992) Regulation of protein serine-threonine phosphatase type-2A by tyrosine phosphorylation. Science 257:1261-1264.

Chen L, Thiruchelvam MJ, Madura K, Richfield EK (2006b) Proteasome dysfunction in aged human α-synuclein transgenic mice. Neurobiol Dis 23:120-126.

Chiang HL, Terlecky SR, Plant CP, Dice JF (1989) A role for a 70-kilodalton heat shock protein in lysosomal degradation of intracellular proteins. Science 246:382-385.

Choi BK, Choi MG, Kim JY, Yang Y, Lai Y, Kweon DH, Lee NK, Shin YK (2013) Large alpha-synuclein oligomers inhibit neuronal SNARE-mediated vesicle docking. Proc Natl Acad Sci U S A 110:4087-4092.

Chu Y, Dodiya H, Aebischer P, Olanow CW, Kordower JH (2009) Alterations in lysosomal and proteasomal markers in Parkinson's disease: Relationship to alpha-synuclein inclusions. Neurobiol Dis 35:385-398.

Chung KKK, Zhang Y, Lim KL, Tanaka Y, Huang H, Gao J, Ross CA, Dawson VL, Dawson TM (2001) Parkin ubiquitinates the α-synuclein–interacting protein, synphilin-1: implications for Lewy-body formation in Parkinson disease. Nat Med 7:1144.

Collier TJ, Kanaan NM, Kordower JH (2011) Ageing as a primary risk factor for Parkinson's disease: evidence from studies of non-human primates. Nat Rev Neurosci 12:359-366.

Collier TJ, Redmond DE, Steece-Collier K, Lipton JW, Manfredsson FP (2016) Is Alpha-Synuclein Loss-of-Function a Contributor to Parkinsonian Pathology? Evidence from Non-human Primates. Front Neurosci 10:12.

Conway KA, Harper JD, Lansbury PT (1998) Accelerated in vitro fibril formation by a mutant [alpha]-synuclein linked to early-onset Parkinson disease. Nat Med 4:1318-1320.

Conway KA, Lee SJ, Rochet JC, Ding TT, Williamson RE, Lansbury PT (2000) Acceleration of oligomerization, not fibrillization, is a shared property of both alpha-synuclein mutations linked to early-onset Parkinson's disease: Implications for pathogenesis and therapy. Proc Natl Acad Sci U S A 97:571-576.

Cookson MR (2006) Hero versus antihero: the multiple roles of alpha-synuclein in neurodegeneration. Exp Neurol 199:238-242.

Corcoran NM, Martin D, Hutter-Paier B, Windisch M, Nguyen T, Nheu L, Sundstrom LE, Costello AJ, Hovens CM (2010) Sodium selenate specifically activates PP2A phosphatase, dephosphorylates tau and reverses memory deficits in an Alzheimer's disease model. J Clin Neurosci 17:1025-1033.

Cremades N, Cohen Samuel IA, Deas E, Abramov Andrey Y, Chen Allen Y, Orte A, Sandal M, Clarke Richard W, Dunne P, Aprile Francesco A, Bertoncini Carlos W, Wood Nicholas W, Knowles Tuomas PJ, Dobson Christopher M, Klenerman D (2012) Direct Observation of the Interconversion of Normal and Toxic Forms of α-Synuclein. Cell 149:1048-1059.

Crews L, Tsigelny I, Hashimoto M, Masliah E (2009) Role of Synucleins in Alzheimer's Disease. Neurotox Res 16:306-317.

Cristobal I, Garcia-Orti L, Cirauqui C, Alonso MM, Calasanz MJ, Odero MD (2011) PP2A impaired activity is a common event in acute myeloid leukemia and its activation by forskolin has a potent anti-leukemic effect. Leukemia 25:606-614.

Cuervo AM, Dice JF (1996) A receptor for the selective uptake and degradation of proteins by lysosomes. Science 273:501-503.

Cuervo AM, Stefanis L, Fredenburg R, Lansbury PT, Sulzer D (2004) Impaired Degradation of Mutant α-Synuclein by Chaperone-Mediated Autophagy. Science 305:1292-1295.

Dahmene M, Berard M, Oueslati A (2017) Dissecting the Molecular Pathway Involved in PLK2 Kinase-mediated alpha-Synuclein-selective Autophagic Degradation. J Biol Chem 292:3919-3928.

Dettmer U, Selkoe D, Bartels T (2016) New insights into cellular α-synuclein homeostasis in health and disease. Curr Opin Neurobiol 36:15-22.

Di Daniel E, Glover CP, Grot E, Chan MK, Sanderson TH, White JH, Ellis CL, Gallagher KT, Uney J, Thomas J, Maycox PR, Mudge AW (2009) Prolyl oligopeptidase binds to GAP-43 and functions without its peptidase activity. Mol Cell Neurosci 41:373-382.

Dickey AS, Strack S (2011) PKA/AKAP1 and PP2A/Bbeta2 regulate neuronal morphogenesis via Drp1 phosphorylation and mitochondrial bioenergetics. J Neurosci 31:15716-15726.

Diogenes MJ, Dias RB, Rombo DM, Vicente Miranda H, Maiolino F, Guerreiro P, Nasstrom T, Franquelim HG, Oliveira LM, Castanho MA, Lannfelt L, Bergstrom J, Ingelsson M, Quintas A, Sebastiao AM, Lopes LV, Outeiro TF (2012) Extracellular alpha-synuclein oligomers modulate synaptic transmission and impair LTP via NMDA-receptor activation. J Neurosci 32:11750-11762.

Dokleja L, Hannula MJ, Myohanen TT (2014) Inhibition of prolyl oligopeptidase increases the survival of alpha-synuclein overexpressing cells after rotenone exposure by reducing alpha-synuclein oligomers. Neurosci Lett 583:37-42.

Ebrahimi-Fakhari D, Wahlster L, McLean PJ (2012) Protein degradation pathways in Parkinson's disease: curse or blessing. Acta Neuropathol 124:153-172.

Ebrahimi-Fakhari D, Cantuti-Castelvetri I, Fan Z, Rockenstein E, Masliah E, Hyman BT, McLean PJ, Unni VK (2011) Distinct roles in vivo for the ubiquitin-proteasome system and the autophagy-lysosomal pathway in the degradation of alpha-synuclein. J Neurosci 31:14508-14520.

Eliezer D, Kutluay E, Bussell R, Jr., Browne G (2001) Conformational properties of alpha-synuclein in its free and lipid-associated states. J Mol Biol 307:1061-1073.

Emmanouilidou E, Stefanis L, Vekrellis K (2010) Cell-produced alpha-synuclein oligomers are targeted to, and impair, the 26S proteasome. Neurobiol Aging 31:953-968.

Fagerqvist T, Lindstrom V, Nordstrom E, Lord A, Tucker SM, Su X, Sahlin C, Kasrayan A, Andersson J, Welander H, Nasstrom T, Holmquist M, Schell H, Kahle PJ, Kalimo H, Moller C, Gellerfors P, Lannfelt L, Bergstrom J, Ingelsson M (2013) Monoclonal antibodies selective for alpha-synuclein oligomers/protofibrils recognize brain pathology in Lewy body disorders and alpha-synuclein transgenic mice with the disease-causing A30P mutation. J Neurochem 126:131-144.

Fellner T, Lackner DH, Hombauer H, Piribauer P, Mudrak I, Zaragoza K, Juno C, Ogris E (2003) A novel and essential mechanism determining specificity and activity of protein phosphatase 2A (PP2A) in vivo. Genes Dev 17:2138-2150.

Finley D, Sadis S, Monia BP, Boucher P, Ecker DJ, Crooke ST, Chau V (1994) Inhibition of proteolysis and cell cycle progression in a multiubiquitination-deficient yeast mutant. Mol Cell Biol 14:5501-5509.

Fuchs J, Nilsson C, Kachergus J, Munz M, Larsson EM, Schule B, Langston JW, Middleton FA, Ross OA, Hulihan M, Gasser T, Farrer MJ (2007) Phenotypic variation in a large Swedish pedigree due to SNCA duplication and triplication. Neurology 68:916-922.

Fujiwara H, Hasegawa M, Dohmae N, Kawashima A, Masliah E, Goldberg MS, Shen J, Takio K, Iwatsubo T (2002) α-Synuclein is phosphorylated in synucleinopathy lesions. Nat Cell Biol 4:160.

Fukunari A, Kato A, Sakai Y, Yoshimoto T, Ishiura S, Suzuki K, Nakajima T (1994) Colocalization of prolyl endopeptidase and amyloid beta-peptide in brains of senescence-accelerated mouse. Neurosci Lett 176:201-204.

Fulop V, Bocskei Z, Polgar L (1998) Prolyl oligopeptidase: an unusual beta-propeller domain regulates proteolysis. Cell 94:161-170.

Fulop V, Szeltner Z, Polgar L (2000) Catalysis of serine oligopeptidases is controlled by a gating filter mechanism. EMBO Rep 1:277-281.

Garcia-Horsman JA, Mannisto PT, Venalainen JI (2007) On the role of prolyl oligopeptidase in health and disease. Neuropeptides 41:1-24.

Gaugler MN, Genc O, Bobela W, Mohanna S, Ardah MT, El-Agnaf OM, Cantoni M, Bensadoun J-C, Schneggenburger R, Knott GW, Aebischer P, Schneider BL (2012)

Nigrostriatal overabundance of α-synuclein leads to decreased vesicle density and deficits in dopamine release that correlate with reduced motor activity. Acta Neuropathol 123:653-669.

George S, Rey NL, Reichenbach N, Steiner JA, Brundin P (2013) alpha-Synuclein: the long distance runner. Brain Pathol 23:350-357.

Goossens F, De Meester I, Vanhoof G, Scharpe S (1996) Distribution of prolyl oligopeptidase in human peripheral tissues and body fluids. Eur J Clin Chem Clin Biochem 34:17-22.

Hannula MJ, Myohanen TT, Tenorio-Laranga J, Mannisto PT, Garcia-Horsman JA (2013) Prolyl oligopeptidase colocalizes with alpha-synuclein, beta-amyloid, tau protein and astroglia in the post-mortem brain samples with Parkinson's and Alzheimer's diseases. Neuroscience 242:140-150.

Hara S, Arawaka S, Sato H, Machiya Y, Cui C, Sasaki A, Koyama S, Kato T (2013) Serine 129 phosphorylation of membrane-associated alpha-synuclein modulates dopamine transporter function in a G protein-coupled receptor kinase-dependent manner. Mol Biol Cell 24:1649-1660, S1641-1643.

Hara T, Nakamura K, Matsui M, Yamamoto A, Nakahara Y, Suzuki-Migishima R, Yokoyama M, Mishima K, Saito I, Okano H, Mizushima N (2006) Suppression of basal autophagy in neural cells causes neurodegenerative disease in mice. Nature 441:885-889.

Harwood AJ (2011) Prolyl oligopeptidase, inositol phosphate signalling and lithium sensitivity. CNS Neurol Disord Drug Targets 10:333-339.

Hasegawa M, Fujiwara H, Nonaka T, Wakabayashi K, Takahashi H, Lee VM, Trojanowski JQ, Mann D, Iwatsubo T (2002) Phosphorylated alpha-synuclein is ubiquitinated in alpha-synucleinopathy lesions. J Biol Chem 277:49071-49076.

He C, Klionsky DJ (2009) Regulation mechanisms and signaling pathways of autophagy. Annu Rev Genet 43:67-93.

He C, Levine B (2010) The Beclin 1 interactome. Curr Opin Cell Biol 22:140-149.

Hershko A, Heller H, Elias S, Ciechanover A (1983) Components of ubiquitin-protein ligase system. Resolution, affinity purification, and role in protein breakdown. J Biol Chem 258:8206-8214.

Hicke L (2001) Protein regulation by monoubiquitin. Nat Rev Mol Cell Biol 2:195-201.

Hirai Y, Fujita SC, Iwatsubo T, Hasegawa M (2004) Phosphorylated alpha-synuclein in normal mouse brain. FEBS Lett 572:227-232.

Hof PR, Young WG, Bloom FE, Belichenko PV, Celio MR (2000) Comparative Cytoarchitectonic Atlas of the C57BL6 and 129 Sv Mouse Brains. Amsterdam: Elsevier.

Hofling C, Kulesskaya N, Jaako K, Peltonen I, Mannisto PT, Nurmi A, Vartiainen N, Morawski M, Zharkovsky A, Voikar V, Rossner S, Garcia-Horsman JA (2016) Deficiency of prolyl oligopeptidase in mice disturbs synaptic plasticity and reduces anxiety-like behaviour, body weight, and brain volume. Eur Neuropsychopharmacol 26:1048-1061.

Hombauer H, Weismann D, Mudrak I, Stanzel C, Fellner T, Lackner DH, Ogris E (2007) Generation of active protein phosphatase 2A is coupled to holoenzyme assembly. PLoS Biol 5:e155.

Hurley JH, Schulman BA (2014) Atomistic autophagy: the structures of cellular self-digestion. Cell 157:300-311.

Iacono D, Geraci-Erck M, Rabin ML, Adler CH, Serrano G, Beach TG, Kurlan R (2015) Parkinson disease and incidental Lewy body disease: Just a question of time? Neurology 85:1670-1679.

Ichai C, Chevallier N, Delaere P, Dournaud P, Epelbaum J, Hauw JJ, Vincent JP, Checler F (1994) Influence of region-specific alterations of neuropeptidase content on the catabolic fates of neuropeptides in Alzheimer's disease. J Neurochem 62:645-655.

Irazusta J, Larrinaga G, González-Maeso J, Gil J, Meana JJ, Casis L (2002) Distribution of prolyl endopeptidase activities in rat and human brain. Neurochem Int 40:337-345.

Iwai A, Masliah E, Yoshimoto M, Ge N, Flanagan L, Rohan de Silva HA, Kittel A, Saitoh T (1995) The precursor protein of non-Aβ component of Alzheimer's disease amyloid is a presynaptic protein of the central nervous system. Neuron 14:467-475.

Jakes R, Spillantini MG, Goedert M (1994) Identification of two distinct synucleins from human brain. FEBS Lett 345:27-32.

Jarho EM, Venalainen JI, Huuskonen J, Christiaans JA, Garcia-Horsman JA, Forsberg MM, Jarvinen T, Gynther J, Mannisto PT, Wallen EA (2004) A cyclopent-2-enecarbonyl group mimics proline at the P2 position of prolyl oligopeptidase inhibitors. J Med Chem 47:5605-5607.

Jiang CH, Tsien JZ, Schultz PG, Hu Y (2001) The effects of aging on gene expression in the hypothalamus and cortex of mice. Proc Natl Acad Sci U S A 98:1930-1934.

Juhász T, Szeltner Z, Fülöp V, Polgár L (2005) Unclosed β-Propellers Display Stable Structures: Implications for Substrate Access to the Active Site of Prolyl Oligopeptidase. J Mol Biol 346:907-917.

Julku UH, Panhelainen AE, Tiilikainen SE, Svarcbahs R, Tammimaki AE, Piepponen TP, Savolainen MH, Myohanen TT (2018) Prolyl Oligopeptidase Regulates Dopamine Transporter Phosphorylation in the Nigrostriatal Pathway of Mouse. Mol Neurobiol 55:470-482.

Kahle PJ, Neumann M, Ozmen L, Haass C (2000a) Physiology and pathophysiology of alpha-synuclein. Cell culture and transgenic animal models based on a Parkinson's disease-associated protein. Ann N Y Acad Sci 920:33-41.

Kahle PJ, Neumann M, Ozmen L, Muller V, Jacobsen H, Schindzielorz A, Okochi M, Leimer U, van Der Putten H, Probst A, Kremmer E, Kretzschmar HA, Haass C (2000b) Subcellular localization of wild-type and Parkinson's disease-associated mutant alpha -synuclein in human and transgenic mouse brain. J Neurosci 20:6365-6373.

Kanaan NM, Manfredsson FP (2012) Loss of functional alpha-synuclein: a toxic event in Parkinson's disease? J Parkinsons Dis 2:249-267.

Karpinar DP et al. (2009) Pre-fibrillar alpha-synuclein variants with impaired beta-structure increase neurotoxicity in Parkinson's disease models. EMBO J 28:3256-3268.

Kauko O, O'Connor CM, Kulesskiy E, Sangodkar J, Aakula A, Izadmehr S, Yetukuri L, Yadav B, Padzik A, Laajala TD, Haapaniemi P, Momeny M, Varila T, Ohlmeyer M, Aittokallio T, Wennerberg K, Narla G, Westermarck J (2018) PP2A inhibition is a druggable MEK inhibitor resistance mechanism in KRAS-mutant lung cancer cells. Sci Transl Med 10.

Kayed R, Head E, Thompson JL, McIntire TM, Milton SC, Cotman CW, Glabe CG (2003) Common structure of soluble amyloid oligomers implies common mechanism of pathogenesis. Science 300:486-489.

Khan NL, Graham E, Critchley P, Schrag AE, Wood NW, Lees AJ, Bhatia KP, Quinn N (2003) Parkin disease: a phenotypic study of a large case series. Brain 126:1279-1292.

Kiffin R, Christian C, Knecht E, Cuervo AM (2004) Activation of chaperone-mediated autophagy during oxidative stress. Mol Biol Cell 15:4829-4840.

Kirik D, Björklund A (2003) Modeling CNS neurodegeneration by overexpression of disease-causing proteins using viral vectors. Trends Neurosci 26:386-392.

Kirik D, Rosenblad C, Burger C, Lundberg C, Johansen TE, Muzyczka N, Mandel RJ, Bjorklund A (2002) Parkinson-like neurodegeneration induced by targeted overexpression of alpha-synuclein in the nigrostriatal system. J Neurosci 22:2780-2791.

Kitada T, Asakawa S, Hattori N, Matsumine H, Yamamura Y, Minoshima S, Yokochi M, Mizuno Y, Shimizu N (1998) Mutations in the parkin gene cause autosomal recessive juvenile parkinsonism. Nature 392:605-608.

Klegeris A, Li J, Bammler TK, Jin J, Zhu D, Kashima DT, Pan S, Hashioka S, Maguire J, McGeer PL, Zhang J (2008) Prolyl endopeptidase is revealed following SILAC analysis to be a novel mediator of human microglial and THP-1 cell neurotoxicity. Glia 56:675-685.

Klucken J, Poehler AM, Ebrahimi-Fakhari D, Schneider J, Nuber S, Rockenstein E, Schlotzer-Schrehardt U, Hyman BT, McLean PJ, Masliah E, Winkler J (2012) Alpha-synuclein aggregation involves a bafilomycin A 1-sensitive autophagy pathway. Autophagy 8:754-766.

Koida M, Walter R (1976) Post-proline cleaving enzyme. Purification of this endopeptidase by affinity chromatography. J Biol Chem 251:7593-7599.

Komatsu M, Waguri S, Chiba T, Murata S, Iwata J, Tanida I, Ueno T, Koike M, Uchiyama Y, Kominami E, Tanaka K (2006) Loss of autophagy in the central nervous system causes neurodegeneration in mice. Nature 441:880-884.

Kramer ML, Schulz-Schaeffer WJ (2007) Presynaptic alpha-synuclein aggregates, not Lewy bodies, cause neurodegeneration in dementia with Lewy bodies. J Neurosci 27:1405-1410.

Kruger R, Kuhn W, Muller T, Woitalla D, Graeber M, Kosel S, Przuntek H, Epplen J, Schols L, Riess O (1998) Ala30Pro mutation in the gene encoding alpha-synuclein in Parkinson's disease. Nat Genet 18.

Kuwahara T, Tonegawa R, Ito G, Mitani S, Iwatsubo T (2012) Phosphorylation of alpha-synuclein protein at Ser-129 reduces neuronal dysfunction by lowering its membrane binding property in Caenorhabditis elegans. J Biol Chem 287:7098-7109.

Laitinen KS, van Groen T, Tanila H, Venalainen J, Mannisto PT, Alafuzoff I (2001) Brain prolyl oligopeptidase activity is associated with neuronal damage rather than beta-amyloid accumulation. Neuroreport 12:3309-3312.

Lam HA, Wu N, Cely I, Kelly RL, Hean S, Richter F, Magen I, Cepeda C, Ackerson LC, Walwyn W, Masliah E, Chesselet M-F, Levine MS, Maidment NT (2011) Elevated tonic extracellular dopamine concentration and altered dopamine modulation of synaptic activity precede dopamine loss in the striatum of mice overexpressing human α-synuclein. J Neurosci Res 89:1091-1102.

Lambeir AM (2011) Interaction of prolyl oligopeptidase with alpha-synuclein. CNS Neurol Disord Drug Targets 10:349-354.

Larrinaga G, Perez I, Blanco L, Sanz B, Errarte P, Beitia M, Etxezarraga MC, Loizate A, Gil J, Irazusta J, Lopez JI (2014) Prolyl endopeptidase activity is correlated with colorectal cancer prognosis. Int J Med Sci 11:199-208.

Lashuel HA, Overk CR, Oueslati A, Masliah E (2012) The many faces of α-synuclein: from structure and toxicity to therapeutic target. Nature Reviews Neuroscience 14:38.

Lashuel HA, Overk CR, Oueslati A, Masliah E (2013) The many faces of alpha-synuclein: from structure and toxicity to therapeutic target. Nat Rev Neurosci 14:38-48.

Lee J, Chen Y, Tolstykh T, Stock J (1996) A specific protein carboxyl methylesterase that demethylates phosphoprotein phosphatase 2A in bovine brain. Proc Natl Acad Sci U S A 93:6043-6047.

Lee JT, Wheeler TC, Li L, Chin LS (2008a) Ubiquitination of alpha-synuclein by Siah-1 promotes alpha-synuclein aggregation and apoptotic cell death. Hum Mol Genet 17:906-917.

Lee KW, Chen W, Junn E, Im JY, Grosso H, Sonsalla PK, Feng X, Ray N, Fernandez JR, Chao Y, Masliah E, Voronkov M, Braithwaite SP, Stock JB, Mouradian MM (2011) Enhanced phosphatase activity attenuates alpha-synucleinopathy in a mouse model. J Neurosci 31:6963-6971.

Lee SJ, Jeon H, Kandror KV (2008b) Alpha-synuclein is localized in a subpopulation of rat brain synaptic vesicles. Acta Neurobiol Exp (Wars) 68:509-515.

Lee Y, Dawson VL, Dawson TM (2012) Animal models of Parkinson's disease: vertebrate genetics. Cold Spring Harb Perspect Med 2.

Leroy E, Boyer R, Auburger G, Leube B, Ulm G, Mezey E, Harta G, Brownstein MJ, Jonnalagada S, Chernova T, Dehejia A, Lavedan C, Gasser T, Steinbach PJ, Wilkinson KD, Polymeropoulos MH (1998) The ubiquitin pathway in Parkinson's disease. Nature 395:451-452.

Liani E, Eyal A, Avraham E, Shemer R, Szargel R, Berg D, Bornemann A, Riess O, Ross CA, Rott R, Engelender S (2004) Ubiquitylation of synphilin-1 and alpha-synuclein by SIAH and its presence in cellular inclusions and Lewy bodies imply a role in Parkinson's disease. Proc Natl Acad Sci U S A 101:5500-5505.

Lilienbaum A (2013) Relationship between the proteasomal system and autophagy. Int J Biochem Mol Biol 4:1-26.

Lim KL, Tan JM (2007) Role of the ubiquitin proteasome system in Parkinson's disease. BMC Biochem 8 Suppl 1:S13.

Lindersson E, Beedholm R, Hojrup P, Moos T, Gai W, Hendil KB, Jensen PH (2004) Proteasomal inhibition by alpha-synuclein filaments and oligomers. J Biol Chem 279:12924-12934.

Liu CW, Corboy MJ, DeMartino GN, Thomas PJ (2003) Endoproteolytic activity of the proteasome. Science 299:408-411.

Liu R, Zhou XW, Tanila H, Bjorkdahl C, Wang JZ, Guan ZZ, Cao Y, Gustafsson JA, Winblad B, Pei JJ (2008) Phosphorylated PP2A (tyrosine 307) is associated with Alzheimer neurofibrillary pathology. J Cell Mol Med 12:241-257.

Longin S, Jordens J, Martens E, Stevens I, Janssens V, Rondelez E, De Baere I, Derua R, Waelkens E, Goris J, Van Hoof C (2004) An inactive protein phosphatase 2A population is associated with methylesterase and can be re-activated by the phosphotyrosyl phosphatase activator. Biochem J 380:111-119.

Lopez A, Herranz-Trillo F, Kotev M, Gairi M, Guallar V, Bernado P, Millet O, Tarrago T, Giralt E (2016) Active-Site-Directed Inhibitors of Prolyl Oligopeptidase Abolish Its Conformational Dynamics. ChemBioChem 17:913-917.

Lowe J, Blanchard A, Morrell K, Lennox G, Reynolds L, Billett M, Landon M, Mayer RJ (1988) Ubiquitin is a common factor in intermediate filament inclusion bodies of diverse type in man, including those of Parkinson's disease, Pick's disease, and Alzheimer's disease, as well as Rosenthal fibres in cerebellar astrocytomas, cytoplasmic bodies in muscle, and mallory bodies in alcoholic liver disease. J Pathol 155:9-15.

Luk KC, Covell DJ, Kehm VM, Zhang B, Song IY, Byrne MD, Pitkin RM, Decker SC, Trojanowski JQ, Lee VM (2016) Molecular and Biological Compatibility with Host Alpha-Synuclein Influences Fibril Pathogenicity. Cell Rep 16:3373-3387.

Luo Y, Nie YJ, Shi HR, Ni ZF, Wang Q, Wang JZ, Liu GP (2013) PTPA activates protein phosphatase-2A through reducing its phosphorylation at tyrosine-307

with upregulation of protein tyrosine phosphatase 1B. Biochim Biophys Acta 1833:1235-1243.

Luth ES, Stavrovskaya IG, Bartels T, Kristal BS, Selkoe DJ (2014) Soluble, prefibrillar alpha-synuclein oligomers promote complex I-dependent, Ca2+-induced mitochondrial dysfunction. J Biol Chem 289:21490-21507.

Machiya Y, Hara S, Arawaka S, Fukushima S, Sato H, Sakamoto M, Koyama S, Kato T (2010) Phosphorylated alpha-synuclein at Ser-129 is targeted to the proteasome pathway in a ubiquitin-independent manner. J Biol Chem 285:40732-40744.

Mak SK, McCormack AL, Manning-Bog AB, Cuervo AM, Di Monte DA (2010) Lysosomal degradation of alpha-synuclein in vivo. J Biol Chem 285:13621-13629.

Mannisto PT, Garcia-Horsman JA (2017) Mechanism of Action of Prolyl Oligopeptidase (PREP) in Degenerative Brain Diseases: Has Peptidase Activity Only a Modulatory Role on the Interactions of PREP with Proteins? Front Aging Neurosci 9:27.

Mantle D, Falkous G, Ishiura S, Blanchard PJ, Perry EK (1996a) Comparison of proline endopeptidase activity in brain tissue from normal cases and cases with Alzheimer's disease, Lewy body dementia, Parkinson's disease and Huntington's disease. Clin Chim Acta 249:129-139.

Mantle D, Falkous G, Ishiura S, Blanchard PJ, Perry EK (1996b) Comparison of proline endopeptidase activity in brain tissue from normal cases and cases with Alzheimer's disease, Lewy body dementia, Parkinson's disease and Huntington's disease. Clin Chim Acta 249:129-139.

Maroteaux L, Campanelli JT, Scheller RH (1988) Synuclein: a neuron-specific protein localized to the nucleus and presynaptic nerve terminal. J Neurosci 8:2804-2815.

Martinez-Vicente M, Vila M (2013) Alpha-synuclein and protein degradation pathways in Parkinson's disease: a pathological feed-back loop. Exp Neurol 247:308-313.

Martinez-Vicente M, Talloczy Z, Kaushik S, Massey AC, Mazzulli J, Mosharov EV, Hodara R, Fredenburg R, Wu DC, Follenzi A, Dauer W, Przedborski S, Ischiropoulos H, Lansbury PT, Sulzer D, Cuervo AM (2008) Dopamine-modified alpha-synuclein blocks chaperone-mediated autophagy. J Clin Invest 118:777-788.

Massey AC, Kaushik S, Sovak G, Kiffin R, Cuervo AM (2006) Consequences of the selective blockage of chaperone-mediated autophagy. Proc Natl Acad Sci U S A 103:5805-5810.

Matsuda T, Sakaguchi M, Tanaka S, Yoshimoto T, Takaoka M (2013) Prolyl oligopeptidase is a glyceraldehyde-3-phosphate dehydrogenase-binding protein that regulates genotoxic stress-induced cell death. Int J Biochem Cell Biol 45:850-857.

McCann H, Stevens CH, Cartwright H, Halliday GM (2014) alpha-Synucleinopathy phenotypes. Parkinsonism Relat Disord 20 Suppl 1:S62-67.

McNaught KS, Mytilineou C, Jnobaptiste R, Yabut J, Shashidharan P, Jennert P, Olanow CW (2002) Impairment of the ubiquitin-proteasome system causes dopaminergic cell death and inclusion body formation in ventral mesencephalic cultures. J Neurochem 81:301-306.

Meier F, Abeywardana T, Dhall A, Marotta NP, Varkey J, Langen R, Chatterjee C, Pratt MR (2012) Semisynthetic, site-specific ubiquitin modification of alpha-synuclein reveals differential effects on aggregation. J Am Chem Soc 134:5468-5471.

Milber JM, Noorigian JV, Morley JF, Petrovitch H, White L, Ross GW, Duda JE (2012) Lewy pathology is not the first sign of degeneration in vulnerable neurons in Parkinson disease. Neurology 79:2307-2314.

Mizushima N, Ohsumi Y, Yoshimori T (2002) Autophagosome formation in mammalian cells. Cell Struct Funct 27:421-429.

Moreno-Baylach MJ, Puttonen KA, Tenorio-Laranga J, Venalainen JI, Storvik M, Forsberg MM, Garcia-Horsman JA (2011) Prolyl endopeptidase is involved in cellular signalling in human neuroblastoma SH-SY5Y cells. Neurosignals 19:97-109.

Moriyama A, Nakanishi M, Sasaki M (1988) Porcine muscle prolyl endopeptidase and its endogenous substrates. J Biochem 104:112-117.

Mulherkar SA, Sharma J, Jana NR (2009) The ubiquitin ligase E6-AP promotes degradation of alpha-synuclein. J Neurochem 110:1955-1964.

Muntane G, Ferrer I, Martinez-Vicente M (2012) alpha-synuclein phosphorylation and truncation are normal events in the adult human brain. Neuroscience 200:106-119.

Murphy KE, Gysbers AM, Abbott SK, Spiro AS, Furuta A, Cooper A, Garner B, Kabuta T, Halliday GM (2015) Lysosomal-associated membrane protein 2 isoforms are differentially affected in early Parkinson's disease. Mov Disord 30:1639-1647.

Myohanen TT, Venalainen JI, Garcia-Horsman JA, Piltonen M, Mannisto PT (2008) Distribution of prolyl oligopeptidase in the mouse whole-body sections and peripheral tissues. Histochem Cell Biol 130:993-1003.

Myohanen TT, Hannula MJ, Van Elzen R, Gerard M, Van Der Veken P, Garcia-Horsman JA, Baekelandt V, Mannisto PT, Lambeir AM (2012) A prolyl oligopeptidase inhibitor, KYP-2047, reduces alpha-synuclein protein levels and aggregates in cellular and animal models of Parkinson's disease. Br J Pharmacol 166:1097-1113.

Myöhänen TT, Venäläinen JI, Tupala E, Garcia-Horsman JA, Miettinen R, Männistö PT (2007) Distribution of Immunoreactive Prolyl Oligopeptidase in Human and Rat Brain. Neurochem Res 32:1365-1374.

Naetar N, Soundarapandian V, Litovchick L, Goguen KL, Sablina AA, Bowman-Colin C, Sicinski P, Hahn WC, DeCaprio JA, Livingston DM (2014) PP2A-mediated regulation of Ras signaling in G2 is essential for stable quiescence and normal G1 length. Mol Cell 54:932-945.

Narhi L, Wood SJ, Steavenson S, Jiang Y, Wu GM, Anafi D, Kaufman SA, Martin F, Sitney K, Denis P, Louis J-C, Wypych J, Biere AL, Citron M (1999) Both Familial Parkinson's Disease Mutations Accelerate α-Synuclein Aggregation. J Biol Chem 274:9843-9846.

Natunen TA, Gynther M, Rostalski H, Jaako K, Jalkanen AJ (2018) Extracellular prolyl oligopeptidase derived from activated microglia is a potential neuroprotection target. Basic Clin Pharmacol Toxicol. (online)

Neumann M, Kahle PJ, Giasson BI, Ozmen L, Borroni E, Spooren W, Muller V, Odoy S, Fujiwara H, Hasegawa M, Iwatsubo T, Trojanowski JQ, Kretzschmar HA, Haass C (2002) Misfolded proteinase K-resistant hyperphosphorylated alpha-synuclein in aged transgenic mice with locomotor deterioration and in human alpha-synucleinopathies. J Clin Invest 110:1429-1439.

Nicot AS, Lo Verso F, Ratti F, Pilot-Storck F, Streichenberger N, Sandri M, Schaeffer L, Goillot E (2014) Phosphorylation of NBR1 by GSK3 modulates protein aggregation. Autophagy 10:1036-1053.

Nixon RA (2013) The role of autophagy in neurodegenerative disease. Nat Med 19:983-997.

Nonaka T, Iwatsubo T, Hasegawa M (2005) Ubiquitination of alpha-synuclein. Biochemistry 44:361-368.

Nykanen NP, Kysenius K, Sakha P, Tammela P, Huttunen HJ (2012) gamma-Aminobutyric acid type A (GABAA) receptor activation modulates tau phosphorylation. J Biol Chem 287:6743-6752.

Odagiri S, Tanji K, Mori F, Kakita A, Takahashi H, Wakabayashi K (2012) Autophagic adapter protein NBR1 is localized in Lewy bodies and glial cytoplasmic inclusions and is involved in aggregate formation in alpha-synucleinopathy. Acta Neuropathol 124:173-186.

Oliveras-Salva M, Van der Perren A, Casadei N, Stroobants S, Nuber S, D'Hooge R, Van den Haute C, Baekelandt V (2013) rAAV2/7 vector-mediated overexpression of alpha-synuclein in mouse substantia nigra induces protein aggregation and progressive dose-dependent neurodegeneration. Mol Neurodegener 8:44.

Otomo C, Metlagel Z, Takaesu G, Otomo T (2013) Structure of the human ATG12~ATG5 conjugate required for LC3 lipidation in autophagy. Nat Struct Mol Biol 20:59-66.

Oueslati A (2016) Implication of Alpha-Synuclein Phosphorylation at S129 in Synucleinopathies: What Have We Learned in the Last Decade? J Parkinsons Dis 6:39-51.

Oueslati A, Schneider BL, Aebischer P, Lashuel HA (2013) Polo-like kinase 2 regulates selective autophagic alpha-synuclein clearance and suppresses its toxicity in vivo. Proc Natl Acad Sci U S A 110:E3945-3954.

Outeiro TF, Klucken J, Bercury K, Tetzlaff J, Putcha P, Oliveira LM, Quintas A, McLean PJ, Hyman BT (2009) Dopamine-induced conformational changes in alpha-synuclein. PLoS One 4:e6906.

Park HJ, Lee KW, Park ES, Oh S, Yan R, Zhang J, Beach TG, Adler CH, Voronkov M, Braithwaite SP, Stock JB, Mouradian MM (2016) Dysregulation of protein phosphatase 2A in parkinson disease and dementia with lewy bodies. Annals of Clinical and Translational Neurology 3:769-780.

Pattingre S, Bauvy C, Carpentier S, Levade T, Levine B, Codogno P (2009) Role of JNK1-dependent Bcl-2 phosphorylation in ceramide-induced macroautophagy. J Biol Chem 284:2719-2728.

Paxinos G, Franklin KBJ (1997) The Mouse Brain in Stereotaxic Coordinates. San Diego: Elsevier Academic Press.

Peng C, Gathagan RJ, Lee VM (2018) Distinct alpha-Synuclein strains and implications for heterogeneity among alpha-Synucleinopathies. Neurobiol Dis 109:209-218.

Penttinen A, Tenorio-Laranga J, Siikanen A, Morawski M, Rossner S, Garcia-Horsman JA (2011) Prolyl oligopeptidase: a rising star on the stage of neuroinflammation research. CNS Neurol Disord Drug Targets 10:340-348.

Perez RG, Hastings TG (2004) Could a loss of alpha-synuclein function put dopaminergic neurons at risk? J Neurochem 89:1318-1324.

Petrucelli L, O'Farrell C, Lockhart PJ, Baptista M, Kehoe K, Vink L, Choi P, Wolozin B, Farrer M, Hardy J, Cookson MR (2002) Parkin protects against the toxicity associated with mutant alpha-synuclein: proteasome dysfunction selectively affects catecholaminergic neurons. Neuron 36:1007-1019.

Phan JA, Stokholm K, Zareba-Paslawska J, Jakobsen S, Vang K, Gjedde A, Landau AM, Romero-Ramos M (2017) Early synaptic dysfunction induced by alpha-synuclein in a rat model of Parkinson's disease. Sci Rep 7:6363.

Pickart CM, Fushman D (2004) Polyubiquitin chains: polymeric protein signals. Curr Opin Chem Biol 8:610-616.

Polymeropoulos MH, Lavedan C, Leroy E, Ide SE, Dehejia A, Dutra A, Pike B, Root H, Rubenstein J, Boyer R, Stenroos ES, Chandrasekharappa S, Athanassiadou A, Papapetropoulos T, Johnson WG, Lazzarini AM, Duvoisin RC, Di Iorio G, Golbe

LI, Nussbaum RL (1997) Mutation in the alpha-synuclein gene identified in families with Parkinson's disease. Science 276:2045-2047.

Qu J, Yan H, Zheng Y, Xue F, Zheng Y, Fang H, Chang Y, Yang H, Zhang J (2018) The Molecular Mechanism of Alpha-Synuclein Dependent Regulation of Protein Phosphatase 2A Activity. Cell Physiol Biochem 47:2613-2625.

Rechsteiner M, Hill CP (2005) Mobilizing the proteolytic machine: cell biological roles of proteasome activators and inhibitors. Trends Cell Biol 15:27-33.

Rincon R, Cristobal I, Zazo S, Arpi O, Menendez S, Manso R, Lluch A, Eroles P, Rovira A, Albanell J, Garcia-Foncillas J, Madoz-Gurpide J, Rojo F (2015) PP2A inhibition determines poor outcome and doxorubicin resistance in early breast cancer and its activation shows promising therapeutic effects. Oncotarget 6:4299-4314.

Roberts HL, Brown DR (2015) Seeking a mechanism for the toxicity of oligomeric alpha-synuclein. Biomolecules 5:282-305.

Rocha EM, De Miranda B, Sanders LH (2018) Alpha-synuclein: Pathology, mitochondrial dysfunction and neuroinflammation in Parkinson's disease. Neurobiol Dis 109:249-257.

Rock KL, Gramm C, Rothstein L, Clark K, Stein R, Dick L, Hwang D, Goldberg AL (1994) Inhibitors of the Proteasome Block the Degradation of Most Cell-Proteins and the Generation of Peptides Presented on Mhc Class-I Molecules. Cell 78:761-771.

Rockenstein E, Nuber S, Overk CR, Ubhi K, Mante M, Patrick C, Adame A, Trejo-Morales M, Gerez J, Picotti P, Jensen PH, Campioni S, Riek R, Winkler J, Gage FH, Winner B, Masliah E (2014) Accumulation of oligomer-prone alpha-synuclein exacerbates synaptic and neuronal degeneration in vivo. Brain 137:1496-1513.

Rossner S, Schulz I, Zeitschel U, Schliebs R, Bigl V, Demuth HU (2005) Brain prolyl endopeptidase expression in aging, APP transgenic mice and Alzheimer's disease. Neurochem Res 30:695-702.

Rott R, Szargel R, Haskin J, Bandopadhyay R, Lees AJ, Shani V, Engelender S (2011) alpha-Synuclein fate is determined by USP9X-regulated monoubiquitination. Proc Natl Acad Sci U S A 108:18666-18671.

Rott R, Szargel R, Shani V, Hamza H, Savyon M, Abd Elghani F, Bandopadhyay R, Engelender S (2017) SUMOylation and ubiquitination reciprocally regulate alpha-synuclein degradation and pathological aggregation. Proc Natl Acad Sci U S A 114:13176-13181.

Rott R, Szargel R, Haskin J, Shani V, Shainskaya A, Manov I, Liani E, Avraham E, Engelender S (2008) Monoubiquitylation of alpha-synuclein by seven in absentia homolog (SIAH) promotes its aggregation in dopaminergic cells. J Biol Chem 283:3316-3328.

Rubinsztein DC (2006) The roles of intracellular protein-degradation pathways in neurodegeneration. Nature 443:780-786.

Ruvolo PP (2016) The broken "Off" switch in cancer signaling: PP2A as a regulator of tumorigenesis, drug resistance, and immune surveillance. BBA Clin 6:87-99.

Sakaguchi M, Matsuda T, Matsumura E, Yoshimoto T, Takaoka M (2011) Prolyl oligopeptidase participates in cell cycle progression in a human neuroblastoma cell line. Biochem Biophys Res Commun 409:693-698.

Salvador N, Aguado C, Horst M, Knecht E (2000) Import of a cytosolic protein into lysosomes by chaperone-mediated autophagy depends on its folding state. J Biol Chem 275:27447-27456.

Savolainen MH, Yan X, Myohanen TT, Huttunen HJ (2015) Prolyl oligopeptidase enhances alpha-synuclein dimerization via direct protein-protein interaction. J Biol Chem 290:5117-5126.

Savolainen MH, Richie CT, Harvey BK, Mannisto PT, Maguire-Zeiss KA, Myohanen TT (2014) The beneficial effect of a prolyl oligopeptidase inhibitor, KYP-2047, on alpha-synuclein clearance and autophagy in A30P transgenic mouse. Neurobiol Dis 68:1-15.

Schmitz C, Hof PR (2005) Design-based stereology in neuroscience. Neuroscience 130:813-831.

Schulz-Schaeffer WJ (2010) The synaptic pathology of alpha-synuclein aggregation in dementia with Lewy bodies, Parkinson's disease and Parkinson's disease dementia. Acta Neuropathol 120:131-143.

Schulz I, Gerhartz B, Neubauer A, Holloschi A, Heiser U, Hafner M, Demuth H-U (2002) Modulation of inositol 1,4,5-triphosphate concentration by prolyl endopeptidase inhibition. Eur J Biochem 269:5813-5820.

Schulz I, Zeitschel U, Rudolph T, Ruiz-Carrillo D, Rahfeld J-U, Gerhartz B, Bigl V, Demuth H-U, Roßner S (2005) Subcellular localization suggests novel functions for prolyl endopeptidase in protein secretion. J Neurochem 94:970-979.

Scott DA, Tabarean I, Tang Y, Cartier A, Masliah E, Roy S (2010) A Pathologic Cascade Leading to Synaptic Dysfunction in α-Synuclein-Induced Neurodegeneration. The Journal of Neuroscience 30:8083-8095.

Shabek N, Herman-Bachinsky Y, Buchsbaum S, Lewinson O, Haj-Yahya M, Hejjaoui M, Lashuel HA, Sommer T, Brik A, Ciechanover A (2012) The size of the proteasomal substrate determines whether its degradation will be mediated by mono- or polyubiquitylation. Mol Cell 48:87-97.

Shaid S, Brandts CH, Serve H, Dikic I (2013) Ubiquitination and selective autophagy. Cell Death Differ 20:21-30.

Shimura H, Schlossmacher MG, Hattori N, Frosch MP, Trockenbacher A, Schneider R, Mizuno Y, Kosik KS, Selkoe DJ (2001) Ubiquitination of a new form of alpha-synuclein by parkin from human brain: implications for Parkinson's disease. Science 293:263-269.

Shin Y, Klucken J, Patterson C, Hyman BT, McLean PJ (2005) The co-chaperone carboxyl terminus of Hsp70-interacting protein (CHIP) mediates alpha-synuclein degradation decisions between proteasomal and lysosomal pathways. J Biol Chem 280:23727-23734.

Shinoda M, Okamiya K, Toide K (1995) Effect of a novel prolyl endopeptidase inhibitor, JTP-4819, on thyrotropin-releasing hormone-like immunoreactivity in the cerebral cortex and hippocampus of aged rats. Jpn J Pharmacol 69:273-276.

Singleton AB et al. (2003) alpha-Synuclein locus triplication causes Parkinson's disease. Science 302:841.

Snyder H, Mensah K, Theisler C, Lee J, Matouschek A, Wolozin B (2003) Aggregated and monomeric alpha-synuclein bind to the S6' proteasomal protein and inhibit proteasomal function. J Biol Chem 278:11753-11759.

Sontag JM, Sontag E (2014) Protein phosphatase 2A dysfunction in Alzheimer's disease. Front Mol Neurosci 7:16.

Spencer B, Potkar R, Trejo M, Rockenstein E, Patrick C, Gindi R, Adame A, Wyss-Coray T, Masliah E (2009) Beclin 1 gene transfer activates autophagy and ameliorates the neurodegenerative pathology in alpha-synuclein models of Parkinson's and Lewy body diseases. J Neurosci 29:13578-13588.

Spillantini MG, Crowther RA, Jakes R, Hasegawa M, Goedert M (1998) alpha-synuclein in filamentous inclusions of Lewy bodies from Parkinson's disease and dementia with Lewy bodies. Proc Natl Acad Sci U S A 95:6469-6473.

Spillantini MG, Schmidt ML, Lee VM, Trojanowski JQ, Jakes R, Goedert M (1997) Alpha-synuclein in Lewy bodies. Nature 388:839-840.

St Martin JL, Klucken J, Outeiro TF, Nguyen P, Keller-McGandy C, Cantuti-Castelvetri I, Grammatopoulos TN, Standaert DG, Hyman BT, McLean PJ (2007) Dopaminergic neuron loss and up-regulation of chaperone protein mRNA induced by targeted over-expression of alpha-synuclein in mouse substantia nigra. J Neurochem 100:1449-1457.

St. P. McNaught K, Belizaire R, Isacson O, Jenner P, Olanow CW (2003) Altered Proteasomal Function in Sporadic Parkinson's Disease. Exp Neurol 179:38-46.

Stadtmueller BM, Hill CP (2011) Proteasome activators. Mol Cell 41:8-19.

Stefanis L, Larsen KE, Rideout HJ, Sulzer D, Greene LA (2001) Expression of A53T mutant but not wild-type alpha-synuclein in PC12 cells induces alterations of the ubiquitin-dependent degradation system, loss of dopamine release, and autophagic cell death. J Neurosci 21:9549-9560.

Sun L, Ii AL, Pham TT, Shanley TP (2015) Study of Protein Phosphatase 2A (PP2A) Activity in LPS-Induced Tolerance Using Fluorescence-Based and Immunoprecipitation-Aided Methodology. Biomolecules 5:1284-1301.

Suzuki H, Osawa T, Fujioka Y, Noda NN (2017) Structural biology of the core autophagy machinery. Curr Opin Struct Biol 43:10-17.

Suzuki K, Sakaguchi M, Tanaka S, Yoshimoto T, Takaoka M (2014) Prolyl oligopeptidase inhibition-induced growth arrest of human gastric cancer cells. Biochem Biophys Res Commun 443:91-96.

Szeltner Z, Rea D, Juhász T, Renner V, Fülöp V, Polgár L (2004) Concerted Structural Changes in the Peptidase and the Propeller Domains of Prolyl Oligopeptidase are Required for Substrate Binding. J Mol Biol 340:627-637.

Szeltner Z, Juhász T, Szamosi I, Rea D, Fülöp V, Módos K, Juliano L, Polgár L (2013) The loops facing the active site of prolyl oligopeptidase are crucial components in substrate gating and specificity. Biochim Biophys Acta 1834:98-111.

Tan S, Wong E (2017) Chapter Fifteen - Kinetics of Protein Aggregates Disposal by Aggrephagy. In: Methods in Enzymology (Galluzzi L, Bravo-San Pedro JM, Kroemer G, eds), pp 245-281: Academic Press.

Tanaka S, Suzuki K, Sakaguchi M (2017) The prolyl oligopeptidase inhibitor SUAM-14746 attenuates the proliferation of human breast cancer cell lines in vitro. Breast Cancer 24:658-666.

Tanaka Y, Engelender S, Igarashi S, Rao RK, Wanner T, Tanzi RE, Sawa A, V LD, Dawson TM, Ross CA (2001) Inducible expression of mutant alpha-synuclein decreases proteasome activity and increases sensitivity to mitochondria-dependent apoptosis. Hum Mol Genet 10:919-926.

Tanik SA, Schultheiss CE, Volpicelli-Daley LA, Brunden KR, Lee VM (2013) Lewy body-like alpha-synuclein aggregates resist degradation and impair macroautophagy. J Biol Chem 288:15194-15210.

Tanji K, Odagiri S, Miki Y, Maruyama A, Nikaido Y, Mimura J, Mori F, Warabi E, Yanagawa T, Ueno S, Itoh K, Wakabayashi K (2015) p62 Deficiency Enhances alpha-Synuclein Pathology in Mice. Brain Pathol 25:552-564.

Tenorio-Laranga J, Mannisto PT, Storvik M, Van der Veken P, Garcia-Horsman JA (2012) Four day inhibition of prolyl oligopeptidase causes significant changes in the peptidome of rat brain, liver and kidney. Biochimie 94:1849-1859.

Tenreiro S, Eckermann K, Outeiro TF (2014a) Protein phosphorylation in neurodegeneration: friend or foe? Front Mol Neurosci 7:42.

Tenreiro S, Reimao-Pinto MM, Antas P, Rino J, Wawrzycka D, Macedo D, Rosado-Ramos R, Amen T, Waiss M, Magalhaes F, Gomes A, Santos CN, Kaganovich D, Outeiro TF (2014b) Phosphorylation modulates clearance of alpha-synuclein inclusions in a yeast model of Parkinson's disease. PLoS Genet 10:e1004302.

Tetzlaff JE, Putcha P, Outeiro TF, Ivanov A, Berezovska O, Hyman BT, McLean PJ (2008) CHIP targets toxic alpha-Synuclein oligomers for degradation. J Biol Chem 283:17962-17968.

Thibaudeau TA, Anderson RT, Smith DM (2018) A common mechanism of proteasome impairment by neurodegenerative disease-associated oligomers. Nat Commun 9:1097.

Tofaris GK, Layfield R, Spillantini MG (2001) α-Synuclein metabolism and aggregation is linked to ubiquitin-independent degradation by the proteasome. FEBS Lett 509:22-26.

Tofaris GK, Razzaq A, Ghetti B, Lilley KS, Spillantini MG (2003) Ubiquitination of alpha-synuclein in Lewy bodies is a pathological event not associated with impairment of proteasome function. J Biol Chem 278:44405-44411.

Tofaris GK, Kim HT, Hourez R, Jung JW, Kim KP, Goldberg AL (2011) Ubiquitin ligase Nedd4 promotes alpha-synuclein degradation by the endosomal-lysosomal pathway. Proc Natl Acad Sci U S A 108:17004-17009.

Toide K, Okamiya K, Iwamoto Y, Kato T (1995) Effect of a novel prolyl endopeptidase inhibitor, JTP-4819, on prolyl endopeptidase activity and substance P- and arginine-vasopressin-like immunoreactivity in the brains of aged rats. J Neurochem 65:234-240.

Trojanowski JQ, Lee VM (1998) Aggregation of neurofilament and alpha-synuclein proteins in Lewy bodies: implications for the pathogenesis of Parkinson disease and Lewy body dementia. Arch Neurol 55:151-152.

Tsigelny IF, Sharikov Y, Wrasidlo W, Gonzalez T, Desplats PA, Crews L, Spencer B, Masliah E (2012) Role of alpha-synuclein penetration into the membrane in the mechanisms of oligomer pore formation. FEBS J 279:1000-1013.

Tsuji S, Morinobu S, Tanaka K, Kawano K, Yamawaki S (2003) Lithium, but not valproate, induces the serine/threonine phosphatase activity of protein phosphatase 2A in the rat brain, without affecting its expression. J Neural Transm (Vienna) 110:413-425.

Ueda K, Fukushima H, Masliah E, Xia Y, Iwai A, Yoshimoto M, Otero DA, Kondo J, Ihara Y, Saitoh T (1993) Molecular cloning of cDNA encoding an unrecognized component of amyloid in Alzheimer disease. Proc Natl Acad Sci U S A 90:11282-11286.

Ulmer T, Bax A, Cole N, Nussbaum R (2005) Structure and dynamics of micelle-bound human alpha-synuclein. J Biol Chem 280.

Uversky VN, Eliezer D (2009) Biophysics of Parkinson's Disease: Structure and Aggregation of α-Synuclein. Curr Protein Peptide Sci 10:483-499.

van Eersel J, Ke YD, Liu X, Delerue F, Kril JJ, Gotz J, Ittner LM (2010) Sodium selenate mitigates tau pathology, neurodegeneration, and functional deficits in Alzheimer's disease models. Proc Natl Acad Sci U S A 107:13888-13893.

Vekrellis K, Xilouri M, Emmanouilidou E, Rideout HJ, Stefanis L (2011) Pathological roles of alpha-synuclein in neurological disorders. Lancet Neurol 10:1015-1025.

Villar-Pique A, Lopes da Fonseca T, Outeiro TF (2016) Structure, function and toxicity of alpha-synuclein: the Bermuda triangle in synucleinopathies. J Neurochem 139 Suppl 1:240-255.

Visanji NP, Wislet-Gendebien S, Oschipok LW, Zhang G, Aubert I, Fraser PE, Tandon A (2011) Effect of Ser-129 phosphorylation on interaction of alpha-synuclein with synaptic and cellular membranes. J Biol Chem 286:35863-35873.

Vogiatzi T, Xilouri M, Vekrellis K, Stefanis L (2008) Wild type alpha-synuclein is degraded by chaperone-mediated autophagy and macroautophagy in neuronal cells. J Biol Chem 283:23542-23556.

Wakabayashi K, Engelender S, Yoshimoto M, Tsuji S, Ross CA, Takahashi H (2000) Synphilin-1 is present in Lewy bodies in Parkinson's disease. Ann Neurol 47:521-523.

Walter R, Shlank H, Glass JD, Schwartz IL, Kerenyi TD (1971) Leucylglycinamide released from oxytocin by human uterine enzyme. Science 173:827-829.

Wandzioch E, Pusey M, Werda A, Bail S, Bhaskar A, Nestor M, Yang JJ, Rice LM (2014) PME-1 modulates protein phosphatase 2A activity to promote the malignant phenotype of endometrial cancer cells. Cancer Res 74:4295-4305.

Watanabe Y, Tatebe H, Taguchi K, Endo Y, Tokuda T, Mizuno T, Nakagawa M, Tanaka M (2012) p62/SQSTM1-dependent autophagy of Lewy body-like alpha-synuclein inclusions. PLoS One 7:e52868.

Webb JL, Ravikumar B, Atkins J, Skepper JN, Rubinsztein DC (2003) Alpha-Synuclein is degraded by both autophagy and the proteasome. J Biol Chem 278:25009-25013.

Wei Y, Pattingre S, Sinha S, Bassik M, Levine B (2008) JNK1-mediated phosphorylation of Bcl-2 regulates starvation-induced autophagy. Mol Cell 30:678-688.

Westermarck J (2018) Targeted therapies don't work for a reason; the neglected tumor suppressor phosphatase PP2A strikes back. FEBS J 0.

Williams RS, Cheng L, Mudge AW, Harwood AJ (2002) A common mechanism of action for three mood-stabilizing drugs. Nature 417:292-295.

Williams RS, Eames M, Ryves WJ, Viggars J, Harwood AJ (1999) Loss of a prolyl oligopeptidase confers resistance to lithium by elevation of inositol (1,4,5) trisphosphate. EMBO J 18:2734-2745.

Winner B, Jappelli R, Maji SK, Desplats PA, Boyer L, Aigner S, Hetzer C, Loher T, Vilar M, Campioni S, Tzitzilonis C, Soragni A, Jessberger S, Mira H, Consiglio A, Pham E, Masliah E, Gage FH, Riek R (2011) In vivo demonstration that alpha-synuclein oligomers are toxic. Proc Natl Acad Sci U S A 108:4194-4199.

Winslow AR, Chen CW, Corrochano S, Acevedo-Arozena A, Gordon DE, Peden AA, Lichtenberg M, Menzies FM, Ravikumar B, Imarisio S, Brown S, O'Kane CJ, Rubinsztein DC (2010) alpha-Synuclein impairs macroautophagy: implications for Parkinson's disease. J Cell Biol 190:1023-1037.

Xie W, Li X, Li C, Zhu W, Jankovic J, Le W (2010) Proteasome inhibition modeling nigral neuron degeneration in Parkinson's disease. J Neurochem 115:188-199.

Xilouri M, Vogiatzi T, Vekrellis K, Park D, Stefanis L (2009) Abberant alpha-synuclein confers toxicity to neurons in part through inhibition of chaperone-mediated autophagy. PLoS One 4:e5515.

Xilouri M, Brekk OR, Polissidis A, Chrysanthou-Piterou M, Kloukina I, Stefanis L (2016) Impairment of chaperone-mediated autophagy induces dopaminergic neurodegeneration in rats. Autophagy 12:2230-2247.

Xilouri M, Brekk OR, Landeck N, Pitychoutis PM, Papasilekas T, Papadopoulou-Daifoti Z, Kirik D, Stefanis L (2013) Boosting chaperone-mediated autophagy in vivo mitigates alpha-synuclein-induced neurodegeneration. Brain 136:2130-2146.

Xing Y, Li Z, Chen Y, Stock JB, Jeffrey PD, Shi Y (2008) Structural mechanism of demethylation and inactivation of protein phosphatase 2A. Cell 133:154-163.

Xu P, Duong DM, Seyfried NT, Cheng D, Xie Y, Robert J, Rush J, Hochstrasser M, Finley D, Peng J (2009) Quantitative proteomics reveals the function of unconventional ubiquitin chains in proteasomal degradation. Cell 137:133-145.

Yabe R, Miura A, Usui T, Mudrak I, Ogris E, Ohama T, Sato K (2015) Protein Phosphatase Methyl-Esterase PME-1 Protects Protein Phosphatase 2A from Ubiquitin/Proteasome Degradation. PLoS One 10:e0145226.

Yabe R, Tsuji S, Mochida S, Ikehara T, Usui T, Ohama T, Sato K (2018) A stable association with PME-1 may be dispensable for PP2A demethylation - implications for the detection of PP2A methylation and immunoprecipitation. FEBS Open Bio 8:1486-1496.

Yamada M, Iwatsubo T, Mizuno Y, Mochizuki H (2004) Overexpression of alpha-synuclein in rat substantia nigra results in loss of dopaminergic neurons, phosphorylation of alpha-synuclein and activation of caspase-9: resemblance to pathogenetic changes in Parkinson's disease. J Neurochem 91:451-461.

Yamakawa K, Izumi Y, Takeuchi H, Yamamoto N, Kume T, Akaike A, Takahashi R, Shimohama S, Sawada H (2010) Dopamine facilitates alpha-synuclein oligomerization in human neuroblastoma SH-SY5Y cells. Biochem Biophys Res Commun 391:129-134.

Yang Q, She H, Gearing M, Colla E, Lee M, Shacka JJ, Mao Z (2009) Regulation of neuronal survival factor MEF2D by chaperone-mediated autophagy. Science 323:124-127.

Yavich L, Tanila H, Vepsalainen S, Jakala P (2004) Role of alpha-synuclein in presynaptic dopamine recruitment. J Neurosci 24:11165-11170.

Yu WH, Dorado B, Figueroa HY, Wang L, Planel E, Cookson MR, Clark LN, Duff KE (2009) Metabolic activity determines efficacy of macroautophagic clearance of pathological oligomeric alpha-synuclein. Am J Pathol 175:736-747.

Zachari M, Ganley IG (2017) The mammalian ULK1 complex and autophagy initiation. Essays Biochem 61:585-596.

Zaffagnini G, Martens S (2016) Mechanisms of Selective Autophagy. J Mol Biol 428:1714-1724.

Zalckvar E, Berissi H, Eisenstein M, Kimchi A (2009a) Phosphorylation of Beclin 1 by DAP-kinase promotes autophagy by weakening its interactions with Bcl-2 and Bcl-XL. Autophagy 5:720-722.

Zalckvar E, Berissi H, Mizrachy L, Idelchuk Y, Koren I, Eisenstein M, Sabanay H, Pinkas-Kramarski R, Kimchi A (2009b) DAP-kinase-mediated phosphorylation on the BH3 domain of beclin 1 promotes dissociation of beclin 1 from Bcl-XL and induction of autophagy. EMBO Rep 10:285-292.

Zarranz JJ, Alegre J, Gomez-Esteban JC, Lezcano E, Ros R, Ampuero I, Vidal L, Hoenicka J, Rodriguez O, Atares B, Llorens V, Gomez Tortosa E, del Ser T, Munoz DG, de Yebenes JG (2004) The new mutation, E46K, of alpha-synuclein causes Parkinson and Lewy body dementia. Ann Neurol 55:164-173.

Zhang W, Wang T, Pei Z, Miller DS, Wu X, Block ML, Wilson B, Zhang W, Zhou Y, Hong J-S, Zhang J (2005) Aggregated α-synuclein activates microglia: a process leading to disease progression in Parkinson's disease. 19:533-542.